# Climate adaptation measures for local flooding of the Dutch national highway network

## A case study on Vught and Sint-Michielsgestel

Petri Krijnen

# Climate adaptation measures for local flooding of the Dutch national highway network

## A case study on Vught and Sint-Michielsgestel

by


## Petri Krijnen


to obtain the degree of Master of Science
at the Delft University of Technology,
to be defended publicly on Wednesday August 18, 2021 at 11:45 AM.

| | | |
|---|---|---|
| Student number: | 5145252 | |
| Project duration: | November 23, 2020 – August 18, 2021 | |
| Thesis committee: | Dr. ir. M.M. Rutten, | TU Delft, supervisor |
| | Dr. E. Mostert, | TU Delft |
| | Dr. ir. A.J. Pel, | TU Delft |
| | Ing. J.B.M. Gerritsen MSc, | Rijkswaterstaat WVL, supervisor |


An electronic version of this thesis is available at `http://repository.tudelft.nl/`.


TU Delft

# Preface

Climate change is a global crisis that will face us for decades to come. Since there is no 'one-size-fits-all-solution' for climate change, we are challenged to take the appropriate necessary actions. The COVID-19 pandemic has highlighted the importance of adaptability and has taught us that you can teach an old dog new tricks. This is promising; *Als wij nou veranderen dan hoeft het klimaat het niet te doen (Loesje).*

Before you lies my thesis on climate adaptation measures for local flooding of the Dutch national highway network. This study concludes my master's degree in Water Management at Delft University of Technology. I enjoyed the process, which allowed me to fulfill my enthusiasm for investigating a 'real' world challenge in climate adaptation from a technological as well as a societal point of view.

I could not have performed this research without the support of others. The online presentations and discussions with my committee members helped me to sharpen my thinking and to bring my work to a higher level. Hans, I thank you for giving me the opportunities to graduate at Rijkswaterstaat and to actively participate in meetings concerning projects and research in the field of climate adaptation of the Dutch national highway network. I am grateful for your guidance, both online as well as in real life, your enthusiasm for the topic and your effort in bringing together the right people for organising the focus group. Martine, I thank you for our regular online meet-ups, during which you provided me with guidance and questions to encourage me to address new aspects in my work. Erik, I thank you for your ideas on organizing a focus group and your clear and practical feedback on all my intermediate versions. Adam, I thank you for your nice questions during the meetings, your positive attitude and for providing me with an article to give me ideas on how to make the traffic engineering perspective on extreme precipitation explicit. Additionally, I would like to express my gratitude for my colleagues at Rijkswaterstaat for *meebrommen* with my thesis, as they call it. A special thanks goes to Tristan, for regularly having a chat and for always making time for discussing ideas on the bucket model and time series analysis on the basis of a spontaneously put together presentation. Moreover, I would like to thank Jacques for involving me in the knowledge exchanges on the hydrological behaviour of porous asphalt. Next, I would like to thank the participants of the focus group, the hydrologists and area manager of waterboard the Dommel for their time and enthusiasm to transfer knowledge and to contribute to this research. Finally, I would like to thank my boyfriend, family and friends for their endless support.

*Petri Krijnen*
*Delft, August 2021*

# Abstract

This master thesis provides an approach to develop Adaptation Pathways to prevent local flooding of the Dutch national highway network, using the A2 between the Vught and Sint-Michielsgestel junctions as a case study. Local flooding as result of extreme precipitation has the highest urgency on the Dutch national highway network, due to its increasing chance of occurrence as a result of climate change and increasing consequences on the traffic flow. Hydrological modelling through a bucket approach, complemented by the groundwater dynamics of time series analysis, was done to quantify a range of tipping points between 6 and 60 mm/hr for the Adaptation Pathways, i.e. the hourly precipitation intensity at which water exceeds the edge line of the road for a precipitation event with a maximum return period of 10 years. This was done for three scenarios that embed uncertainties in interception and infiltration parameters and variations in the boundary conditions of groundwater levels. The bucket approach revealed that processes of interception by porous asphalt and sewer discharge are most influential to delay the tipping point, whereas infiltration is the least influential to delay the tipping point. The modelling results showed that adaptation measures that result in (1) an increase in the storage capacity of the catchment of the road (either on the road itself or in the verge) or (2) an increase in the discharge capacity of the catchment of the road are possible to control flooding of the case highway. Possible adaptation measures to increase the storage capacity on the road that were identified are cleaning porous asphalt, increasing the thickness of the porous asphalt and installing a Plastic Road. Possible adaptation measures to increase the storage capacity of the verge that were gathered are removing the top layer of the verge, installing an infiltration trench, raising the road and creating a descending verge. An increase in the discharge capacity of the catchment of the road can be established through a new sewer layout, increasing the sewer capacity and installing manholes with holes. A focus group revealed the interests of stakeholders with respect to flooding. (1) Traffic flow, (2) water buffering capacity, (3) water quality, (4) ecological value and (5) costs and maintenance reflect the criteria relevant to the stakeholders of the focus group and therefore provide information on the societal robustness of an adaptation measure. A scorecard ranked the potential adaptation measures according to the defined criteria which indicate the societal robustness of adaptation measures. Overall, the design of Adaptation Pathways for measures to prevent local flooding on the Dutch national highway network revealed a wide range of possible futures for the defined measures, in which the fulfillment of the T=10 year design storm that is associated with 2050 requirement is either already met or possible through the implementation of adaptation measures. The combination of the Adaptation Pathways map together with the scorecard provided an assessment of the climate resilience of the A2 as an integral part of the surrounding environment. It was found that the designed Adaptation Pathways promote incremental changes, such as cleaning porous asphalt and enlarging the sewer capacity, which enhance path-dependency. Moreover, it was discovered that using a combination of Adaptation Pathways with a scorecard provides insight on transformational adaptation measures that focus on achieving hydrologic neutrality. Hydrologic neutrality can be either be achieved by storing precipitation in the catchment of the road or by discharging precipitation to a nearby location out-side the catchment of the road, where it is used. The findings of the research can be generalized to others places of the Dutch national highway network, to the design of Adaptation Pathways elsewhere and to a variety of climate effects. Finally, as the transformational change towards hydrologically neutral highways complies with the principles of systematic water management of the $21^{st}$ century and low impact development, one could argue for generalization towards hydrologically neutral highways.

**Keywords:** extreme precipitation, highway network, local flooding, time series analysis, bucket model, focus group, climate adaptation measures, Adaptation Pathways

# List of Figures

# List of Tables

# Contents

# 1 Introduction

## 1.1. Research context

### 1.1.1. Climate change and extreme precipitation on the Dutch national highway network

Climate scenarios from the Dutch meteorological institute predict extensive changes in the climate for the coming half century (Attema et al., 2014). Regarding the 2050 climate scenarios, precipitation in the Netherlands will undergo an average increase of 2.5% to 5.5%. In summer, the maximum hourly intensity of rainfall will increase significantly by 5.5% to 25%. Hence, the climate scenarios exhibit a range in uncertainty. Beersma et al. (2018b) state that the uncertainty for extreme precipitation events is especially significant. Firstly, this is caused by the statistical uncertainty associated with the long return periods [1] characterizing extreme precipitation events, because of the limited amount of extreme precipitation observations. Secondly, uncertainty arises from the lack of theoretical understanding on the effects of atmospheric dynamics and microphysics on the magnitude of convective [2] extreme precipitation events (Lenderink et al., 2017).

The Dutch national highway network (HWN), presented in Figure 1.1, is a 3100 km long network of great social interest, because it facilitates 80% of the domestic transport and it is used by 3 million road users a day (Leijstra et al., 2018; Bles et al., 2020). The HWN is due to its extent susceptible to extreme precipitation events. In a study by Beersma et al. (2018a) the frequency of occurrence of extreme precipitation somewhere on the HWN was derived (Table 1.1). Table 1.1 for example illustrates that a precipitation depth exceeding 60 mm in 60 minutes occurs on average 6 times a year on the HWN. Since all 3780 HWN radar sections with a size of 0.9 $km^2$ each are regarded, a single extreme precipitation event is measured multiple times when the shower travels over radar sections. According to Beersma et al. (2018a) Table 1.1 underestimates the actual precipitation extremes of the dataset under study because of attenuation of the radar signal in case of extreme precipitation and must therefore be used as a lower limit for the annual frequency of extreme precipitation. The future increase in precipitation extremes due to global warming will likely result in increased values of Table 1.1 for future datasets (Lenderink et al., 2017; Beersma et al., 2018a).

Table 1.1: Average annual frequency of occurrence of extreme precipitation events based on the Dutch meteorological radar dataset from 2008 to 2017 at any location on the HWN, i.e. regarding all 3780 HWN radar sections with an area of 0.9 $km^2$ each (Beersma et al., 2018a).

| Precipitation duration (min) | > 20 mm | > 30 mm | > 40 mm | > 60 mm | > 80 mm | > 100 mm |
|---|---|---|---|---|---|---|
| 15 | 135 | 13 | 1.7 | 0 | 0 | 0 |
| 60 | 1142 | 218 | 60 | 6.2 | 0.8 | 0.2 |
| 90 | 1757 | 363 | 108 | 15 | 2.8 | 0.4 |
| 120 | 2409 | 501 | 154 | 23 | 4.8 | 0.9 |

[1] Return period T is the average number of years in between precipitation events that exceed a certain magnitude (Savenije, 2006)

[2] Convection is a precipitation mechanism that arises from the vertical instability of the air and results in short, local precipitation events with high rainfall intensities in temperate climates during summer (Luxemburg and Coenders, 2011)


Figure 1.1: Map of the Dutch national highway network, indicated by the red lines (Kerngis Droog, 2020).

### 1.1.2. Effects of extreme precipitation from a traffic engineering perspective

From a traffic engineering perspective the increase in extreme precipitation events will have a large impact on traffic flow. Impacts on traffic flow are reductions in capacity of the road network and travel speed, demand effects, loss of driving safety due to limited visibility and both economic as well as personal costs associated with e.g. the increase in the occurrence of incidents (Axelsen et al., 2016; Snelder and Calvert, 2016; Leijstra et al., 2018; Lázaro, 2020). Demand effects reflect behavioural changes of road users such as cancellation of their trip and changes in departure time and destination (Snelder and Calvert, 2016; Lázaro, 2020). In their literature review on what is empirically known on the performance of the road network with respect to adverse weather conditions, Snelder and Calvert (2016) illustrate that precipitation significantly increases the number of accidents. Whereas research shows varying quantification of the increase in accidents due to adverse weather conditions, precipitation is believed to cause an increase in the number of accidents of at least 75%. Whereas the number of accidents increases, Snelder and Calvert (2016) remark that precipitation tends to decrease the severity of incidents. It is believed that the latter is related to the decrease in travel speed in case of adverse weather conditions (Koetse and Rietveld, 2009). It is also pointed out that precipitation after a dry spell leads to a relatively strong increase in the number of accidents. Reasons for this are slipperiness of the road due to the clearing of accumulated oil by precipitation and risky driving behaviour of road users, because people slowly adjust their driving behavior after a prolonged period of drought (Koetse and Rietveld, 2009).

Quantification of the aforementioned impacts on the traffic flow is scarce for the HWN (Snelder and Calvert, 2016), but the impacts of extreme precipitation on the HWN have been experienced occasionally in the past years. Examples are on the A10 highway in July 2014 (Figure 1.2), on the A20 highway in October 2013 and the A74 highway in June 2016 (e.g. Bles et al., 2020). According to Fortuin (2021) the impacts of extreme precipi-

tation on traffic flow are on average experienced 15 minutes after the occurrence of extreme precipitation on the radar. The review by Snelder and Calvert (2016) reveals that the economic costs associated with changes in traffic and transport due to a single extreme precipitation event causing water nuisance in the Netherlands vary between €414 million and €1.1 billion. The few existing insights in quantification of reductions in capacity, speed and demand effects in the Netherlands show capacity reductions of 1.9% to 11% for heavy rain (i.e. >1 mm), speed reductions of 11 km/hour and a decrease in demand effects of 7.7% (Snelder and Calvert, 2016). Moreover, several studies make the impact of waterfilm formation on the road explicit. A study by Evans et al. (2020) shows that a waterfilm with a depth between 100 and 300 mm causes a vehicle speed reduction towards 20 km/h. Willway et al. (2008) and Bles et al. (2012) state that extreme precipitation events are likely to cause hydroplaning, i.e. a dangerous driving condition that occurs when water causes a loss of contact between the tires and the road. According to Bles et al. (2012) cars are prone to undergo hydroplaning at speeds exceeding 72 km/h in combination with a waterfilm with a minimum depth of 2.5 mm and an extent of 9 m respectively. Additionally, transitions between road sections with opposite slopes are prone to hydroplaning accidents due to the accumulation of runoff at the zero slope in the centre of the transition (Bles et al., 2012).


Figure 1.2: Local flooding of the A10 highway after a precipitation event of 40 mm in one hour in July 2014 (Volkskrant, 2014).

Due to the long service life[3] of infrastructure, as well as the significant costs related to the loss of safety and accessibility of roads, it is important to consider climate change when planning and designing transportation infrastructure. According to the Ministry of Public Works and Water Management (2020) the climate effect of local flooding has the highest urgency on the HWN due to its increasing chance of occurrence and thereafter increasing consequences on the traffic flow. Local flooding concerns pluvial flooding, runoff and flooding of the stormwater drainage system (Table 1.2). Whereas this research focuses on local flooding, it can be considered important to be aware of other types of flooding on road infrastructure as well (Table 1.2).

Table 1.2: Types of flooding and associated impact of one occurring event on the Dutch national highway network (Bles et al., 2012).

| **Type of flooding** | | **Impact of one occurring event** | |
|---|---|---|---|
| | | **Duration** | **Area** |
| Failure of flood defence | flooding from sea and large rivers | weeks to months | dike ring areas (numerous square kilometres) |
| | flooding from small rivers/canals | days to weeks | polder areas (several square kilometres) |
| Water system in the area around the road is not capable for discharge of water | pluvial flooding (overland flow after precipitation) | hours to a day | local, deepened road sections (several metres to kilometres) |
| | increase of groundwater levels | weeks to months | regional |
| Road surface is not capable for discharge of water | run-off on the road | minutes to hours | local (several metres to kilometres) |
| | flooding of the stormwater drainage system | minutes to hours | local (several metres to kilometres) |

[3]The pavements and stormwater drainage systems of the HWN are designed for a service life of 20 and 50 years respectively (Rijkswaterstaat, 2020b; Rijkswaterstaat, 2020a)

## 1.2. Problem statement

### 1.2.1. Previous research

Following the Delta Program on Spatial Adaptation, the Ministry of Infrastructure and Water Management has formulated the goal that in 2050 the Netherlands will be designed as water-resilient as possible (Bles et al., 2012). Water-resilience can in this way be defined as understanding an interconnected socio-spatial hydrological system as the system adapts and changes in an uncertain and unpredictable environment (Davoudi et al., 2012). Thereafter, the Ministry of Infrastructure and Water Management has started the Climate-proof Networks project to fulfil the two main ambitions. The first ambition is to gain sufficient insight into the impact of climate change on the performance of the HWN by 2020. Secondly, an overview of how to act in order to have the HWN set up in a water-resilient manner by 2050 must be created.

Research programs and pilot studies contributing to fulfilling the first ambition with respect to flooding entail limitations and do not yet fulfil the second ambition, i.e. providing foresight into the use of the HWN in relation to climate adaptation measures. Bles et al. (2012) produced a map of the Dutch national highway network showing the vulnerable locations for flooding for both the current climate (blue spots) as well as the future climate in 2050 (red spots). Limitations of this study are the use of a grid size accuracy of 100m, the assumption that roads are maintained adequately and the lack of analysing the actual impact of flooding. More recent studies on the effect of flooding on the HWN are the National Stresstest and the Climate Impact Atlas (Bles et al., 2020; Klimaateffectatlas, 2020). The Stresstest builds on the research by Bles et al. (2012) and provides insight into the vulnerability of the highway network to waterfilm formation at an extreme precipitation event on a grid resolution of 100m, by categorizing the entire HWN (Figure 1.3a). Limitations of this study are the use of a grid size accuracy of 100m and the lack of analysing the actual impact of flooding. The Climate Impact Atlas on the other hand does map out the impact of flooding associated with climate change on a national scale, for example due to extreme precipitation events and changing groundwater regimes (Figure 1.3b). The Climate Impact Atlas provides an indication of the water depth that can occur as a consequence of extreme precipitation. Figure 1.3b reveals a scattered distribution of the water depth consequences over the Netherlands, since spatial differences within extreme rainfall have not been demonstrated (Klimaateffectatlas, 2020). The simulations are executed with the 'Rainfall overlay' of Tygron and throughout the simulation the model calculates how much precipitation will infiltrate, runoff and end up in the sewer (Slager, 2018). Several modelling choices bring along limitations that leave room for improvement:

- It is assumed that the sewer system is optimally functioning, i.e. without blockages or maintenance backlog and that a uniform sewer discharge capacity of 20 mm/hour is applicable everywhere. In reality, sewer capacities vary.

- The simulations are performed with a spatial resolution of 2 by 2 metres based on AHN2, the digital elevation map of the Netherlands mapped between 2007 and 2012. Concerning the spatial resolution, room for improvement is twofold. On the one hand recent developments influencing the land surface elevation and thereby water depths that can occur as a consequence of extreme precipitation can be included. On the other hand, a higher resolution produces more detailed results and possibly better estimations of water depths.

- The infiltration values used in the simulations are based on simplified topographic and soil classification maps. Slager (2018) reveals that variation of infiltration values can be significant on short distances and heavily relies on antecedent conditions to the precipitation event. Thereafter, room for improvement through the variation of infiltration values can be identified.

Next to precipitation, the Climate Impact Atlas provides an indication of the changing Mean High Groundwater Level according to the most extreme climate scenario of the Dutch meteorological institute. The distribution of the changing Mean High Groundwater Level (MHGL), i.e. an averaged high groundwater level and thus not a maximum groundwater level, reveals that particularly high sandy grounds are prone to an increase of the MHGL (Figure 1.3b). In the simulation, local conditions and processes, e.g. groundwater dynamics and the functioning of local drainage, have not been included.


(a) Sensitivity to waterfilm formation (GeoWeb Stresstest HWN, 2019).

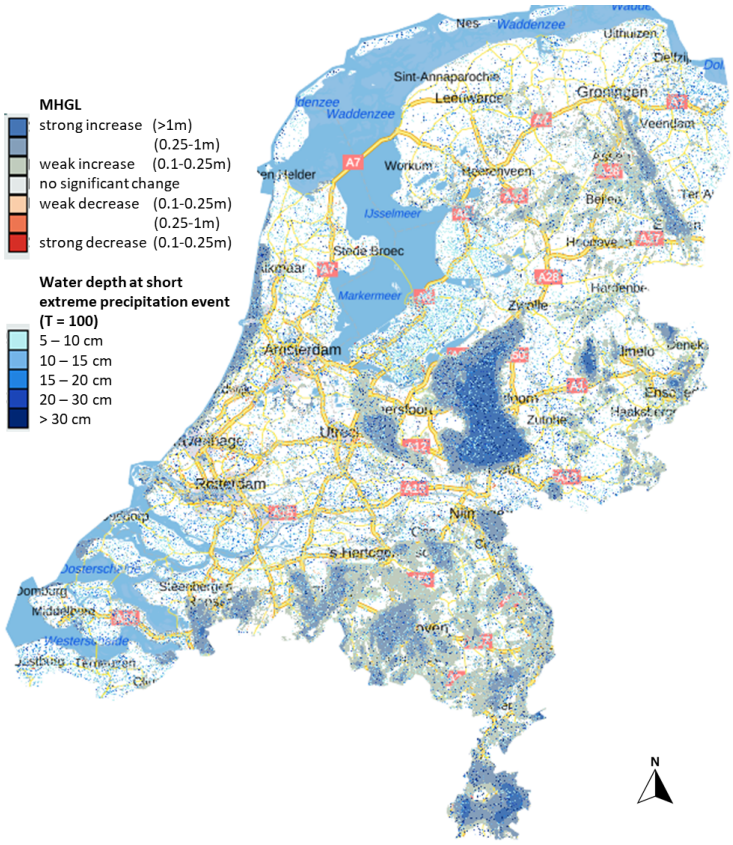


(b) Consequences of a T = 100 year (70 mm of precipitation in 2 hours) precipitation event and the expected increase in Mean High Groundwater Level (MHGL) up to 2050 due to climate change (Klimaateffectatlas, 2020).

Figure 1.3: Results of research programs on the climate effect of local flooding

### 1.2.2. Methodology and scientific relevance

Adaptation Pathways provide a methodology to support the development of an adaptive plan that is able to deal with conditions of deep uncertainties (Haasnoot et al., 2013). Uncertainty can be defined as limited knowledge about future, past or current events (Walker et al., 2012). Various levels of uncertainty can be distinguished for purposes of determining ways to deal with uncertainty. A high level of uncertainty is associated with deep uncertainty, a notion that implies that it is possible to enumerate conceivable representations of the system, plausible futures and relevant outcomes of interest without being able to rank these representations, futures and outcomes (Walker et al., 2012; Haasnoot et al., 2013). Climate change is a concrete example of deep uncertainty due to to the lack of knowledge on the magnitude and speed of climate change and on the consequences of climate change on a local scale (see limitations of previous research in section 1.2.1).

A methodology to evaluate measures concerning water management under the deep uncertainty climate change is Adaptation Pathways (Kwakkel et al., 2015). The use of Adaptation Pathways for implementing climate-resilient water management has gained popularity throughout recent years (Bloemen et al., 2018; Werners et al., 2021). This can be related to the advantages of Adaptation Pathways, such as clear visualization and providing the means of motivating decision-makers to accommodate for future developments by linking short-term decisions to long-term tasks. Adaptation Pathways reveal sequences of actions to achieve an objective under uncertain changing conditions (Kwakkel et al., 2015), e.g. the objective of preventing local flooding of the HWN under increasing precipitation intensities. Adaptation Pathways can be illustrated in the form of a map (figure 1.4), in which the effectiveness of a measure is plotted against a normative parameter which can be associated with the objective, for example precipitation intensity associated with flooding. The overview indicates a variety of pathways, i.e. a combination of one or more measures that may be taken in order to be prepared for future developments.

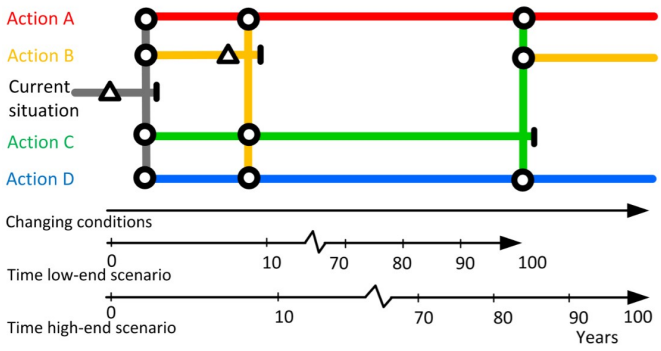


Figure 1.4: Example of an Adaptation Pathways map (Kwakkel et al., 2015). The changing conditions and time scales of scenarios are shown on the horizontal axes underneath the diagram, the length of the coloured horizontal lines indicates the extent to which the (package of) measures is compliant and the vertical coloured lines that run to and from a circle indicate how to switch between measures.

The first scientific challenge that arises from Adaptation Pathways is societal robustness on a local scale. Societal robustness forms a common criterion for making decisions under uncertainty by indicating the performance in a multi-stakeholder setting (Marchau et al., 2019). A societal robust adaptation measure meets multiple objectives of the relevant stakeholders over many scenarios and therefore provides a better trade-off than other potential adaptation measures in the Adaptation Pathways map (Marchau et al., 2019). Since different stakeholders fulfil different responsibilities and have various preferences, an adaptation measure might meet the objectives of one stakeholder, while not meeting the objectives of another stakeholder. In this respect adaptation outcomes and goals can be regarded ambiguous (Werners et al., 2021). Adaptation Pathways have mostly been designed for well-resourced national scale studies such as the Dutch Delta Programme and Los Angeles County (Marchau et al., 2019; Werners et al., 2021), but further application on a local scale must be explored (Marchau et al., 2019). To start with, studying Adaptation Pathways on a local scale can be regarded important because local governments are more technically and financially resource-constrained to implement big projects compared to national governments. Secondly, decisions on adaptation at a local scale rely heavily on consensus within local constitutes, because of differences in responsibilities and preferences (Barnett et al., 2014). According to Barnett et al. (2014) and Bloemen et al. (2018) local Adaptation Pathways are a promising method to contribute to the quality of the plans and to the commitment of stakeholders for the monitoring and implementation of plans.

A recent example of a local Adaptation Pathways approach on the HWN without the inclusion of societal robustness is the InnovA58 project, a Dutch project aimed at increasing the resilience of the A58 highway and its surrounding environment for the effects of climate change (Leijstra et al., 2018). In the research, the developed Adaptation Pathways reveal possible measures that increase resilience to e.g. flooding. In the project it was proved difficult to integrate information from stakeholders with information of the road itself, because the possible measures mainly focus on the functionality of the road and not on making integral solutions to create matching solutions with other goals related to e.g. nature. An example of a matching solution is a culvert that serves both as a drain for excess precipitation as well as an underpass for wildlife. Unlike the research by Leijstra et al. (2018) this thesis will contribute to the aforementioned scientific challenge by exploring the societal robustness of local Adaptation Pathways.

The second scientific challenge that arises from Adaptation Pathways is model robustness. In order to create the Adaptation Pathways the deeply uncertain future must be quantified through modelling. In the field of hydrology a model can be defined an encapsulation of our knowledge on the processes in the real world (Savenije, 2009). The use of an appropriate model structure remains a big challenge for hydrologists (Clark et al., 2008; Gupta et al., 2012). Moreover, parameter uncertainty can be regarded an issue due to e.g. a lack of observations, unreliable observations, non-observable quantities and heterogeneity of hydrological systems (Gharari et al., 2014; Hrachowitz and Clark, 2017). It can generally be stated that models should be detailed enough to represent the dominant processes and natural variability in the system (Booij, 2003). Moreover, the model should be robust, i.e. able to maintain the desired system characteristics in case of disturbances and a wide range of plausible futures (Mens et al., 2011; Marchau et al., 2019). In case of increasing model complexity issues such as a lack of parameter constraints that cause instable model solutions arise.

Regarding the exploratory nature of Adaptation Pathways and the common problem of a lack of data in rainfall-runoff modelling (Hrachowitz et al., 2014) a robust modelling approach can be chosen by combining a lumped hydrological model and time series analysis. According to Nijzink et al. (2016) lumped hydrological models are able to capture dominant hydrological systems across various spatial scales, since the model domain is represented as a single entity without spatial discretization (Hrachowitz and Clark, 2017). In general, lumped conceptual models are bucket models, which rely on forcing [$LT^{-1}$] and storages [L], i.e. buckets, which interact through fluxes [$LT^{-1}$] (Nijzink et al., 2016; Hrachowitz and Clark, 2017). Examples of forcing are precipitation and evaporation and examples of fluxes are runoff, infiltration and discharge. Savenije (2009) and Hrachowitz and Clark (2017) state that bucket models, despite being conceptual in design and therefore associated with a level of abstraction, are robust if well tested and are at a macroscale able to relate individual components to stores and fluxes in nature. Due to the aforementioned common problem of a lack of data a way to increase the potential of bucket models is by involving observation-based process identification (Hrachowitz and Clark, 2017). Thereafter, it is in this thesis explored whether time series analysis can contribute to the latter by involving observations. A time series constitutes a set of chronologically successive observations of a certain variable (Von Asmuth, 2012; Van Geer, 2012). Time series analysis is a data-based approach to model the dynamical behaviour of a system by translating input signals (e.g. precipitation) to output signals (groundwater heads) (Von Asmuth et al., 2002; Collenteur et al., 2019). In the field of hydrology, time series analysis allows the hydrologist to understand why groundwater heads vary the way they do (Bakker and Schaars, 2019). In contrast to a conceptual hydrological model, time series analysis requires a small number of parameters. Thereby the uncertainty that arises from the necessary parameterizations in conceptual modelling is avoided (Bakker and Schaars, 2019).

Nowadays combining the qualities of time series analysis and hydrological modelling is not a common practice (Obergfell et al., 2019). Berendrecht et al. (2006) and Collenteur et al. (2020) explored the combination of time series analysis with a lumped, conceptual model with three natural reservoirs; the root zone, the unsaturated zone and the saturated zone. Collenteur et al. (2020) for example uses the FLEX model to account for soil water dynamics by combining time series analysis with a bucket approach with two connecting buckets (Figure 2.4a); an interception reservoir and a root zone reservoir (Fenicia et al., 2006; Collenteur et al., 2020). However, the applicability of the combination on other settings involving anthropogenic processes such as highway runoff and sewer discharge has not been studied before. Therefore, it will be explored whether the complementarity of time series analysis of natural processes with a bucket approach involving both natural and anthropogenic processes enhances robust hydrological modelling.

## 1.3. Research objective

This thesis will provide insight into the aforementioned societal and scientific challenges, by fulfilling the following research objective;

**To design Adaptation Pathways of measures to prevent flooding as a result of extreme precipitation on the Dutch national highway network.**

In order to study the use of Adaptation Pathways in a local, context-specific, multi-stakeholder setting a case area is needed. Regarding the case area, availability of local information is required to explore the complementary use of time series analysis of the natural hydrological processes and a lumped, conceptual bucket approach involving both natural as well as anthropogenic hydrological processes influencing the HWN. The A2 between the Vught and Sint-Michielsgestel junctions of the HWN meets both requirements and therefore is considered suitable to serve as case area in this thesis. The A2 case area with its surroundings is located south of the city of 's-Hertogenbosch in the Netherlands (Figure 1.5).

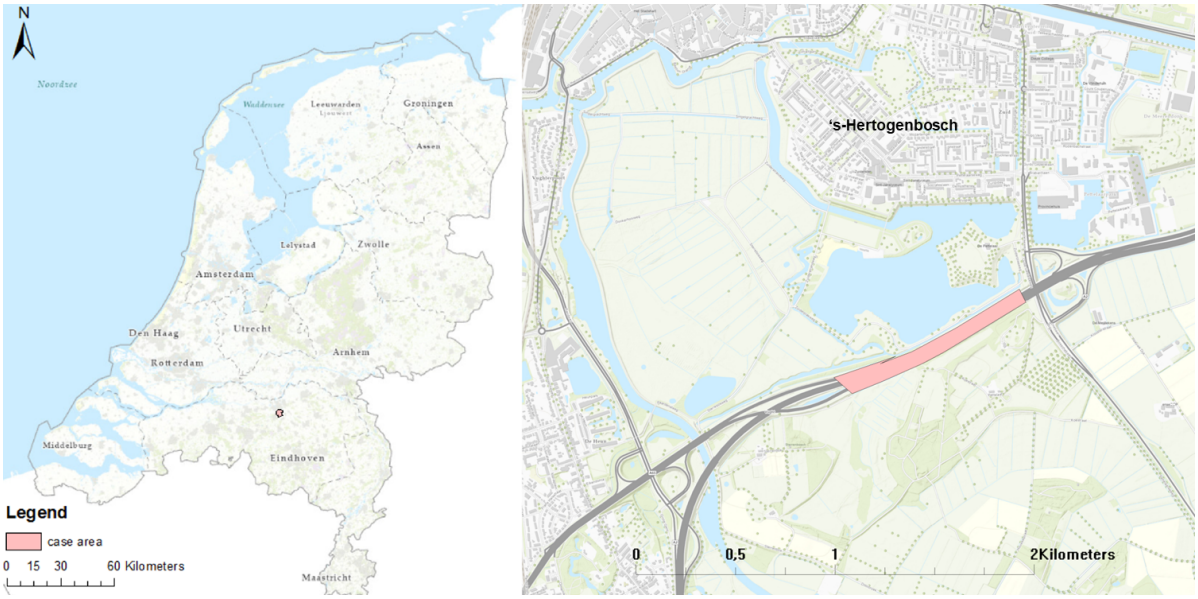


Figure 1.5: Location of case area (Kerngis Droog, 2020).

## 1.4. Research questions

In order to fulfill the research objective, the following research questions are posed;

1. How can flooding of the A2 between the Vught and Sint-Michielsgestel junctions be described and explained?
   (a) What does the hydrological system of the A2 between the Vught and Sint-Michielsgestel junctions look like?
   (b) How can a robust quantitative model of the hydrological system of the A2 between the Vught and Sint-Michielsgestel junctions be constructed?
   (c) Which scenarios should be used to reflect the effect of the increase in extreme precipitation intensities due to climate change on the A2 between the Vught and Sint-Michielsgestel junctions?
   (d) How do the scenarios influence the flooding of the A2 between the Vught and Sint-Michielsgestel junctions?
2. What are possible measures to prevent flooding of the A2 between the Vught and Sint-Michielsgestel junctions of the Dutch national highway network?
3. What are the interests of the stakeholders involved with respect to the flooding and to measures against flooding of the A2 between the Vught and Sint-Michielsgestel junctions of the Dutch national highway network?

4. What Adaptation Pathways of measures for flood control of the A2 between Vught and Sint-Michielsgestel junctions can be designed with the inclusion of stakeholder interests?

5. Can the results of the case study be generalized?

## 1.5. Reader guide

Throughout the report the research questions will be answered. To start with, Chapter 2 presents the methodology used in the research by illustrating the link between quantitative and qualitative research in Adaptation Pathways. Chapter 3 describes the case area, thereby providing a base for the creation of the hydrological model and Adaptation Pathways. Chapters 4 and 5 focus on the results of hydrological modelling by time series analysis and a bucket approach respectively in order to answer the first research question. Chapter 6 focuses on the societal robustness of adaptation measures gathered through a focus group. Chapter 7 illustrates the design of Adaptation Pathways with a scorecard, by combining the quantitative and qualitative findings from previous chapters. Thereafter, an answer to the second, third and fourth research questions is provided. Chapter 8 discusses the results obtained in previous chapters through comparison with results of other research, reflection on the methodology and by reflection on possibilities for generalization of the research. The latter provides an answer to the fifth research question. In Chapter 9 all findings are summarized and recommendations are presented.

# 2

# Methodology

To fulfill the objective to design adaptation strategies of measures to prevent flooding of the Dutch national highway network as a result of extreme precipitation this research was carried out using a case study approach and a mixed-mode design that combines quantitative and qualitative research (Bhattacherjee, 2012) (Figure 2.1). Whereas quantitative research aims at identifying general relations by deduction, qualitative research aims at understanding unique characteristics by induction (Mostert, 2018). According to Johnson and Onwuegbuzie (2004) and Bhattacherjee (2012) the joint use of quantitative and qualitative data is successful, because it acknowledges the importance of the physical, natural world as well as the importance of reality and the influence of human experience. Therefore the mixed-mode design can provide insights that might be missed when either quantitative or qualitative research is used. Moreover, Johnson and Onwuegbuzie (2004) state that mixed-mode design can be used to increase the generalizability of the results (research question 5).

Figure 2.1 reveals the structure of the research. To start with, quantitative data collection (section 2.4) provided input for time series analysis and the bucket model which describe and explain flooding (research question 1) and simulate possible measures to prevent flooding (research question 2). Qualitative data collection (section 2.5) revealed the interests of stakeholders with respect to flooding (research question 3). The design of Adaptation Pathways was established by combining findings of earlier research questions (research question 4).

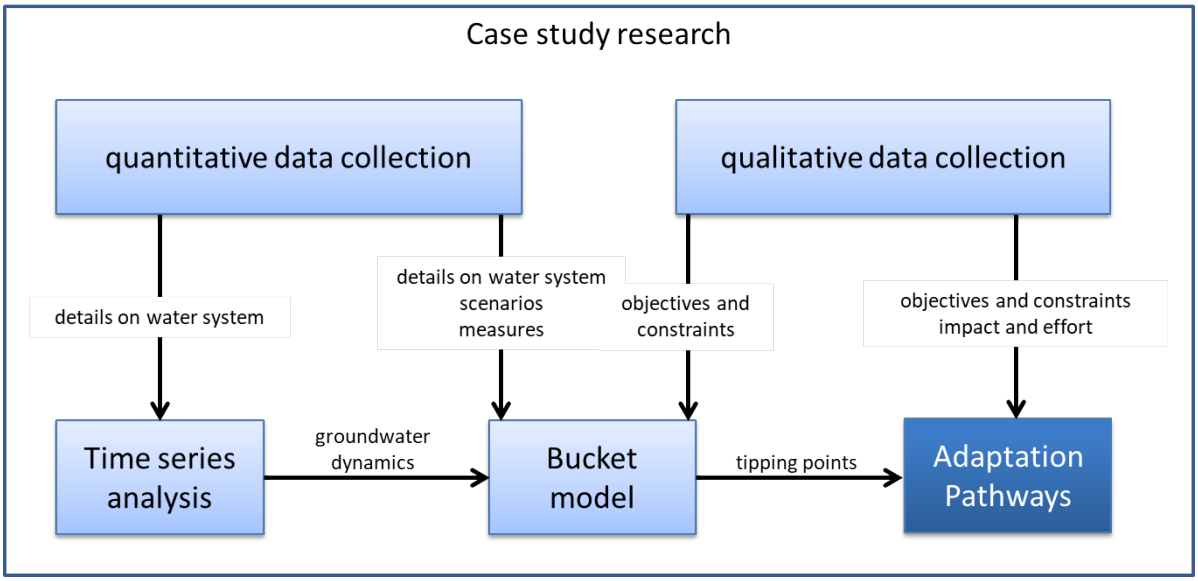


Figure 2.1: Visual representation of links between methods

## 2.1. Case study

Case study is the intensive studying of a phenomenon within its real-life context in one or a few settings (Bhattacherjee, 2012). Case studies allow for the use of all types of data and offer good possibilities for bringing together literature, disciplines and experts (Mostert, 2018).

The A2 between the Vught and Sint-Michielsgestel junction is part of the HWN and was selected as case area for the design of Adaptation Pathways due to its economic relevance, suspected susceptibility to local flooding and practical considerations. To start with, the A2 route of the HWN connects two powerful Dutch economic regions (Brainport Eindhoven and the Northern Randstad) and is therefore of high economic relevance (Tijhuis and Beentjes, 2019). Although the A2 between the Vught and Sint-Michielsgestel junctions is not regarded a bottleneck for traffic disruptions due to economic growth and mobility trends (Tijhuis and Beentjes, 2019), flooding as a result of extreme precipitation can have a large impact on the traffic flow (section 1.1.2). Secondly, according to a pilot study on the A2 route between Deil and Vught (Huveneers, 2018), the Climate Effect Atlas and Stresstest the A2 between the Vught and Sint-Michielsgestel junctions can be regarded a vulnerable location to local flooding as a result of extreme precipitation (Figure 2.2). Figure 2.2 reveals water depths up to 30 centimeters on the highway under consideration as a result of a precipitation event with a return period of 100 years and sensitivity to waterfilm formation due to the absence of a stormwater sewer. Thirdly, practical considerations contribute to the choice of the Vught and Sint-Michielsgestel case. Zwart (2020) assessed the geohydrological situation of the case area and its surroundings. Therefore, quantitative data such as groundwater level measurements and some information on dimensions of the sewer system are available.

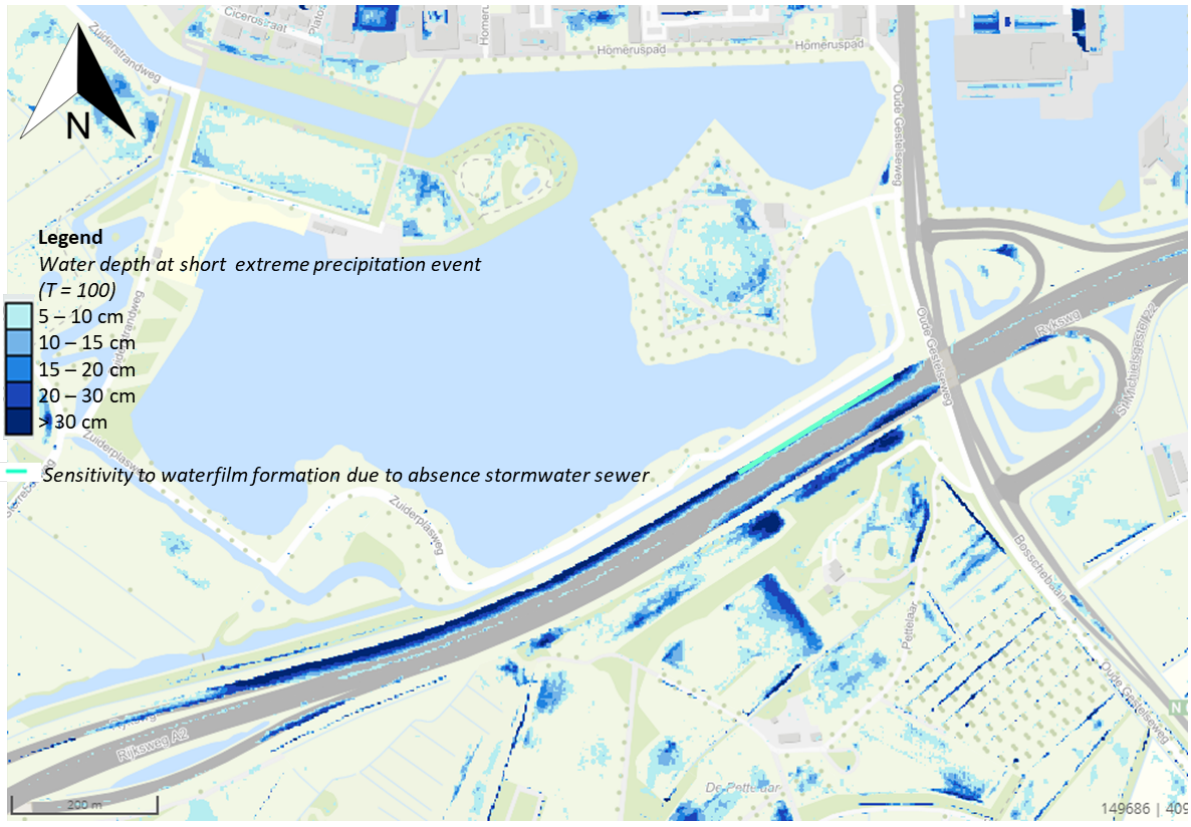


Figure 2.2: Sensitivity of the case highway to waterfilm formation (after GeoWeb Stresstest HWN, 2019) and impact of a T = 100 year (70 mm of precipitation in 2 hours) precipitation event (after Huveneers, 2018; Klimaateffectatlas, 2020).

## 2.2. Hydrological modelling

The choice of the hydrological modelling techniques, i.e. the complementary use of time series analysis and a bucket model, relies on the societal challenge of improving limitations of current research programs with respect to flooding and the scientific challenge of model robustness (section 1.2.2). Time series analysis is used to explore whether findings on groundwater dynamics through time series analysis can increase the potential of a bucket model (Figure 2.1). A bucket model provides the means to simulate the quantitative effects of scenarios that reflect the increase in extreme precipitation intensities due to climate change, to quantify the effects of measures against local flooding and to determine adaptation tipping points for each scenario (Figure 2.1). Adaptation tipping points are a central concept in Adaptation Pathways and indicate the moment at which the system is not able to achieve its objective and alternatives are necessary (Kwadijk et al., 2010). In this thesis, the tipping points indicate at which hourly precipitation intensity the consequences of flooding exceed the flooding standards, i.e. the hourly precipitation intensity at which water exceeds the edge line of the road for a precipitation event with a maximum return period of 10 years.

### 2.2.1. Time series analysis

Time series analysis is a data-based approach to model the dynamical behaviour of a hydrological system by translating input signals to output signals (Von Asmuth et al., 2002; Collenteur et al., 2019). In the field of hydrology, transfer function noise (TFN) modelling is a popular method of time series analysis (Collenteur et al., 2020). In TFN models stresses such as precipitation, evaporation, surface water levels and pumping time series form the input signals which force a response of the output signal, i.e. a groundwater head time series (Collenteur et al., 2019; Collenteur et al., 2020). The use of TFN models allows a geohydrologist

1. to understand a system by quantifying the separate influences of the stresses which compose the output signal (Von Asmuth et al., 2002; Van Geer, 2012; Pezij et al., 2020).

2. to assess the quality of available data by detecting errors and outliers in the observed times series (Collenteur et al., 2019).

3. to forecast the output signal at non-observed periods, both in the past (filling in data gaps) and future (studying scenarios) (Von Asmuth et al., 2002; Van Geer, 2012).

4. to analyse the effects of interventions in a system and trends throughout time, such as seasonal and long-term temporal variability (Van Geer, 2012; Collenteur et al., 2019). In regions with shallow groundwater tables, such as the case area, knowledge on the variability in groundwater heads can be regarded important for economic and ecological purposes (Collenteur et al., 2019) and can contribute to understanding the role of groundwater in the phenomenon of local flooding.

Moreover, a development in TFN modelling is the ability of TFN models to calibrate parameters associated with rainfall-runoff models using groundwater levels (Collenteur et al., 2020).

Figure 2.3 illustrates that a TFN model consists of a deterministic model and a stochastic noise model (Von Asmuth et al., 2002). Whereas the deterministic part allows the model to find parameter values such that the residuals are minimized (Bierkens and Van Geer, 2007), the stochastic noise model computes the residuals in the model outcomes by identifying white noise through statistical treatment of general errors without reference to the system (Bierkens and Van Geer, 2007; Von Asmuth, 2012). White noise is the result of random processes that cannot be modelled (Collenteur et al., 2019) and is for example associated with measurement errors in the input series. A clear trend in the residuals next to white noise indicates that a stress is missing from the model (Collenteur et al., 2019). The reasoning behind minimizing the residuals in the deterministic part is that the model strives to explain as much of the output signal as possible with the input signals. The combination of a deterministic with a stochastic approach results in a so-called gray box model (Collenteur et al., 2019). In contrast to deterministic groundwater models, gray models have the advantage of easily being set up without requiring detailed knowledge on subsurface characteristics (Collenteur et al., 2019; Pezij et al., 2020). This prevents equifinality, meaning that parameters compensate for uncertainties in other parameters or in the model structure due to a high number of parameters with insufficient model constraints in the deterministic part (Von Asmuth, 2012).

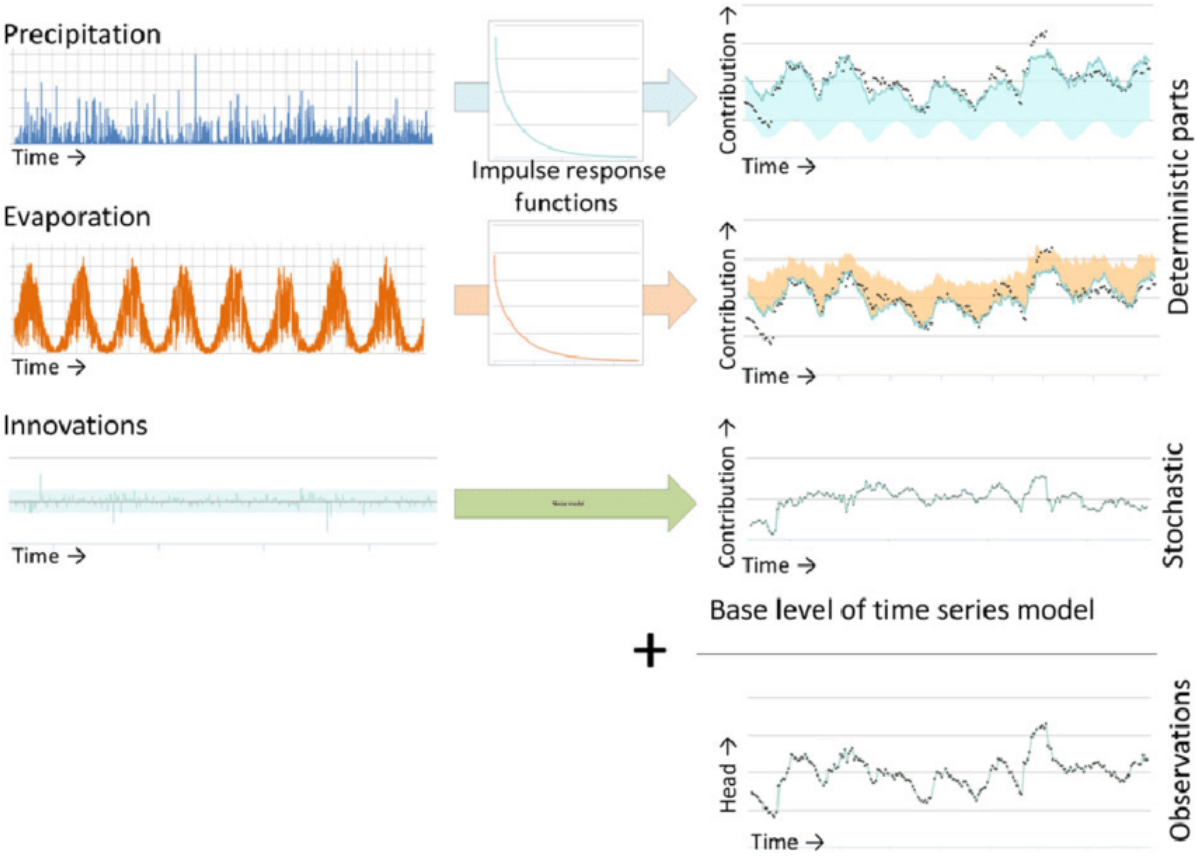


Figure 2.3: Schematic representation of a TFN model. In the deterministic part of the TFN model observed precipitation and evaporation time series are transferred by impulse response functions to their contribution to the observed groundwater head time series. The stochastic noise model computes the residuals. The sum of the base groundwater level, i.e. the steady state groundwater head when all stresses are zero, and the contribution of the deterministic and stochastic parts results in the observed head time series (Zaadnoordijk et al., 2019).

In TFN modelling a transformation by an impulse-response function is applied to one or more deterministic input series (Von Asmuth et al., 2002; Pezij et al., 2020). Different stresses are associated with different types of impulse response functions (Collenteur et al., 2019). Nowadays, predefined, physically realistic impulse response functions are used in TFN modelling (Collenteur et al., 2019; Collenteur et al., 2020; Pezij et al., 2020). These functions are characterized by shape parameters that can be adjusted to optimize the fit between the measured and modelled heads. As aforementioned, optimization is aimed at explaining as much of the output signal as possible with the input signals. It is therefore important to note that through TFN modelling optimal values will be provided given the model structure, so it cannot be guaranteed that the response function used is the optimal one to explain the observed time series (Van Geer, 2012). A frequently applied impulse response function for precipitation and evaporation for example is the scaled gamma distribution (Pezij et al., 2020). Appendix A.1 provides more details on the basic equations of TFN modelling.

A stress can consist of the combined contribution of multiple stresses. In TFN modelling of groundwater head time series net groundwater recharge is a well-known function that describes the contribution of both precipitation and evaporation stresses. Models that accurately describe the net groundwater recharge are under development (Collenteur et al., 2019). Currently available models for net groundwater recharge are either based on a linear function of precipitation and potential evaporation (Zaadnoordijk et al., 2019); Collenteur et al., 2021) or on a non-linear response of recharge to precipitation using soil-water balance concepts (Collenteur et al., 2021);

- In case of a linear response of recharge the output signal is simply a sum of the effects of all individual deterministic stresses (Von Asmuth, 2012). The linear response of recharge can therefore be estimated by a factor $f$, which gives the ratio between the impulse response functions for precipitation $P$ [$LT^{-1}$] and potential evaporation $E_p$ [$LT^{-1}$] (Obergfell et al., 2019; Zaadnoordijk et al., Zaadnoordijk et al.);

$$R = P - fE_p \tag{2.1}$$

  The value of $f$ [-] is in between 0 and 2, thereby allowing the actual evaporation to vary between zero and twice the potential reference evaporation (Collenteur et al., 2020). If the net groundwater recharge is positive the contribution of precipitation $P$ is larger than the contribution of evaporation and vice versa. Van Der Hauw (2012) states that $f$-values larger than 2 imply that influences have incorrectly been modelled as evaporation. It is important to note that $f$ does not account for seasonal and temporal variability (Obergfell et al., 2019). According to Zaadnoordijk et al. (2019) the linear model provides a good fit for the net groundwater recharge in temperate climates characterized by shallow groundwater levels (up to a few metres depth) and negligible runoff. According to Obergfell et al. (2019) and Collenteur et al. (2020) factor $f$ does not guarantee accurate estimation of recharge and cannot easily be appraised.

  A possible reason for inaccurate simulation of groundwater head output series by assuming a linear relationship between precipitation and potential evaporation in the TFN model is the physical knowledge that groundwater systems can be strongly non-linear (Berendrecht et al., 2006). Treshold non-linearities due to drainage levels and perched water tables[1], extreme rainfall events that result in significant runoff (Peterson and Western, 2014; Collenteur et al., 2019) and soil water dynamics in the unsaturated zone are possible causes for non-linear groundwater recharge (Berendrecht et al., 2006; Collenteur et al., 2021). The latter can be related to the dependency of the unsaturated zone storage capacity on the water table depth and the influence of saturation of the unsaturated zone on the hydraulic conductivity and therefore groundwater recharge (Berendrecht et al., 2006).

- In case of a non-linear response of recharge in a groundwater system, the non-linear FLEX model can be used (Collenteur et al., 2021). The FLEX recharge model accounts for soil water dynamics in the unsaturated zone by using a bucket approach with two connecting buckets (Figure 2.4a); an interception reservoir and a root zone reservoir (Fenicia et al., 2006; Collenteur et al., 2020). The FLEX model can be applied to areas with shallow groundwater levels that are not significantly affected by capillary rise (Collenteur et al., 2020). In the FLEX model precipitation $P$ [$LT^{-1}$] and potential evaporation $E_P$ [$LT^{-1}$] form the input signals which influence the water balances for the reservoirs and therefore force groundwater recharge $R$ [$LT^{-1}$]. In the model, the groundwater recharge is calculated by the approximation of Campbell (Collenteur et al., 2020);

$$R = k_s \left( \frac{S_r}{S_{r,max}} \right)^{\gamma} \tag{2.2}$$

  with saturated conductivity $k_s$ [$LT^{-1}$], storage in the rootzone reservoir $S_r$ [L] and rootzone reservoir storage capacity $S_{r,max}$ [L]. Moreover, the degree of non-linearity of the recharge flux with respect to the degree of saturation of the unsaturated zone is present in the formula as $\gamma$ [-]. The larger the value for $\gamma$, the more non-linear the recharge flux with respect to the saturation of the unsaturated zone (Figure 2.4b). The values for $S_r$ and $S_{r,max}$ are obtained through the water balances of the reservoirs. It is important to note that unlike the linear recharge model, the use of the non-linear FLEX recharge model in TFN modelling allows calibration of parameters such as $\gamma$, $k_s$, $S_{i,max}$ and $S_{r,max}$, next to the response function parameters and base level $d$ of the model (equation A.1).

Examples of available tools for TFN modelling are the commercial Menyanthes (Von Asmuth, 2012) and the open source Python code Pastas (Collenteur et al., 2019; Pezij et al., 2020). Whereas Pastas allows the possibility to incorporate the non-linear FLEX-model, Menyanthes does not. In this thesis linear recharge is modelled with Pastas and Menyanthes. Non-linear recharge is modelled with the FLEX-model of Pastas.

[1] A perched water table means that an unconfined groundwater lies on top of the unsaturated zone because of physical soil horizons (Berendrecht et al., 2006; Hendriks, 2010),

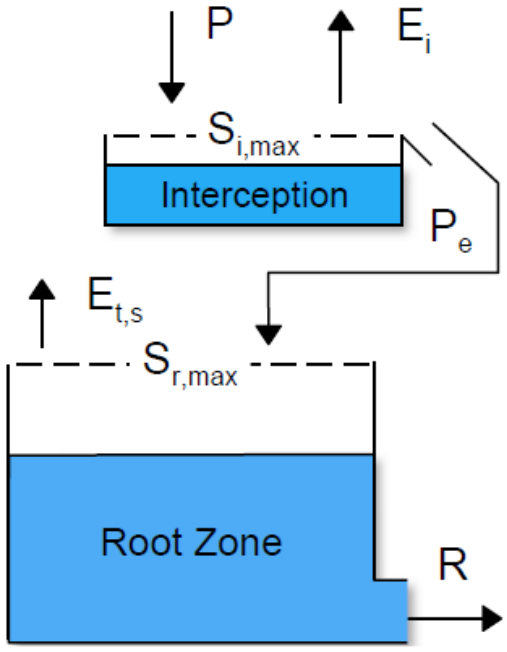


(a) Conceptual model for the FLEX model with reservoirs represented by blue buckets [L] and fluxes along arrows [$LT^{-1}$] (Collenteur et al., 2020). In case the maximum interception capacity $S_{i,max}$ is reached, a treshold non-linearity as effective precipitation $P_e$ is routed towards the root zone reservoir and is partitioned into storage $S_r$, evapotranspiration $E_{t,s}$ and groundwater recharge R.

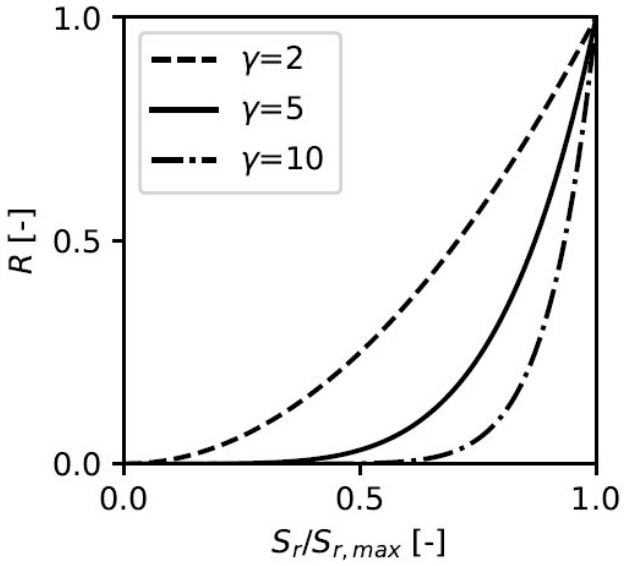


(b) Relationship between groundwater recharge R and the degree of saturation of the root zone ($S_r/S_{r,max}$), in case the saturated conductivity is set to $k_s = 1$ (Collenteur et al., 2020).

Figure 2.4: FLEX model

### 2.2.2. Bucket approach

A bucket model is a conceptual framework to model the dominant hydrological processes in a system without deep knowledge of local conditions, thereby avoiding extensive work on modelling precise structures and high computational costs (Zeisl et al., 2018). Despite its simplicity a general idea on water quantity distribution and behaviour of the water system can be generated with a bucket model (Gharari, 2016). A bucket model consists of single entities without spatial discretizations, i.e. buckets, which interact through fluxes and rely on forcing. A bucket model is created according to a deductive top-down approach, in which the observed patterns are described directly at the scale of the system by testing and refining the model based on learning from data (Hrachowitz and Clark, 2017).

## 2.3. Adaptation Pathways

The choice of designing Adaptation Pathways relies on the societal challenge of providing insight into the use of the HWN in relation to climate adaptation measures and the scientific challenge of societal robustness. In this study Adaptation Pathways provide a way to illustrate adaptation tipping points for each scenario and (sequences of) measures against local flooding (research questions 1 and 2). Therefore, Adaptation Pathways can be regarded a bottom-up approach, i.e. a vulnerability assessment of the system under investigation (Kwadijk et al., 2010). In order to account for the scientific challenge of societal robustness, insight must be provided into the performance of the Adaptation Pathways in a local setting of multiple stakeholders which fulfil different responsibilities and have different ideas, interests and perspectives. Such qualitative data on the performance of Adaptation Pathways (research question 3) is in this research presented with the Adaptation Pathways in the form of a scorecard (Figure 2.5) (Haasnoot et al. 2013; Kwakkel et al., 2015). In a scorecard, a pathway is judged on the basis of a set of performance criteria retrieved from the qualitative data collection (section 2.5). Thereby, societal robustness of the designed Adaptation Pathways can be identified.

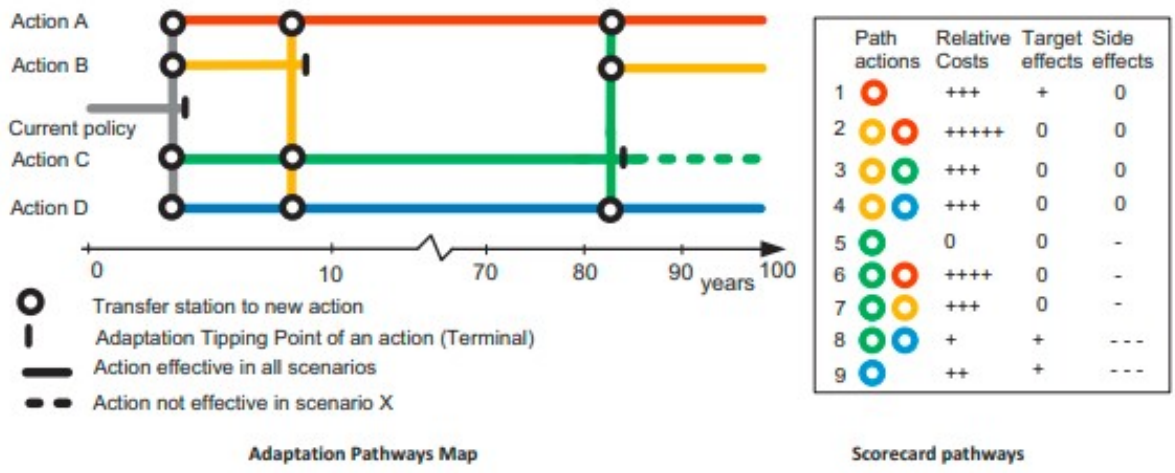


Figure 2.5: An example of an Adaptation Pathways map and a scorecard (Haasnoot et al., 2013). In the scorecard each package of measures is given a score for each assessment criterium (e.g. ++, +, 0, -, -).

## 2.4. Quantitative data collection

Quantitative data on water system characteristics and flooding-related processes within the case area were retrieved from research by Zwart (2020), policy documents, (international) literature, a field visit with the area administrator from the Dommel waterboard and databases such as Dinoloket, the Rijkswaterstaat Geographic Information Systems (GIS) Database and the Dutch Digital Elevation Model AHN3, which has a grid resolution of 0.5 by 0.5 metres.

## 2.5. Qualitative data collection

Qualitative data on ideas, interests, objectives, constraints and perspectives were gathered through an online focus group. Objectives and constraints were also collected using document analysis. A focus group can be defined as an organized group discussion to facilitate interaction between participants and to explore a particular set of issues (Kitzinger, 2005). The ability of a focus group to encourage interaction between participants allows the exploration of societal societal robustness of measures against local flooding of the A2 due to extreme precipitation. The online session with a duration of 2 hours consists of three parts; the collection of objectives and constraints of stakeholders, a brainstorm for measures against flooding of the A2 due to extreme precipitation in small groups and a discussion on the impact and effort of the gathered measures during the brainstorm. The inclusion of a brainstorm part was chosen to fulfill the the pragmatic consideration to create willingness among participants to participate and to facilitate the design of societal robust Adaptation Pathways. Chapters 6 and 7 provide more details on the qualitative data collection.

# 3

# Case area: the A2 highway between the Vught and Sint-Michielsgestel junctions

## 3.1. Topographic time travel: from Moerasdraak to A2

The A2 highway between the Vught and Sint-Michielsgestel junctions is surrounded by the Bossche Broek, an area that has fulfilled a broad range of functions throughout time; means of defence, natural floodplain, agricultural land, sand extraction, water retention, Natura 2000 and providing the grounds for the A2 highway. The Bossche Broek is a 200 hectare nature reserve in the valley of the river Dommel in the Dutch province of North Brabant. It is directly adjacent to the city centre of 's-Hertogenbosch and the A2 highway (Figure 3.1b). Its name is related to its nature, as a *broek* refers to a low-lying area that remains wet due to seepage or regular flooding of a nearby river. Throughout various centuries, the Bossche Broek functioned as the main means of defence for the city of 's-Hertogenbosch, as its inhabitants could inundate it, thereby keeping enemies outside the city walls (Figure 3.1a). With its *Ondergelopen Weyden* (English: flooded meadows) 's-Hertogenbosch was known as the *Onoverwinnelijke Moerasdraak* (English: invincible swamp dragon) that was part of the Spanish Netherlands. In 1629, the city was laid siege on by the Dutch Republic through the art of hydraulic engineering. The river Dommel and the river Aa, the main streams feeding the Bossche Broek, were diverted by means of a double forty kilometre dike and the Bossche Broek was drained with horse mills. Throughout the 17th and 18th century the case area was part of the Zuiderfrontier, a military defence line (De Monte and Van De Vrede, nd).

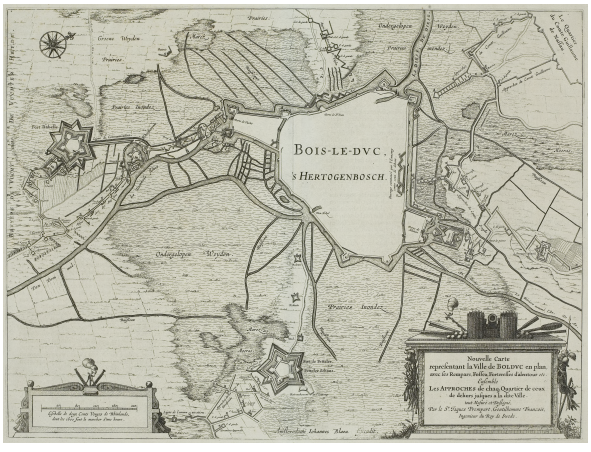


(a) 1629: "Bois-Le-Duc (Dutch: 's-Hertogenbosch) is a fortified city surrounded by fortresses swamps and inundations (Obtained from TU Delft Beeldbank).

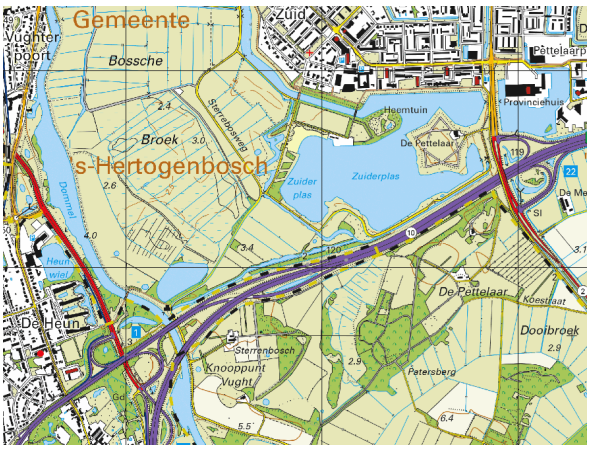


(b) 2020: A2 highway in purple between the Vught junction (west, kmr 121.0) and Sint-Michielsgestel junction (east, kmr 119.0), bordered by the Zuiderplas and the city of 's-Hertogenbosch and crossing the Bossche Broek (Obtained from topotijdreis.nl)

Figure 3.1: Locator maps of case area for the years 1629 and 2020. Both maps show the pentagonal, star-shaped De Pettelaar.

Until the 1970s the Bossche Broek functioned partly as a natural floodplain of the Dommel river. Afterwards, within the framework of agricultural land consolidation, quays were laid around the area and the land was made suitable for agricultural use (Sterk, 2021). In 1995, the former function of the Bossche Broek as inundation area was recalled by the breach of the dike along the Dommel river, causing the Bossche Broek and the A2 to flood and become impassable for two weeks (Figure 3.2). Immediately after this event, a flood protection program called HoWaBo was raised and the Bossche Broek was redesigned into a water retention area in case of high waters; a quay was realized along the highway, inlet works were built and a pumping station was installed to gradually pump the retained water back into the river Dommel (Arcadis, 2006). The A2 cuts the Bossche Broek in half and the southern and northern parts together provide 8.6 million $m^3$ of storage. The northern and southern parts are connected by culverts and two badger tunnels which run underneath the A2. Since the redesign of the Bossche Broek, extreme high water situations have not been encountered (Sterk, 2021).


Figure 3.2: Flooded A2 as a result of a dike breach of the Dommel river in 1995 (Brabants Historisch Informatie Centrum, 1995)

Next to its water retention function the Bossche Broek is part of the Natura 2000 network, a network of nature protection areas for rare and threatened species in the territory of the European Union (Zwart, 2020). Within the Bossche Broek various projects have been released as from 2015 in the context of recovery and reinforcement of the northern Bossche Broek. Deepening and widening of ditches and raising water levels are measures that amongst others should benefit the burnet blue and the large loach. Moreover, along the highway drainage ditches were filled up and infiltration trenches were installed to drain precipitation and seepage slowly between the quays. This was done in order to prevent a decrease in seepage flux [1] in the Bossche Broek which benefits nature.

Currently, the province of Noord-Brabant, in collaboration with Staatsbosbeheer and the Dommel waterboard intend to raise the water level in the Zuiderplas on the southern edge of 's-Hertogenbosch so that the regional seepage water no longer ends up in the Zuiderplas, but in the Bossche Broek, thereby favouring the abiotic conditions for valuable Natura 2000 vegetation (Zwart, 2020). The Zuiderplas is a recreative lake with an average depth of 10 meters and originates from sand extraction activities for the reconstruction of Den Bosch after the Second World War (Figure 3.1b). Moreover, an intention to increase (ground)water levels in the southern Bossche Broek to favour Natura 2000 species exists (Chapter 6).

The A2 route of the HWN connects two powerful Dutch economic regions; Brainport Eindhoven and the Randstad (Tijhuis and Beentjes, 2019). In the 1960s a motorway around 's-Hertogenbosch was regarded necessary and a four-lane thruway, having two lanes for traffic in each direction, was therefore built. As a result of the expansion of 's-Hertogenbosch and an increase in traffic congestion, the highway has been expanded to a ten-lane road throughout the years, having five lanes for traffic in each direction. The final road widening on the northern lanes has been finished in 2010 and in 2013, a final lane was added to the southern lanes. The Vught junction (Figure 3.1b) connects the A2 with the A65 into the direction of the city of Utrecht and is fully connected to the Vughterweg (a bypass) by a partial cloverleaf interchange. At the Sint-Michielsgestel junction (3.1a), the parallel southern and northern lanes of the A2 are connected to the N617 Bosschebaan by a partial cloverleaf interchange as well (Tijhuis and Beentjes, 2019).

[1] Seepage is the upward flow of groundwater, because the hydraulic head at some depth has a higher level than the water table (Hendriks, 2010)

## 3.2. Elevation and geomorphology

The natural elevation and soil properties can be related to the geomorphological formation of the case area, which influences the hydrological system in the case area. Figure 3.3a reveals that the Bossche Broek and the case highway are relatively low-lying elements compared to the rest of the surrounding landscape. Whereas the ground level in the area surrounding the A2 under consideration (marked by case highway in Figure 3.3a) varies between approximately +2.3 m NAP in the northern Bossche Broek and +6.8 m NAP just south of the A2, the A2 under consideration is located at an elevation of approximately NAP +3.1 m to NAP +4.2 m. Moreover, a relatively low-lying curvature can be observed south of the A2, which can be regarded a remnant of a meandering channel (Figures 3.3a and 3.3b).

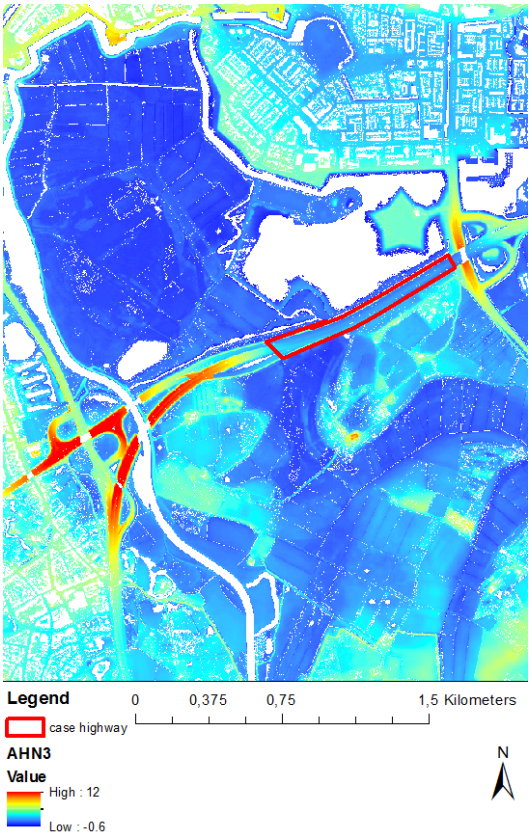


(a) Elevation levels of case area in mNAP (AHN3)

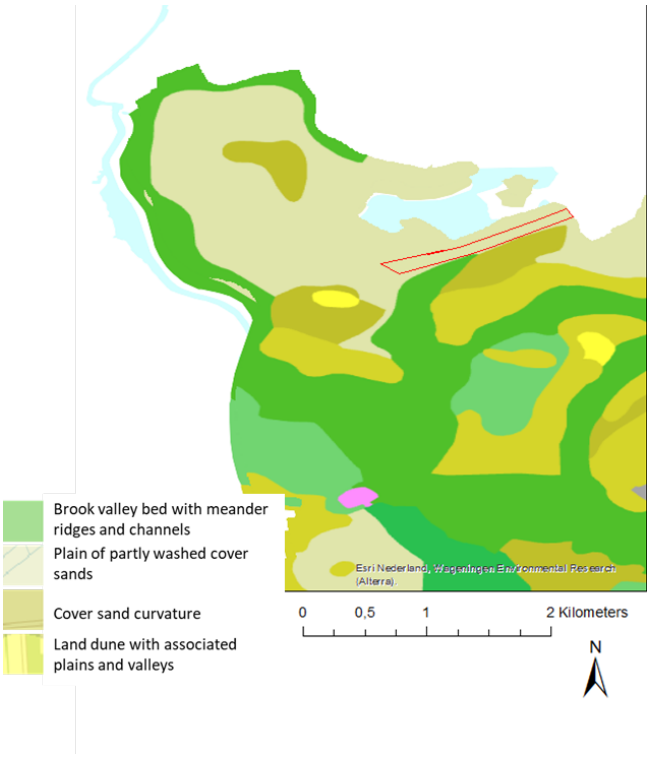


(b) Geomorphological classificiation of case area (BRO PDOK)

Figure 3.3: Ground level and geomorphology

Regarding the geomorphological formation of the case area, 's-Hertogenbosch is located in the Roer Valley Graben, which has actively subsided by approximately two kilometres since the late Oliogocene (25 million years BP) (IVN, 2012). During the Pleistocene, local rivers deposited the sandy formation of Stramproy on top the confining clayey Waalre formation layer, after which the Rhine and Meuse deposited the coarse sandy Sterksel Formation (Table 3.1). During the last glacial period, the Weichselien, the Netherlands was subject to polar winds, which caused the eolian deposits to be blown away from the North Sea bottom and deposit as cover sand ridges and loess. This deposition is called the Boxtel formation and in the case area a fluvial clay layer with a relatively low permeability is present in it, thereby confining the aquifer below (Table 3.1). An aquifer can be depicted as a subsurface layer that easily stores and transmits groundwater (Hendriks, 2010). The east-west oriented sand ridges were located perpendicular to the north-south sloping landscape due to the direction of soil subsidence and the flow path of the river Dommel. Therefore, drainage by the river Dommel was restricted and as a consequence water from the river Dommel was retained, allowing swamps to develop on top of the Pleistocene depositions. Brooks and rivers interrupted the sand ridge at several locations and the remnants of cover sand now form the relatively high cover sand curvatures (Figures 3.3a and 3.3b). The project area is thus situated in a transition zone between the relatively high sandy soils of the province of Noord-Brabant and the Meuse system. The Holocene deposits cover approximately the top 5

metres below ground level (Table 3.1). A few fluvial clay, peat and loam layers interrupt this sandy top layer locally. In the research by Zwart (2020) a saturated hydraulic conductivity of the Holocene top layers of 0.1 to 2.04 m/d was determined using a falling head method and the grain size distribution. Moreover, the soil was classified as loamy sand to sandy loam. It can be hypothesized that relatively coarse deposits with higher hydraulic conductivities will be encountered in the outer bends of the remnants of meandering channels and the cover sand curvatures, whereas finer deposits with lower hydraulic conductivities will be encountered in the inner bends of the meandering channels (Figure 3.3b). At the location of the A2, the natural underground has been modified by the addition of non-natural deposits, because the verges along the A2 have been raised manually. The raised verges consist of moderate to very fine sands, interrupted by clay layers in the top 2 meters (Zwart, 2020).

Table 3.1: Stratigraphic nomenclature of soil in the case area as from the Pleistocene (BRO Regis II).

| **Stratigraphic nomenclature by depositional setting** | **Bottom stratigraphic layer [m NAP]** |
|---|---|
| *Holocene deposits (sand interrupted by fluvial clay, peat and loam layers)* | -2 |
| *Boxtel formation (sand)* | -12 |
| *Boxtel formation (clay)* | -18 |
| *Boxtel, Sterksel and Stramproy formations (sand)* | -90 |

## 3.3. Regional water system

### 3.3.1. Groundwater

The regional groundwater system is illustrated in Figure 3.4, which reveals that the overall groundwater flow is oriented from southeast to northwest. This is the case for both the phreatic as well as the confined aquifer. The presence of a nearly continuous little permeable clay layer at a depth of approximately -16 m NAP allows seepage to occur, i.e. upward flow when the water table and hydraulic heads at different depths do not coincide (Hendriks, 2010). Due to the aforementioned geologic and geomorphologic conditions the water will flow from the southern higher sandy areas towards the northern, relatively low-lying areas near 's-Hertogenbosch. Water that has infiltrated in the more upstream areas passes the poorly permeable layer and has a relatively high hydraulic head. As a result, the case area is prone to diffuse seepage through the confining clayey Boxtel formation layer. Limited knowledge exists on the magnitude of the upward seepage flux, but it is expected to be small when regarding results from the study by Zwart (2020). During the summer of 2020 a weir in the Bossche Broek was temporarily raised to test whether the seepage flux would cause the surface water level in the Bossche Broek to rise. The latter was not the case, since the surface water level remained constant. Therefore it can be hypothesized that the upward seepage flux is very small, i.e. equal to the evaporation.

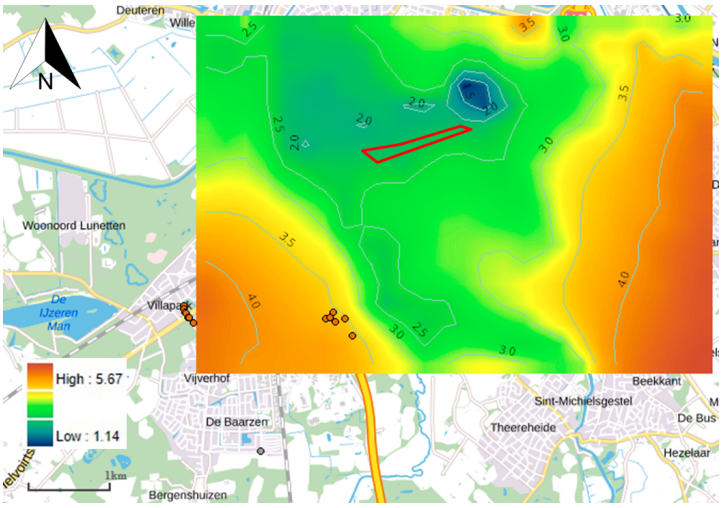


Figure 3.4: Hydraulic head contours [m NAP] in the phreatic aquifer in 2005, with measurement locations in orange. The red area coincides with the A2 highway (TNO, nd).

### 3.3.2. Surface water

The surface water system in the project area consists of ditches regulated by means of a pumping station (Figure 3.5). The Segers pumping station pumps surface water from the Dungense ditch into the Dommel river. The Dungense ditch runs parallel to the A2 and drains water from the A2, the Bossche Broek and an upstream agricultural area and has a water level of 1.90 m+NAP under normal conditions. The Segers pumping station regulates this level set by the Dommel waterboard by starting to pump at a level of 2.00 m +NAP and switching off again at a level of +1.90 m NAP. In practice, the 1.90m NAP is not always maintained (area administrator waterboard De Dommel, 2021). A weir between the surface water in the Bossche Broek (including the Zuiderplas) and the Dungense Ditch is present (Figure 3.5) and has throughout its past always been open, allowing for free exchange of water in the Bossche Broek and the Dungense ditch (Zwart, 2020).

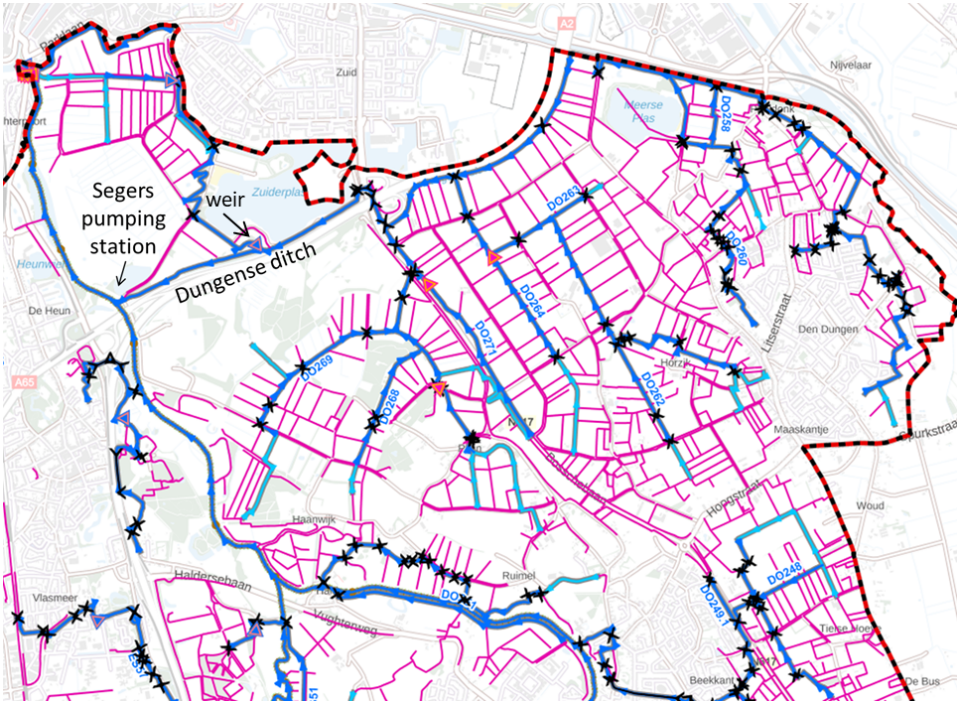


Figure 3.5: Catchment of the Segers pumping station with in blue A-watercourses and in pink B-watercourses (legger from waterboard De Dommel)

## 3.4. Local water system; catchment of the road

### 3.4.1. Typical cross-sections

Two typical cross-sections of the case highway can be illustrated, regarding the cross-slope of the highway, the presence of water retaining sheet piles, groundwater measurements, the type of manholes and the relative location of the stormwater sewer system and drainage pipes underneath the road. To start with, the cross-slope of the A2 changes when travelling when traveling to Utrecht. Between hectometre post 119.5 and 120.0 both lanes of any cross-section along the A2 slope from south to north (Figure 3.6). Between hectometre post 119.0 and 119.5 the A2 runs down from the centre verge to both side verges (Figure 3.7). Secondly, water retaining sheet piles have been constructed along the entire southern verge, but not along the entire northern verge of the A2 (Figures 3.7 and 3.6). The sheet piles reach a depth of a few meters into the ground, up to a maximum of approximately 8 m and therefore do not reach the depth of the confined aquifer (Table 3.1). As the regional groundwater flow in the unconfined aquifer is oriented from southeast to northwest, the sheet piles will influence the local groundwater situation and provide a backwater effect on the southern side of water retaining sheet piles in the southern verge. The groundwater measurements (indicated by PASM in Figures 3.7 and 3.6) will be discussed in section 2. Differences in the relative location of the stormwater sewer system and drainage pipes will be discussed in section 3.4.2.

Similarities in the cross-sections can be found in the presence of asphalt, a road foundation and underground structures. Figures 3.7 and 3.6 reveal that double-layered, porous asphalt (ZOABTW) constitutes the top of the asphalt layer of the case study area. According to research by Wareco (Zwart, 2020) the double-layered porous asphalt has a total thickness of 11 cm (3 cm of fine asphalt on top of an 8 cm of coarse asphalt) and is situated on top of a thicker layer of an old, impermeable asphalt layer (thickness values of 37cm and 27 cm were found). Underneath the asphalt of the A2, a soil package of stabilization sand (approximately 0.33 m), mixed and concrete granulate (0.30 to 0.45 m) and a sand bed (0.35 to 0.50 m) are present (Zwart, 2020). Due to the jamming of drills the exact dimensions are not known (Zwart, 2020).

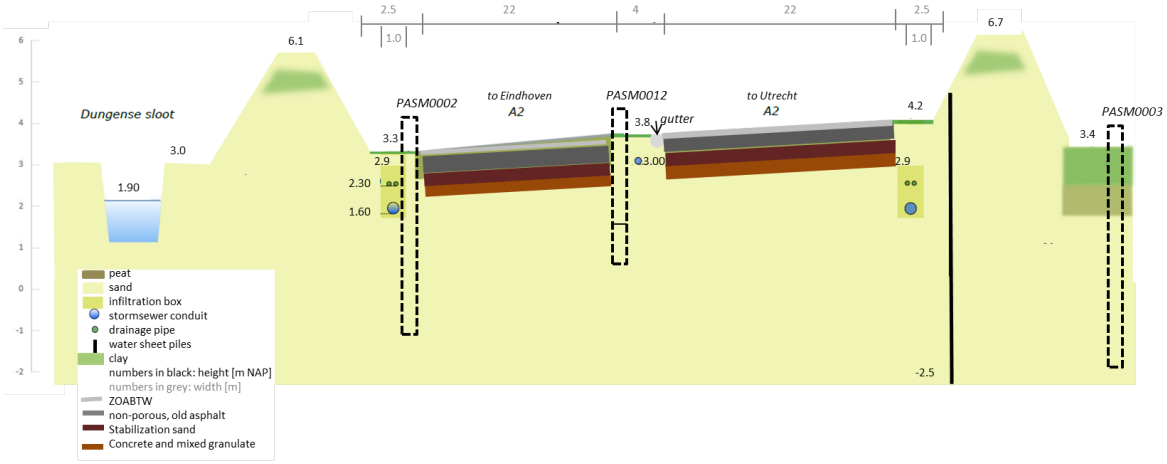


Figure 3.6: Schematic representation of the A2 cross-section near hectometre post 119.95 (representative for the A2 between hectometre posts 119.5 and 120.0). The filter depths of the piezometers (PASM..) are indicated by the dotted black lines.

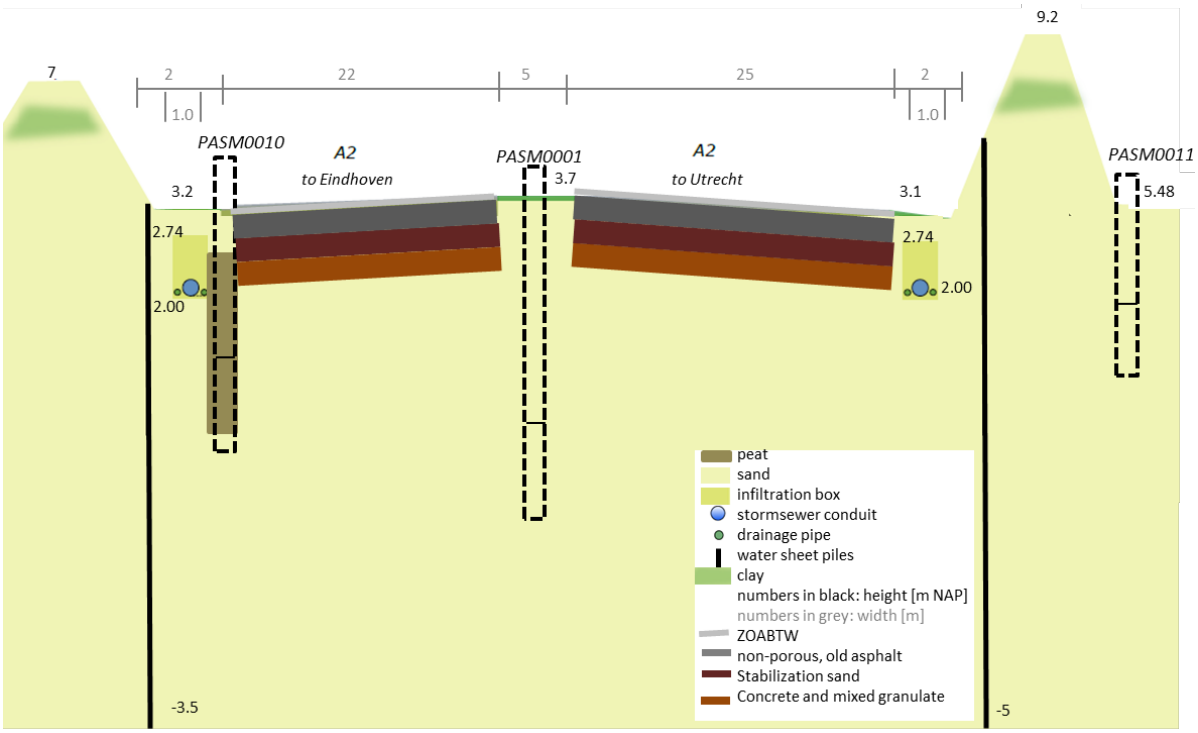


Figure 3.7: Schematic representation of the A2 cross-section near hectometre post 119.1 (representative for the A2 between hectometre posts 119.0 and 119.5). The filter depths of the piezometers (PASM..) are indicated by the dotted black lines

### 3.4.2. Sewer system

The sewer system design of the road is featured by a freely draining stormwater sewer towards various outflow locations on the Dungense ditch (Figure 3.8). The stormwater sewer system consists of stormwater conduits (impermeable) and drainage pipes (permeable) and can be encountered in the northern verge, in parts of the central verge and in the southern verge of the A2 between hectometre posts 120.2 and 119.0 (Figure 3.8).The sewer system in the northern verge originates from 2010 and the sewer system in the central and southern verges originates from 2012. These years correspond with the final road widening events (section 3.1).

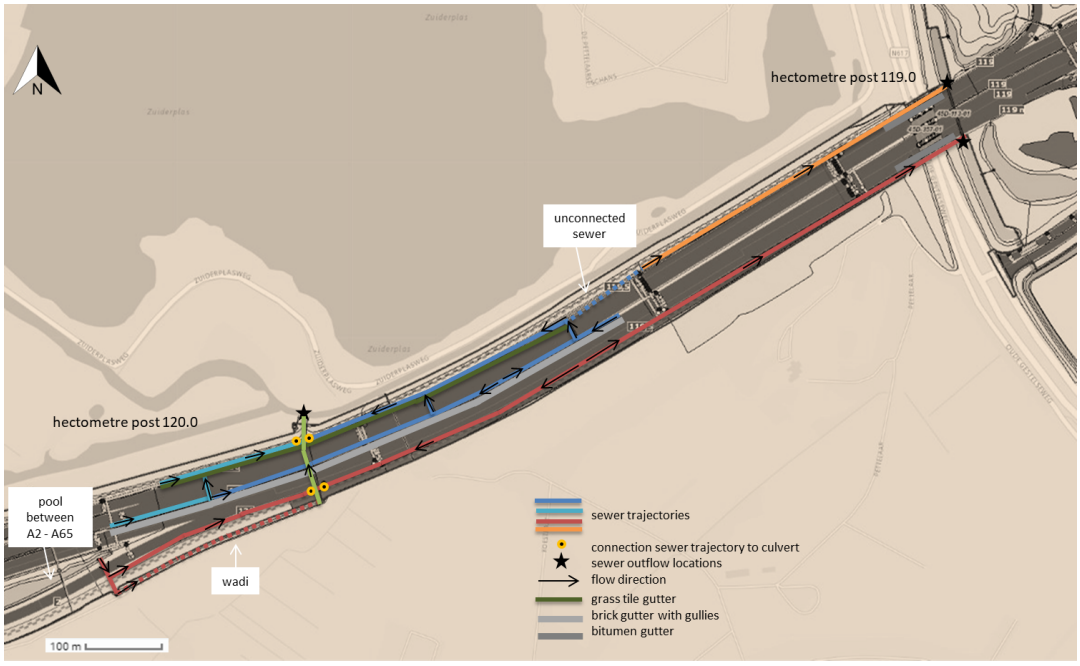


Figure 3.8: Schematic representation of sewer system (after Field visit 24-02-2021, Zwart, 2020; Kerngis Droog, 2021)

The stormwater system consists of several trajectories (Figure 3.8):

1. The blue trajectory discharges to the sewer outflow location on the Dungense ditch near hectometre post 119.9. In the northern verge of the blue trajectory, two drainage pipes and a stormwater conduit run parallel to the A2 (Zwart, 2020). The invert levels of the drainage pipes are relatively high compared to the invert levels of the stormwater conduit (Figures 3.6 and 3.9). The dimensions of the stormwater system of this trajectory are relatively large compared to the other trajectories (Zwart, 2020; Kerngis Droog, 2021). In the central verge only stormwater conduits are present, which are connected to the northern verge by means of conduits running underneath the northern lane at several locations (Zwart, 2020, Kerngis Droog, 2021). The light and dark blue trajectories discharge to the main culvert (Figure 3.8) from the west and east respectively. The dashed line indicates an unconnected sewer trajectory, which is characterized by the absence of a stormwater sewer conduit and the presence of two unconnected drainage pipes. Thereby, this part of the stormwater sewer system does not fulfil a dewatering function.

Figure 3.9: In the blue trajectory the drainage pipes are located above the stormwater conduit (below water level in picture) (Zwart, 2020).

In the northern verge a grass tile gutter is directly adjacent to the northern lane. Precipitation can infiltrate in this gutter, thereby reaching an infiltration trench containing the drainage pipes and stormwater conduits. Water that is drained by the permeable drainage pipes will be collected in the stormsewer conduits and will be transported towards the Dungense ditch (law of communicating vessels). Moreover, it is important to note that the manholes along the blue trajectory are characterized by holes, through which direct inflow into the stormsewer system is facilitated.

In the central verge a brick gutter with gullies is directly adjacent to the southern lane. The brick gutter collects runoff from the southern lane and the gullies allow collection of water into the stormwater conduits in the central verge. The stormwater conduits in the central verge thus do not collect infiltrating water, but direct runoff from the southern A2 lane.

2. The orange trajectory discharges to the northern sewer outflow location on the Dungense ditch near hectometre post 119.0 and is characterized by two drainage pipes and a stormwater conduit which run parallel to the A2 (Zwart, 2020). The invert levels of the drainage pipes are similar to the invert levels of the stormwater conduit (Figures 3.7 and 3.10).

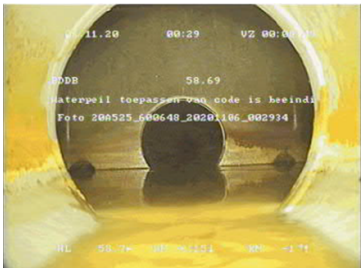

Figure 3.10: In the orange trajectory the drainage pipes are located at the same invert level as the stormwater conduit (Zwart, 2020).

Figures 3.8 and 3.11 reveal that a bitumen gutter with mounting walls and gullies is present adjacent to the northern lane. The bitumen gutter collects runoff from the northern lane and the gullies allow collection of water into the stormwater conduit. The mountain wall holds back runoff from the verge to enter the gutter. The remainder of the orange trajectory does not have a gutter, nor gullies. The manholes that the orange trajectory is characterized by do not contain holes. Therefore, stormwater drainage is reliant on the infiltration of precipitation in the northern verge, thereby reaching an infiltration trench containing the drainage pipes and stormwater conduits. As a consequence, water collected by the permeable drainage pipes through infiltration will be transported towards the Dungense ditch by means of the impermeable stormwater conduits, which act as collection pipes for the water intercepted by the drainage pipes (law of communicating vessels).


Figure 3.11: Bitumen gutter with rectangular gutter in northern verge near junction Sint-Michielsgestel (Field visit 24-02-2021).

3. The red trajectory discharges to the southern sewer outflow location on the Dungense ditch near hectometre post 119.0 and to the sewer outflow location on the Dungense ditch near hectometre post 119.9. Whereas the southern stormwater system was not inspected (Zwart, 2020), a system of two drainage pipes and a stormwater conduit running parallel to the A2 is expected to be present. The red trajectory discharges to the main culvert (Figure 3.8) from the west and from the east. Next to precipitation on the road and in the verges, this trajectory transports water from a pool between the A2 and A65 towards the outflow location of the Dungense sloot near hectometre post 119.9. Moreover, the red trajectory is characterized by a wadi which is located outside the raised verges to the south of the A2 between hectometre posts 120.2 and 119.9 (Figures 3.12a and 3.12b). Field investigation (24-2-2021) revealed that the wadi was considerably full of water and thereby functions as a drainage ditch, instead of a percolation trench (Figure 3.12a). At the connection to the culvert at hectometre post 120.2, the wadi had some significant amount of sludge and the culvert appeared to be nearly submerged (Figure 3.12a). These observations imply that the transport from the pool between the A2 and A65 towards the wadi is hardly possible. Moreover, one could speak of deferred maintenance, as the sludge layer results in clogging of the wadi, preventing infiltration of water into the soil. At the connection of the wadi to the main culvert at hectometre post 119.9, one can hear water flowing into the culvert, implying discharge from the wadi towards the northern outflow location on the Dungense ditch near hectometre post 119.9. The functioning of the connection between the wadi and the main culvert at this location however could not be observed, due to the overgrown wadi (Figure 3.12b). Near the Sint Michielsgestel junction a bitumen gutter with mounting walls and gullies is present adjacent to the southern lane. The gutter with gullies is similar to Figure 3.11. The bitumen gutter collects runoff from the northern lane and the gullies allow collection of water into the stormwater conduit. The mountain wall holds back runoff from the verge to enter the gutter. The remainder of the red trajectory does not have a gutter, nor gullies. Therefore stormwater drainage is reliant on the infiltration of precipitation in the southern verge, thereby reaching an infiltration trench containing the drainage pipes and stormwater conduits. As a consequence, water collected by the permeable drainage pipes through infiltration will be transported towards the Dungense ditch by means of the impermeable stormwater conduits, which act as collection pipes for the water intercepted by the drainage pipes (law of communicating vessels).

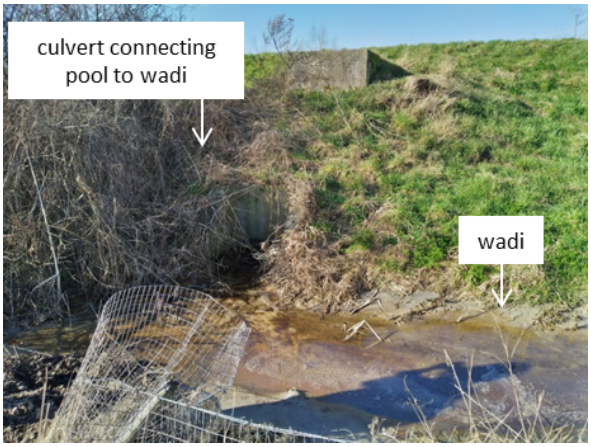


(a) Outflow location of culvert connecting the pool between the A2 and A65 to the wadi. Sludge is present (Field visit 24-02-2021).


(b) Overgrown wadi at location of culvert which connects the wadi to the Dungense sloot (Field visit 24-02-2021).

Figure 3.12: Wadi south of A2

The main culvert (green in Figure 3.8) that passes underneath the A2 near hectometre post 119.9 connects the red and blue trajectories and drains the water intercepted by these trajectories towards the Dungense sloot (Figure 3.8). Field investigation (24-2-2021) confirmed the presence of a non-return valve at the outflow location and the presence of a trash rack around the outflow location (Figure 3.13a). The culvert is separated from to the drainage pipes and stormwater conduits in the side verges by means of a mounting wall (Figure 3.13b). The presence of a mountain wall probably enables the settlement of contaminants from the A2 into the sewer system, before being released into the Dungense ditch. The level of this mountain wall is probably set at +1.85 m NAP (As-Built) and is thus slightly lower than the target level of +1.90 m NAP for the Dungense ditch. The relative location of the target level of the Dungense ditch and the mountain walls can be considered

peculiar because it is a freely draining system, but the presence of a return valve prevents water from flowing from the Dungense sloot into the stormwater system. Due to the mounting walls, the stormwater sewer system of the blue trajectory is always partially filled with water up to a level of +1.85 m NAP. This results in a loss of storage capacity of the stormwater conduit system. Therefore, there is always a limited storage capacity in the system for precipitation from the road. In the event of a peak shower, this could result in the malfunctioning of the stormsewer system.


(a) Outflow location of stormwater sewer system A2 to Dungense sloot near hectometre post 119.9

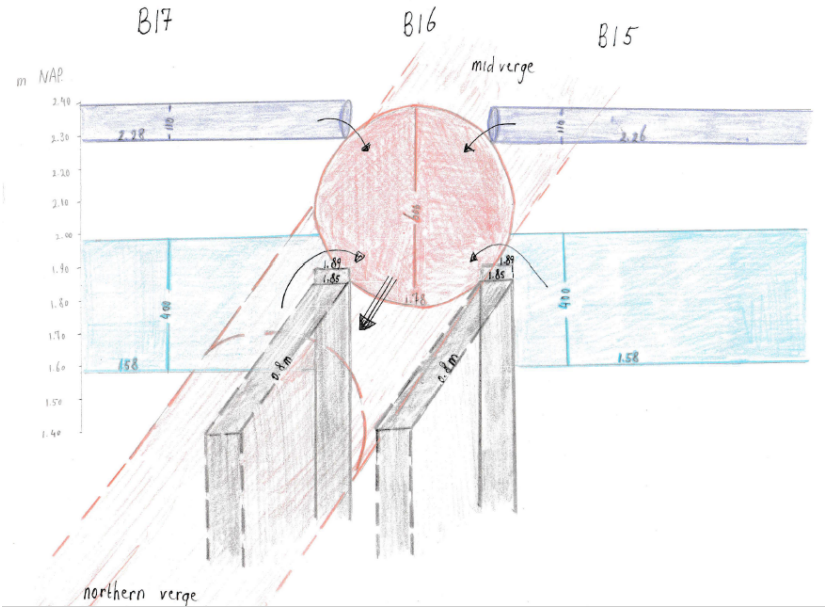


(b) Mounting wall schematisation at connection northern verge stormwater sewer system to main culvert. Purple: drainage pipes, blue: stormwater conduits, black: mounting walls, brown: main culvert (perpendicular to other conduits)

Figure 3.13: Main culvert

Infiltration trenches are present in the northern verge. Infiltration trenches are filled with course stones and thereby create a reservoir (Van De Ven, 2009). The packet of reservoir rock material is surrounded by a filtermat to prevent washing in of surrounding soil. The trenches should be positioned at least above the highest groundwater level (Van De Ven, 2009). In the Wareco investigation two drillings showed the presence of infiltration trenches at a depth of 46 cm and 41 cm below ground level. The trenches consist of gravel and gravel diameters of at least 5-8 cm, with outliers up to 12-13 cm, were encountered. Whereas the presence of gravel made drilling towards the bottom of the drainage trenches impossible, it is expected that in the blue trajectory the drainage pipes are not situated at the bottom of the infiltration trench, due to the relative location of the drainage pipes compared to the stormwater conduit (Figure 3.6). On the other hand, it is expected that in the orange trajectory, the drainage pipes are situated at the bottom of the infiltration trench, together with the stormwater conduit (Figure 3.7).

### 3.4.3. Groundwater

In the case area various monitoring wells have in the past or in the present measured groundwater heads. At the end of October 2019, Brabant Water positioned several phreatic piezometers near the A2 and in the southern part of the city of 's-Hertogenbosch to collect hourly measurements to predict the effect of raising the Zuiderplas (PASM0001, PASM0002 and PASM0003 in Figure 3.14). In November 2020, on behalf of Rijkswaterstaat, three extra piezometers have been added near the A2 to study the drainage depth underneath the A2 (PASM0010, PASM0011 and PASM0012 in Figure 3.14). These piezometers collect hourly measurements as well. Piezometers PASM0002 and PASM0010 measure the phreatic groundwater head in the northern verge, directly adjacent to the A2 highway, near hectometre post 119.9 and 119.1 respectively. Piezometers PASM0012 and PASM0001 measure the phreatic groundwater head in the central verge, near hectometre post 119.9 and 119.1 respectively. At the location of PASM0012, however, measurements have registered only for the short period of a few days, due to a flat battery of the groundwater head transmitter. Piezometers

PASM0003 and PASM0011 measure the phreatic groundwater head at the south of the raised verges, outside of the sheet piling, to measure the backwater effect at the sheet piling (Figures 3.7 and 3.6). It can be noted that PASM0003 is located in the remnant from a meandering channel (Figure 3.3a).

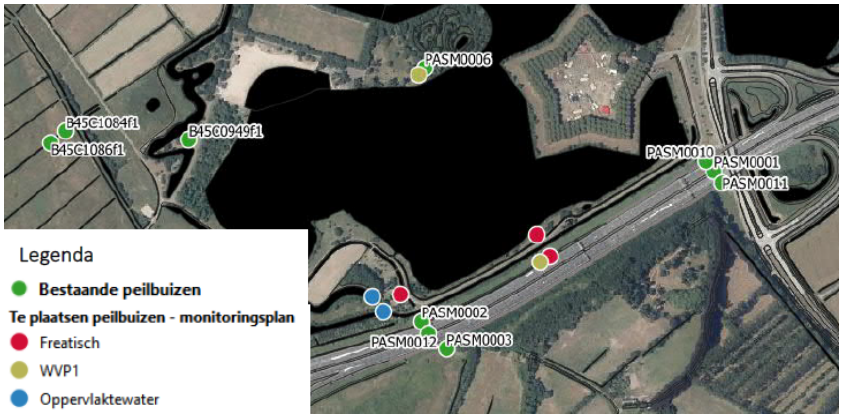


Figure 3.14: Location current and future piezometers (Zwart, 2020)

At cross-section 119.1, the measurements of PASM0010, PASM0001 and PASM0011 can be studied (Figures 3.7 and 3.15). Throughout the measurement period, a backwater effect by the sheet piling ranging between 0 and 15 centimetres can be observed. The backwater effect can be drawn from comparison between PASM0010 and PASM0011, assuming that the measurements of PASM0010 coincide with groundwater heads in the southern verge directly adjacent to the A2. Regarding the presence of sheet piling on both sides of the A2 at this hectometre post, the sloping of the A2 towards the verges and the similar widths of the southern and northern lane, this assumption can be justified. Comparing PASM0010 and PASM0001 reveals the absence of bulging underneath the highway. Instead, the groundwater level near PASM0010 is overall a few centimetres higher than the groundwater head at PASM0001. It can be hypothesized that this is related to the infiltration of water in the side verges.

At cross-section 119.95, the groundwater fluctuation is more significant, as the groundwater head difference between PASM0003 and PASM0002 is approximately 25 cm. Horizontal seepage through the remnant of the meandering river channel can cause this. It is hard to judge whether a bulging effect is significant, as the measurement series of PASM00012 is very short.

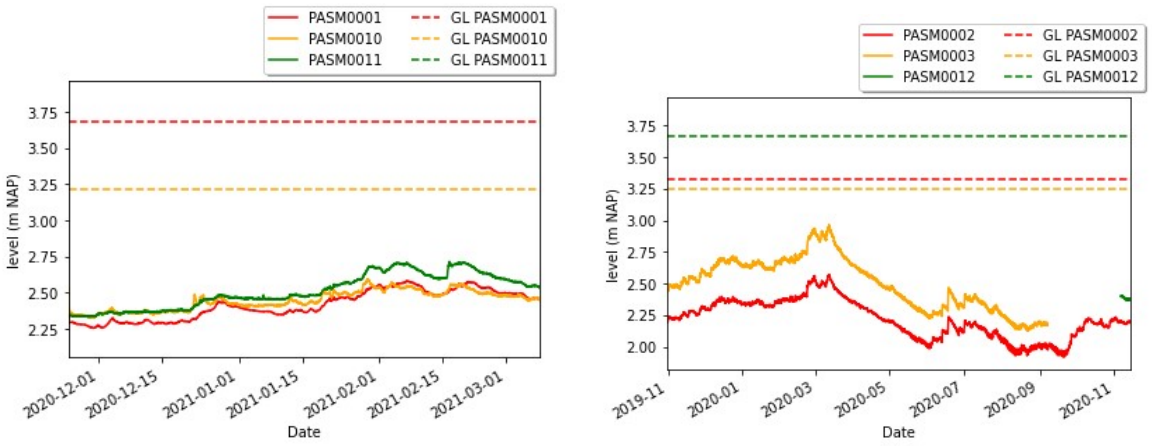


Figure 3.15: Groundwater time series and groundlevel (GL) of PASM0001, PASM0002, PASM0003, PASM0010, PASM0011 and PASM0012 (Obtained from Wareco Water Data and Hydronet). GL of PASM0011 is at 5.5 m NAP and is therefore not represented in the figure.

## 3.5. Stakeholders and roles

Regarding the A2 and its surroundings, various stakeholders can be identified that fulfill various roles. Appendix 6 and Chapter 7 elaborate on objectives and constraints of the stakeholders.

In order to fulfill their role as asset manager the governmental organisation Rijkswaterstaat must ensure the present and future continuation of the operational functions of the HWN and therefore various performance agreements, decrees and requirements have been defined (Chapter 7). The maintenance costs for the HWN amounted to approximately € 825M in 2018 and additionally € 1,163M was spent on new construction projects (Bles et al., 2020). In the case area, Rijkswaterstaat is responsible for the operation of the A2. This amount is in the same order of magnitude as the economic costs associated with changes in traffic and transport due to a single extreme precipitation event causing water nuisance in the Netherlands (section 1.1.2).

The responsibilities of the Province of Noord-Brabant include spatial planning and environmental- and nature management (Mostert, 2019).

Waterboards De Dommel and Aa en Maas are responsible for regional surface water management, regulation of groundwater extractions, management of flood defenses, and water treatment (Mostert, 2019). In and around the case area (Figure 3.16), the waterboards fulfill management tasks regarding HoWaBo (waterboards Aa en Maas and De Dommel) and the Dungense ditch (waterboard De Dommel).

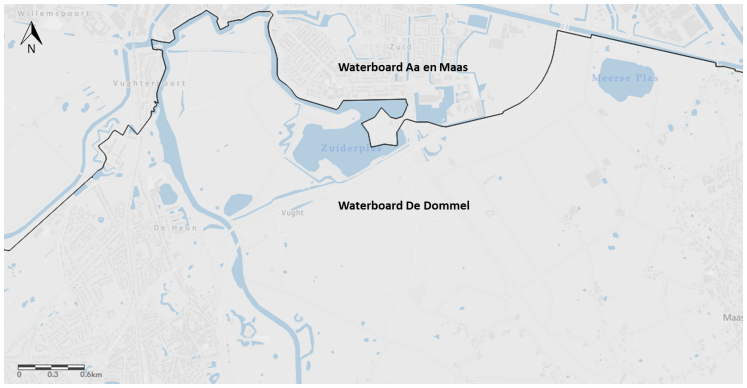


Figure 3.16: Boundaries between waterboards De Dommel and Aa en Maas. The case area lies within the area of Waterboard De Dommel (Kerngis Droog, 2021).

Staatsbosbeheer is a legal entity with a statutory task, receiving subsidy from the Provinces. The organization is established by law and as an independent administrative body of the national government, falling within the domain of the Ministry of Agriculture, Nature and Food Quality (LNV). The statutory task is to manage and sustainably bring the sites to societal use. Staatsbosbeheer has a broad social role and in this respect cannot be characterized as a nature conservation organization, but rather as a green utility company. Staatsbosbeheer plays an important role in the responsibility of the Ministry of Agriculture, Nature and Food Quality for achieving international goals such as Natura 2000. Thereafter, Staatsbosbeheer performs nature restoration tasks in the Bossche Broek in the context of nature restoration Natura 2000.

Brabants Landschap is a Public Benefit Institution for nature protection in the province of Noord-Brabant. The own income of Brabants Landschap consists of revenues from the management of nature areas and buildings, contributions, contribution of the National Postcode Lottery, estates, donations and gifts, interest and investments, purchase subsidies, management subsidies, project subsidies and grants for Landscape Management. In the case area Brabants landschap is responsible for preserving estates.

# 4

# Hydrological model: time series analysis

## 4.1. Input data

Three groundwater head time series from monitoring wells in the case area constitute the output signal of the TFN model and precipitation and evaporation time series of the Gilze-Rijen automatic weather station form the stresses of the TFN model (Figure 4.1). The Gilze-Rijen automatic weather station is chosen as the source for two main reasons; proximity to the case area and measurement frequency;

1. The Gilze-Rijen automatic weather station is at a relatively close distance of 28.81 kilometres to the south-west of the case area. Regarding the proximity to the case area and the prevailance of south-western winds in the Netherlands (KNMI), precipitation events that are measured at the Gilze-Rijen automatic weather station are likely to occur in the case area as well. As a consequence of the prevailing wind direction, the automatic weather station of Gilze-Rijen is preferred over other nearby automatic weather stations.

2. Since the monitoring wells measure the groundwater level hourly, it makes sense to aim at obtaining the same measurement frequency for the input stresses. Moreover, regarding the quick rainfall-runoff processes induced by the presence of the pavement in the case area (Van De Ven, 2009), i.e. the highway, and the relatively shallow groundwater tables that characterize the case area (section ), fast groundwater recharge processes are expected. Therefore, an hourly measurement frequency of precipitation series is desired in order to evaluate the response of the peak flow on the groundwater level. The automatic weather stations of the Dutch meteorological institute, such as the Gilze-Rijen station, measure precipitation on an hourly basis. On the contrary, manual rain gauges from the Dutch meteorological institute measure precipitation on a daily basis. Even though some manual rain gauges are closer to the case area than the automatic Gilze-Rijen weather station, the Gilze-Rijen station is preferred as a source for the stresses due to its measurement frequency.

### 4.1.1. Visual check of input data

To start with, Figure 4.1 reveals a significant difference between the length of the groundwater head time series and the lengths of the precipitation and evaporation time series. A potential pitfall of time series analysis through TFN modelling is the requirement of sufficiently long time series (Collenteur et al., 2019). Von Asmuth (2012) states that ideally the length of the start-up period is as long as the memory of the groundwater system, implying that an observation series with a length of several times the memory is desired. However, no consensus has been reached on this topic yet and research is needed on determination of the effect of the length of the used time series on the accuracy of groundwater head estimation through TFN modelling (Collenteur et al., 2020).

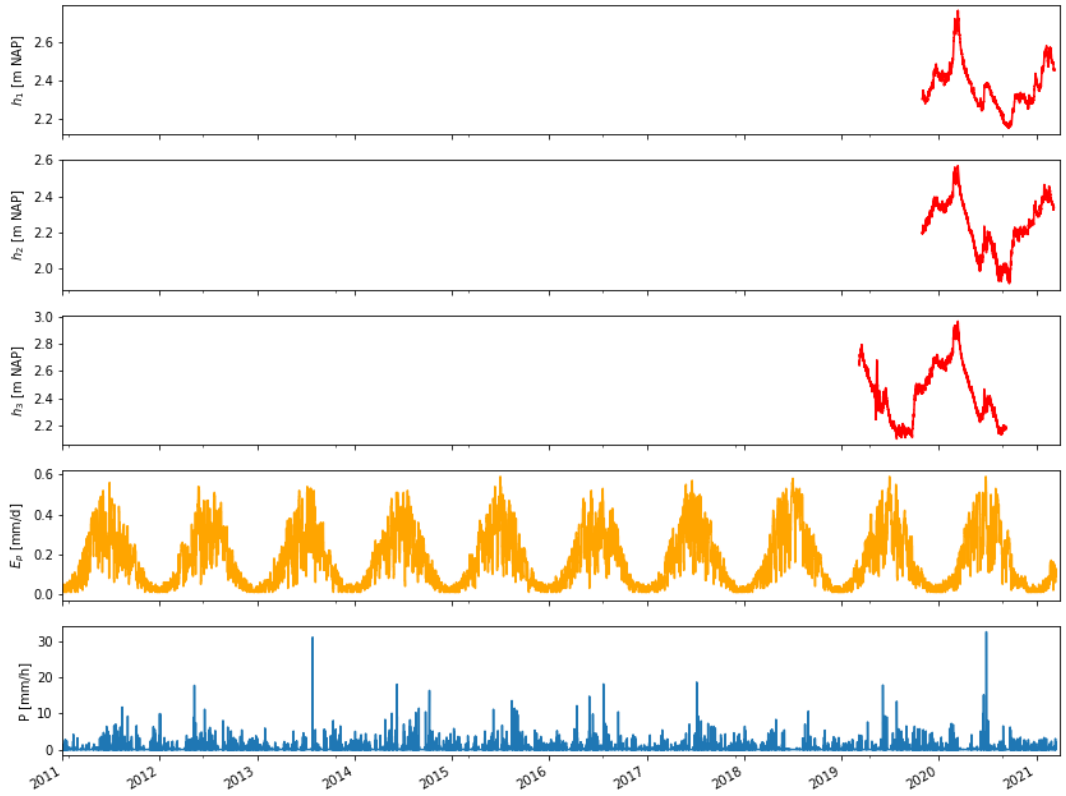


Figure 4.1: Time series of observed groundwater heads $h_1$, $h_2$ and $h_3$ associated with monitoring wells PASM0001, PASM0002 and PASM0003 in Figures 3.7 and 3.6 and time series of potential evaporation $E_p$ and precipitation $P$ from the automatic Gilze-Rijen weather station. $h_1$, $h_2$ and $h_3$ and $P$ have an hourly observation frequency and $E_p$ is observed daily. $h_1$, $h_2$ and $h_3$ have an observation length of 495, 493 and 550 days respectively, whereas $P$ and $E_p$ have an observation length of approximately 10 years.

Secondly, Figure 4.2, an enlarged version of Figure 4.1, visualizes trends;

1. Figure 4.2 reveals that $h_1$, $h_2$ and $h_3$ (associated with PASM0001, PASM0002 and PASM0003 respectively) overall show comparable fluctuations at the same moment in time. Therefore it can be hypothesized that the groundwater levels on the whole respond in a similar way to the stresses at the various locations along the highway in the case area. Whereas the patterns are similar, the groundwater levels are different. The differences between the locations may be owed to differences in the fractions of precipitation that infiltrate into the ground, differences in physical aspects of the soil and to influences of nearby objects such as the presence of sheet piles and storm sewer and drainage systems.

2. The relation between the groundwater levels and evaporation measurements seems physically plausible, because seasonal variation can be detected. The seasonal variation reveals the simultaneous occurrence of high potential evaporation $E_p$ amounts and relatively low groundwater levels during summer and the simultaneous occurrence of low evaporation amounts and relatively high groundwater levels during winter. It is important to note that the potential evaporation indicates the upper boundary of evaporation, because it is not constrained by the availability of water (Savenije, 2006). The actual evaporation will therefore always be lower than the potential evaporation.

3. In contrast to the potential evaporation, the groundwater head and precipitation time series reveal non-constant, irregular patterns. Therefore, it can be hypothesized that precipitation events cause an irregular groundwater head response. Examples of this hypothesis are the relatively high groundwater levels in March 2020, which might be the result of a antecedent, relatively rainy period and the sudden increases in groundwater levels in July 2020 after relatively large precipitation events.

Thirdly, the visual check allows identification of white noise. Figure 4.2 reveals a peculiar fluctuation in the $h_3$ groundwater level head in May 2019. This might be a measurement error.

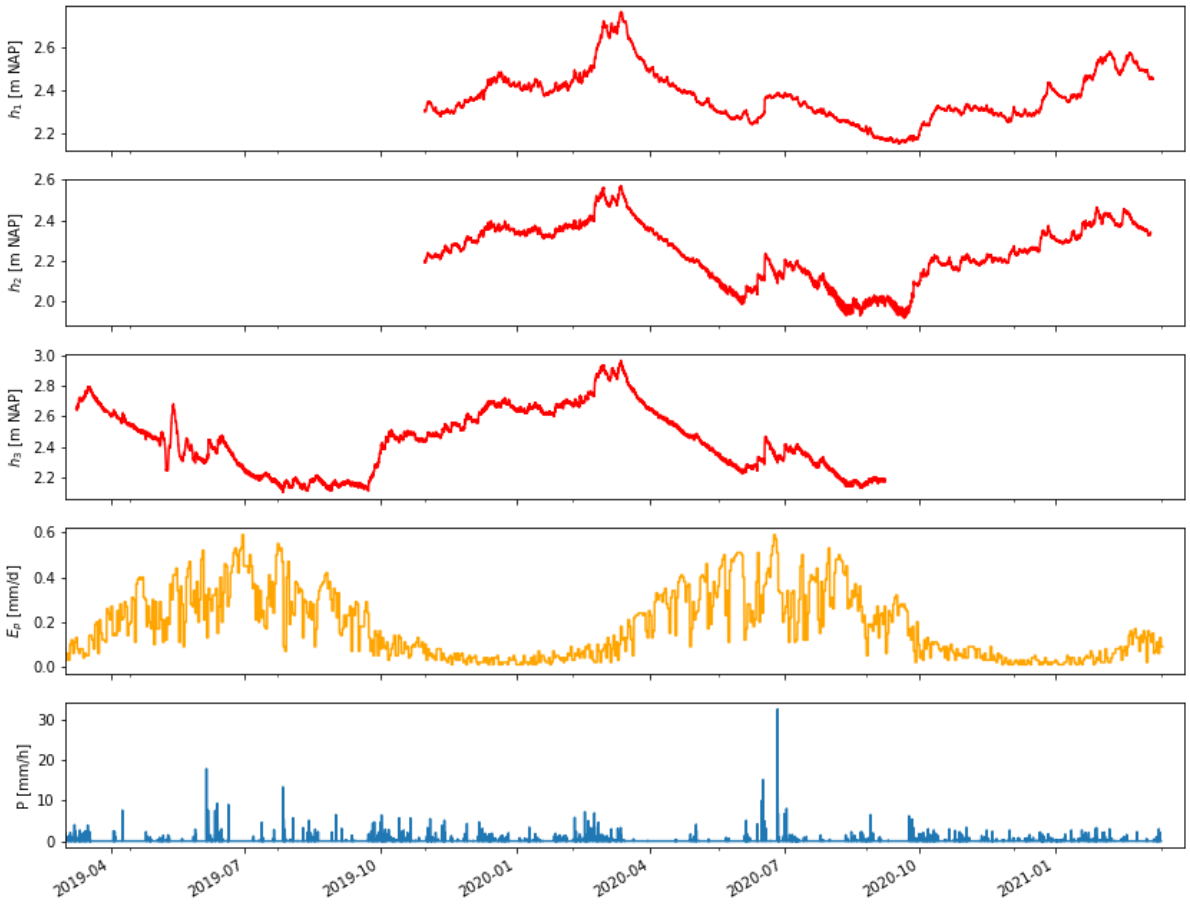


Figure 4.2: Enlarged version of time series of observed groundwater heads $h_1$, $h_2$ and $h_3$ associated with monitoring wells PASM0001, PASM0002 and PASM0003 in Figures 3.6 and 3.7 and time series of potential evaporation $E_p$ and precipitation $P$ from the automatic Gilze-Rijen weather station. $h_1$, $h_2$ and $h_3$ and $P$ have an hourly observation frequency and $E_p$ is observed daily. $h_1$, $h_2$ and $h_3$ have an observation length of 495, 493 and 550 days respectively, whereas $P$ and $E_p$ have an observation length of approximately 10 years.

### 4.1.2. Missing, insignificant and unsuitable input data

No measurements on discharge by the storm sewer and drainage system have been executed and therefore these discharge processes could not be added as stresses in the TFN model.

The water level of the Dungense sloot is an insignificant stress for the TFN model. Available measurements on the water level of the Dungense ditch were implemented as a stress in the TFN model to test whether inclusion of the surface water improved the TFN simulation. However, addition of the surface water level stress did not improve, nor deteriorate, the TFN simulations. Therefore, it was assumed that the surface water is of insignificant influence to the groundwater head time series underneath the highway. This assumption is in line with the lay-out of the sewer system, since the presence of the valves (section 3.4.2) suggests no inflow from the Dungense ditch into the sewer system and thereafter no recharge of the groundwater with surface water through the drainage pipes in proximity of the highway.

The groundwater head series of PASM0010, PASM0011 and PASM0012 (sectoin 2) are unsuitable for TFN modelling. Menyanthes was used to lengthen the short groundwater head series of PASM0010, PASM0011 and PASM0012. This was done by testing the aforementioned purpose of forecasting the groundwater head output signal at non-observed periods in the past by elongating the available time series. Filling in data gaps in the past using the measurement series of PASM0010, PASM0011 and PASM0012 and available precipitation and evaporation series as stresses, however, resulted in groundwater heads exceeding the ground level significantly at various moments in time (e.g. Figure 4.3). Since this is physically unrealistic, it can be speculated that the length of time series PASM0010, PASM0011 and PASM0012 is insufficient for proper time series analysis.

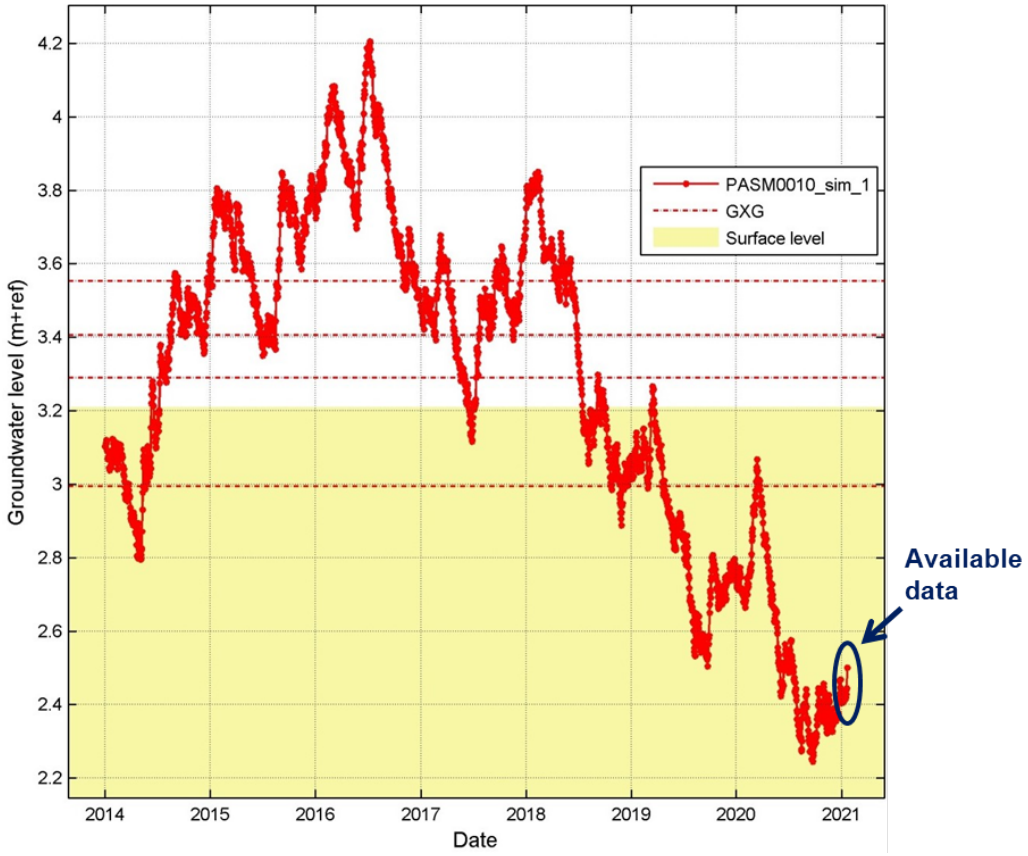


Figure 4.3: Menyanthes simulation of elongation of PASM0010 groundwater head time series (in red), based on the available data of the groundwater head measurements of PASM0010 (indicated by the blue circle), and the available evaporation and precipitation measurement series with a length equal to the elongation period. The surface level is indicated in yellow.

## 4.2. Results time series analysis

In time series analysis, the goodness-of-fit of the TFN model can be expressed in several ways, of which one is the explained variance percentage (EVP). The EVP indicates which part of the variance in the groundwater head observations ($\sigma_h^2$) is present in the model and is therefore not caused by the variance of the residuals ($\sigma_r^2$) (Von Asmuth, 2012; Collenteur et al., 2021);

$$EVP = \frac{\sigma_h^2 - \sigma_r^2}{\sigma_h^2} \times 100 \tag{4.1}$$

The value of the EVP varies between 0% and 100%. A perfect simulation of the groundwater head observations is obtained at an EVP of 100%, i.e. residuals are absent, but as a rule of thumb an EVP of 70% is generally accepted (Pezij et al., 2020). Other parameters to check the goodness-of-fit are for example the root mean squared error and the Nash-Sutcliffe coefficient (Collenteur et al., 2021).

### 4.2.1. Linear groundwater recharge

The scaled gamma distribution impulse response function (equation A.4) for precipitation and evaporation was used to simulate the observed groundwater head series according to linear groundwater recharge (equation 2.1) at the resolutions of an hour and a day. To start with, the simulation reveals poor EVP values for the simulation of groundwater series PASM0001 and PASM0002 with a time step of an hour (table 4.1). In the simulations the amplitude of the groundwater heads are significantly insufficient. A possible reason for this is that at this resolution, the relationship between recharge and measured rainfall and reference evaporation is actually nonlinear. The simulation of PASM0003 with a one hour time step seems acceptable regarding the EVP (table 4.1).

Table 4.1: EVP values for the Pastas simulations of groundwater head time series PASM0001, PASM0002 and PASM0003, using a scaled gamma distribution impulse response function and a linear recharge model and two different time steps Δt.

| | **PASTAS** | |
|---|---|---|
| **piezometer ID** | **Δt = 1 hour** | **Δt = 1 day** |
| *PASM0001* | 41% | 86% |
| *PASM0002* | 24% | 97% |
| *PASM0003* | 73% | 96% |

It is possible that at PASM0003 relatively fast groundwater recharge occurs due to e.g. favourable groundwater recharge conditions (e.g. a high permeability). However, regarding the fit report observations, it can be hypothesized that a stress is missing. A trend can namely be observed in the residuals (graph in the middle of Figure 4.4), i.e. an underestimation of the observed groundwater heads in spring and summer and an overestimation in autumn and winter time by the model. A missing stress or inertia of the groundwater system might be related to this. A possible missing stress is the aforementioned phreatic, horizontal groundwater flow towards piezometer PASM0003, as a result of water discharge through the remnant from the meandering channel.

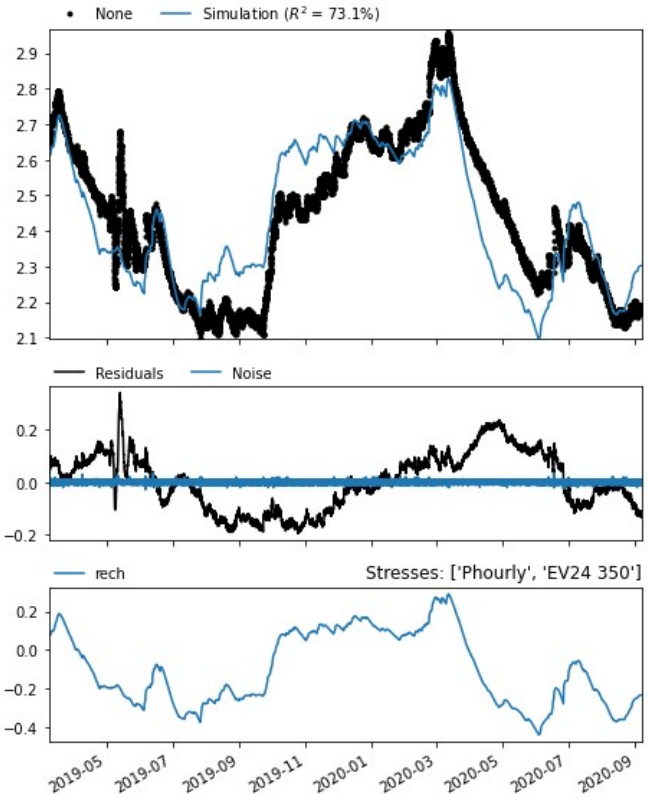


Figure 4.4: Illustration of the Pastas simulation of groundwater head time series PASM0003, using a scaled gamma distribution impulse response function, a linear recharge model and a time step of one hour. From top to bottom the simulated groundwater levels, the model residuals and noise and the simulated contribution of recharge to the observed groundwater heads are illustrated.

TFN modelling tools allow for the resampling of time series, which enables the user to study groundwater head responses at different time steps. Whereas the model performances of the TFN simulations with linear groundwater recharge are poor when using an hourly time step, EVP values can be considered promising when taking a time step of a day (Table 4.1). This implies that for a daily time step, groundwater head time series can be well simulated with a linear recharge function of precipitation and potential evaporation. The latter was tested both in Menyanthes and in Pastas (see Figures A.1 of Appendix A.2 and Figures A.2, A.3 and A.4 of Appendix A.3). To check plausibility of the model simulations, the model parameters such as evaporation factor f and the model residuals were analysed (Table 4.2). Whereas the parameter values of PASM0001 deviate most between the Menyanthes and Pastas simulations, it can be stated that overall the calibrated parameter values coincide relatively well. Regarding the high EVP values for both the Menyanthes and Pastas

simulations (Table 4.2) it can be stated that the precipitation and evaporation measurement time series are able to explain most of the groundwater head time series. As aforementioned, the residuals can reveal a missing stress from the model. However, since no clear trend in the residuals is visible and the autocorrelation of the noise is negligible (Figures A.2, A.3 and A.4), it can be stated that no significant stress is missing. According to Von Asmuth et al. (2008) and Pezij et al. (2020) autocorrelation of the noise implies that the white noise assumption is invalid.

Table 4.2: Calibrated parameter values for Menyanthes (M) and PASTAS (P) simulations of the TFN model with linear recharge (EVP = explained variance percentage, d = groundwater base level, f = evaporation factor, A = gain, $t_{mem}$ = memory of the system). Estimated standard errors of the parameters are between brackets.

| **Parameter** | **EVP [%]** | | **d [m]** | | **f [-]** | | **A [mm]** | | $t_{mem}$ **[days]** | |
|---|---|---|---|---|---|---|---|---|---|---|
| | **M** | **P** | **M** | **P** | **M** | **P** | **M** | **P** | **M** | **P** |
| *PASM0001* | 92 | 86 | 1.3 | 2.2 (6.9%) | 0.67 (0.7%) | 0.67 (36.4%) | 964 (3.1%) | 210 (34.3%) | 1185 | 600 |
| *PASM0002* | 97 | 97 | 2.2 | 2.2 (1.4%) | 1.25 (0.8%) | 1.22 (11.2%) | 109 (0.7%) | 126 (9.8%) | 153 | 350 |
| *PASM0003* | 97 | 96 | 2.6 | 2.5 (2.0%) | 1.67 (0.9%) | 1.41 (13.3%) | 122 (0.8%) | 169 (13.0%) | 184 | 400 |

Next to analysing the influence of precipitation and evaporation on the groundwater head time series, TFN modelling was also used to quantify trends in the system by generating groundwater statistics. Both the mean high groundwater level (MHGL) and mean low groundwater level (MLGL) were computed in different ways by Menyanthes and Pastas. In Menyanthes, MHGL and MLGL computation was done by forecasting the groundwater head output signal at non-observed periods in the past by elongating the available time series. In order to do this, daily KNMI precipitation and evaporation measurement series from 2014 to March 2021 were used as input signals, forcing the groundwater head time series. 2014 was chosen as the starting year, because prior to 2014 the last significant changes to the physical system, i.e. the addition of lanes, have been made to the road system. Leaving out years prior to 2014 is done, because the effects of physical change cannot be predicted by a stochastic model. Menyanthes calculates the MHGL and MLGL by first computing the average for the three highest/lowest groundwater levels of every year and thereafter averaging the resulting values over all measured years. In Pastas, the MHGL and MLGL are approximated by taking quantiles of the timeseries values ($q_{MHGL}$=0.94 and $q_{MLGL}$=0.06) per year and calculating the mean of the quantiles. Quantiles can be defined as particular parts of a data set that determine how many values are above or below a certain limit. Table 4.3 reveals that the different statistic computation methods reveal relatively similar groundwater statistics.

Table 4.3: Computed groundwater statistics (MHGL and MLGL) of the TFN simulations of linear groundwater recharge with a time step of one day in Menyanthes and Pastas.

| | **Menyanthes** | | **PASTAS** | |
|---|---|---|---|---|
| **Piezometer ID** | **MLGL [m NAP]** | **MHGL [m NAP]** | **MLGL [m NAP]** | **MHGL [m NAP]** |
| *PASM0001* | 2.28 | 2.64 | 2.28 | 2.55 |
| *PASM0002* | 2.01 | 2.43 | 2.16 | 2.42 |
| *PASM0003* | 2.20 | 2.76 | 2.16 | 2.78 |

### 4.2.2. Non-linear groundwater recharge

Section 2.2.1 reveals that a possible reason for inaccurate simulation of groundwater head output series is the assumption of a linear relationship between precipitation and potential evaporation in the TFN model. Therefore, the FLEX recharge model was used to study soil water dynamics in the unsaturated zone. Implementing the FLEX recharge model on the available time series and using $\Delta$t=1 day results in very low EVP values, approaching 0. Whereas it would be expected that low $\gamma$ values would be generated due to little non-linearity, no good model fit was created at all. A possible explanation for this could be an insufficient warm-up time (Collenteur et al., 2021). A long warm-up time can be regarded more important for a non-linear recharge model, compared to a linear recharge model, because in the non-linear recharge model the recharge flux strongly depends on the initial saturation level of the root zone. This is not the case in the linear recharge model (Collenteur et al., 2020). For TFN simulation of the FLEX recharge model with a time step of $\Delta$t = 1 hour, the groundwater head measurement series are characterized by significantly more observation points. Implementing the FLEX recharge model ($\Delta$t = 1 hour), seven parameters were estimated; non-linear recharge model parameters $k_v$, $k_s$, $\gamma$ and $S_{r,max}$, parameters A and a from the exponential response function

(equation A.5) and groundwater base level d (equation A.1). The results of the simulations are shown in Figures A.5, A.6 and A.7. Instead of the scaled gamma response function the exponential response function was applied in the TFN model with non-linear recharge. This choice was made because the non-linear recharge model already causes a delayed response on the groundwater (Collenteur et al., 2021) and to enhance model parsimony, i.e. to create a simple model with great explanatory predictive power (Collenteur et al., 2020). Figures A.5, A.6 and A.7 reveal that the values of $S_{i,max}$ and $l_p$ have not changed throughout the simulation, but are fixed. The fixation of the parameters was done, because it appeared that the values of $S_{i,max}$ and $l_p$ were hard to calibrate. Using the same approach as Collenteur et al. (2020) and Collenteur et al. (2021), values for $S_{i,max}$ and $l_p$ were fixed to sensible values, thereby decreasing the amount of parameters to be calibrated. The value of $l_p$ is based on Collenteur et al. (2020) and the value of $S_{i,max}$ is derived from Gerrits (2009), Gerrits (2010) and Collenteur et al. (2020) and is based on literature values for grass. Figures A.5, A.6 and A.7 reveal that FLEX TFN simulations with hourly time steps generate acceptable EVP results, with the exception of PASM0002.

Table 4.4: Calibrated parameter values for PASTAS simulations of the TFN model with non-linear recharge and Δt=1 hour (EVP = explained variance percentage, $S_{r,max}$ = rootzone reservoir storage capacity, $k_s$ = saturated conductivity, $\gamma$ = degree of non-linearity, d = groundwater base level). Estimated standard errors of the parameters are between brackets.

| **Parameter** | **EVP [%]** | $S_{r,max}$ **[mm]** | $k_s$ **[mm/d]** | $\gamma$ **[-]** | **d [m]** |
|---|---|---|---|---|---|
| *PASM0001* | 78 | 358.5 (99.9%) | 203.1 (411.5%) | 3.4 (28.2%) | 2.26 (2.1%) |
| *PASM0002* | 60 | 1.2 (14.3%) | 2.4 (12.1%) | 5.5 (10.9%) | 2.02 (12.4%) |
| *PASM0003* | 90 | 24.8 (4.7%) | 1.0 (10.5%) | 50.0 (10.9%) | 2.12 (1.9%) |

Since the EVP value of the TFN simulation of PASM0002 is below the rule-of-thumb value of 70% (table 4.4), the results from this simulation will not be used for parameter estimation. The poor fit of PASM0002 might be related to the absence of a fast reservoir in the FLEX model (Figure 2.4a). Thereafter, non-linearities due to drainage levels and extreme rainfall events that cause significant runoff and sewer discharge are not covered by the TFN simulation. Table 4.4 overall reveals high $\gamma$ values, indicating non-linear behaviour of the groundwater recharge system at the resolution of one hour. However, table 4.4 also reveals that the calibrated optimal parameter values of PASM0001 are characterized by large standard errors and that they differ significantly from the values of piezometer PASM0003.

# 5

# Hydrological model: bucket approach

## 5.1. Structure of the bucket models

With the knowledge on the case area (Chapter 3) and the generated statistics on groundwater dynamics (Chapter 4) a bucket model can be defined for each of the two typical cross-sections in the case area (Figure 5.1). The bucket models rely on forcing [$LT^1$] and storages [L], i.e. buckets, which interact through fluxes [$LT^1$] (Nijzink et al., 2016; Hrachowitz and Clark, 2017). Details on the mathematical representation of the forcing, buckets and fluxes can be found in Appendix B.1.

### 5.1.1. Similarities in the structure of the buckets models

Overall, the bucket models for the cross-sections (Figures 3.6 and 3.7) show many similarities. To start with, the forcing, buckets and fluxes associated with interception in the catchment of the road will be described. Figure 5.1 reveals that precipitation (P) is intercepted by the porous asphalt (ZOABTW) and the verge. A part of the interception buckets is lost through evaporation E and the remainder is distributed by runoff and infiltration in the verge. It is assumed that no infiltration takes place from the porous asphalt, because it is situated on top of impervious, non-porous old asphalt.

Secondly, the model structure associated with water in the soil below ground level will be illustrated. As infiltration enters the soil, it is directed into an infiltration trench or into the unsaturated zone, which represents the zone above the groundwater level where water can temporarily be stored (Figure 5.1). Interaction between the unsaturated zone and the phreatic groundwater is established by percolation and capillary rise. Capillary rise is a process at which pores pull water upwards and is specifically evident for small pores and dry soils (Hendriks, 2010). Percolation is the downward, gravity-driven movement of water within the unsaturated zone towards the groundwater table (Hendriks, 2010). It is important to note that the term recharge in the time series analysis corresponds with percolation in the bucket approach. Interaction between the phreatic groundwater and the deep regional, confined groundwater can be generated through seepage and recharge (Figure 5.1). Recharge refers to the replenishment of the regional, confined groundwater under the influence of gravity (Hendriks, 2010).

Thirdly, the model structure associated with transport of water out of the catchment of the road will be elaborated on. Both the infiltration trench and the phreatic groundwater drain into drainage pipes, which are connected to the stormwater sewer conduits at manholes. Consequently, water collected in the drainage pipes is transported through the impermeable stormwater conduits and overflows into the Dungense ditch, where it leaves the catchment of the road. A pump releases the water from the catchment of the road, along with upstream discharge, into the river Dommel.

### 5.1.2. Differences between the structure of the buckets models

The differences between the structure of the bucket models are related to the routing of runoff and the presence of sheet piles;

- Runoff at the cross-section at hectometre post 119.1 is solely routed towards the verge, due to the absence of holes in most of the manhole covers along this part of the road. At the cross-section of 119.95, on the other hand, runoff is both routed towards the verge and the stormwater sewer, because the manhole covers along this cross-section are featured by holes.
- Due to the absence of sheet piling on the northern side of the highway at hectometre post 119.95, seepage towards a wadi that is located along the highway takes place. Seepage in this case constitutes the movement of water through the soil towards the surface water of the wadi (De Ridder et al., 1994). This is not the case at hectometre post 119.1, where the sheet piling obstructs this type of seepage.

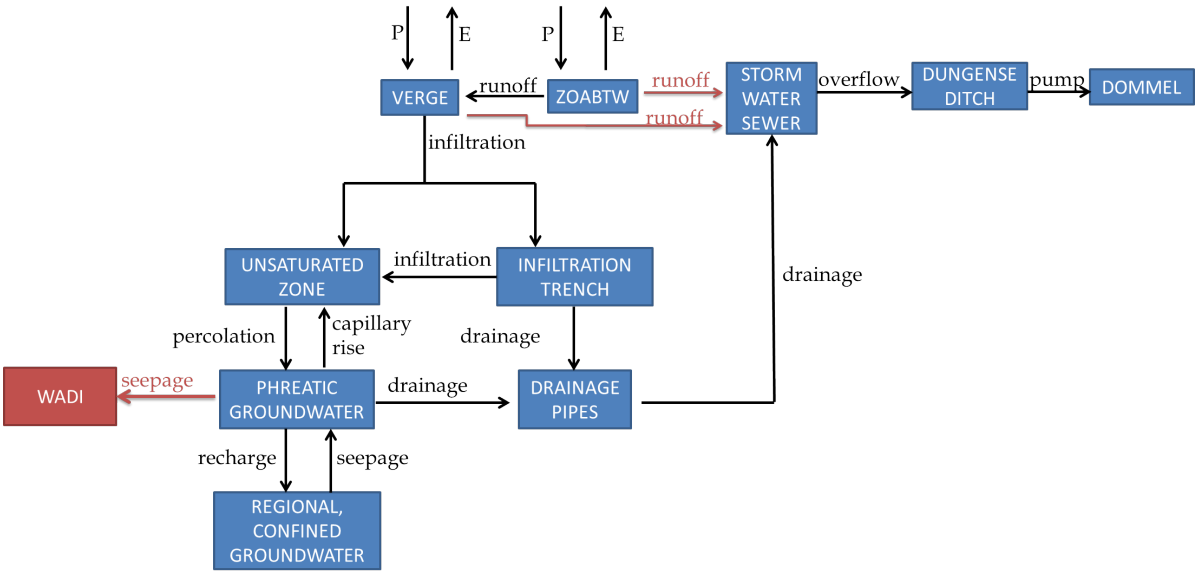


Figure 5.1: Structure of the bucket models for cross-sections 119.1 and 119.95 (Figures 3.7 and 3.6), with forcing P and E [$LT^{-1}$], buckets in the rectangles [L] and fluxes along arrows [$LT^{-1}$]. The buckets and fluxes in red are only applicable to cross-section 119.95.

## 5.2. Assumptions and simplifications

The model structure brings along several assumptions and simplifications, which are listed below and are presented in Figure 5.2. More detailed elaboration on the assumptions and simplifications can be found in Appendix B.1. The implications of the assumptions and simplifications are discussed in section 8.2.2.

- All fluxes from bucket X to bucket Y are limited by three factors; the available storage in bucket X, the available storage in bucket Y and the transport capacity from X to Y.
- It is assumed that water is instantaneously travelling from bucket X to bucket Y, which can be compared to a glass of water getting knocked over after which water is spread over the surface instantly. Whereas routing is ignored, the mass balance is conserved.
- All fluxes and buckets are expressed in unit depth [L], considering the area ratios [$L^2$] of the buckets. For example, if the area of X constitutes 20 $m^2$ and the area of Y constitutes 10 $m^2$ and if the outflow from bucket X is 20 mm/hr, then the inflow to bucket Y is $20 \times \frac{20}{10} = 40$ mm/hr.
- Precipitation only occurs in the form of steady rainfall which is distributed homogeneously over the case area.
- Evaporation, horizontal runoff through the porous asphalt and discharge by drainage pipes are not incorporated in the bucket models. These processes are relatively slow compared to the intensity of an extreme precipitation event and therefore have a negligible influence on the model outcome.

- Two infiltration mechanisms can be distinguished; infiltration excess overland flow and saturation excess overland flow. In case of infiltration excess overland flow, the rainfall rate is larger than the soil infiltration capacity and therefore ponded infiltration starts occurring (Brevnova, 2001; Hendriks, 2010). The process of infiltration excess overland flow is physically approximated by the Green and Ampt 1D infiltration model. The model simplifies infiltration through a step-like approximation, assuming a sharp wetting front (Brevnova, 2001; Hendriks, 2010; Kale and Sahoo, 2011), a constant saturated hydraulic conductivity and a constant capillary suction. The latter two assumptions imply the absence of soil layering and a deep groundwater table. In case of saturation excess overland flow, on the other hand, the soil infiltration capacity is larger than the precipitation intensity throughout the precipitation event and the water table rises to the land surface due to a limited amount of available storage in the unsaturated zone (Hendriks, 2010). In the approximation of saturation excess overland flow it is assumed that no recharge to the regional, confined groundwater occurs.
- Groundwater dynamics are encapsulated by the results of time series analysis (Chapter 4). Using the input precipitation and evaporation time series of the Gilze-Rijen automatic weather station, time series analysis amongst others generated an output of MHGL and MLGL groundwater statistics (Table 4.3). In the bucket approach the lowest MLGL and highest MHGL of each piezometer from Table 4.3 represent the boundary conditions for the available water storage below ground level, i.e. the MLGL and MHGL are a simplified representation of groundwater dynamics.
- The stormwater sewer is modelled as a discharge model with initial losses. The stormwater sewer only comes into play in case puddles in the verge starts to form, i.e. when infiltration excess overland flow or saturation excess overland flow occurs. The reason for this assumption is the lack of drainage routes for rainwater from the highway into the direction of the manholes, as water originating from the porous asphalt is forced to flow along the verge slopes parallel to the highway to reach the manholes. As a result of this assumption, 100% runoff from the porous asphalt and the verge is assumed in case the stormwater sewer comes into play.
- Incomplete information on the sewer layout led to the following simplifications:
  - Separate modelling of overflow for each stormwater trajectory.
  - Application of the standard weir formula. This implies that the connecting culvert near hectometre post 119.95 is not included in the sewer calculations and that sufficient discharge into the Dungense ditch through the main culvert occurs to fulfill the condition of free flow over the weir.
  - It is assumed that interaction with the drainage pipes does not influence sewer overflow.

  As a result of these aforementioned simplifications, the robust rational method in combination with hydraulic calculations was used to approximate the storage and discharge capacity of the storm water sewer. The rational method simplifies the rainfall-runoff processes associated with the sewer as follows;
  - The return period of rainfall specifies the occurrence of flooding. On the one hand this means that the rational method produces the worst case flow. On the other hand this implies that local problems such as blockages causing flooding events at short return periods are not taken into account.
  - The hydrological response between rainfall and flow in the system is linear.
  - The catchment imperviousness is constant throughout the precipitation event.
  - Discharge in the sewer flows at a constant pipe-full velocity.
- It is assumed that the Dungense ditch has an unlimited storage and discharge capacity. A first reason for this is that it is assumed that in case of an extreme precipitation event local flooding occurs before the precipitation has reached the surface water. Moreover, precipitation losses and delay processes in the upstream agricultural area imply that a large part of the precipitation has not reached the Dungense ditch yet at the time of the event. Another reason is that the presence of a non-return valve at the connection between the sewer system and the Dungense ditch facilitates discharge towards the Dungense ditch. According to Van Wijk (2021) from waterboard De Dommel the non-return valve is designed to open in case of sewer discharge as easily as it closes in case a difference in water level occurs. Whereas no specific information on the design of the non-return valve could be retrieved, Van Wijk (2021) therefore believes the resistance against discharge to the Dungense ditch to be negligible.

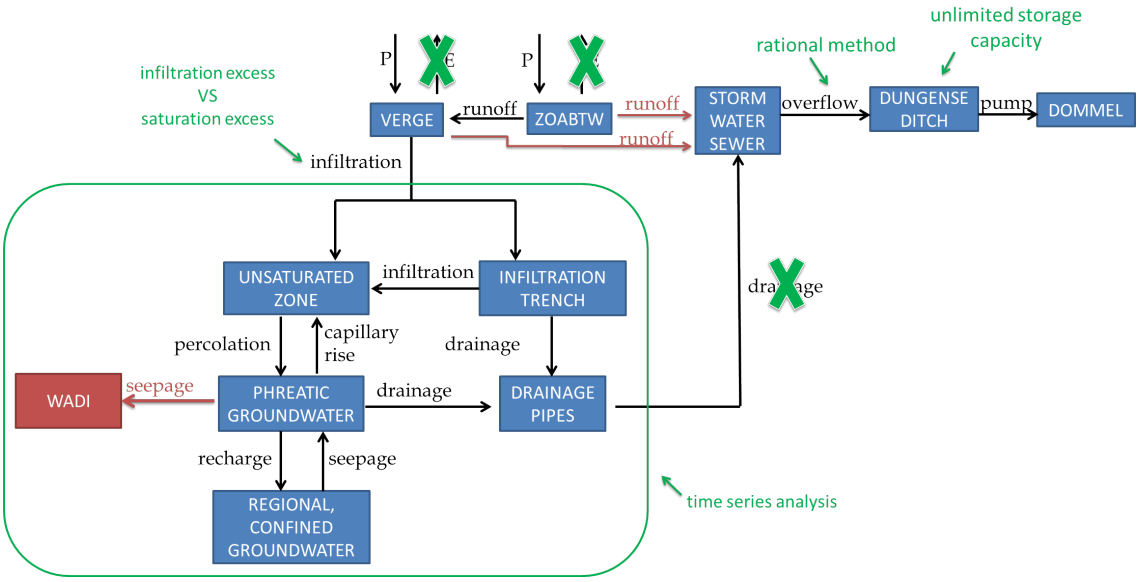


Figure 5.2: Structure of the bucket model for cross-sections 119.1 and 119.95, with buckets [L] and fluxes and forcing along arrows [$LT^{-1}$]. Assumptions and simplifications are indicated in green (see preceding text for clarification) and the buckets and fluxes in red are only applicable to cross-section 119.95.

## 5.3. Scenarios

In order to embed uncertainties in parameters and variations in boundary conditions three plausible scenarios have been defined to calculate tipping points as a result of the increase of extreme precipitation for the bucket models of the two typical cross-sections in the case area; a worst case, a best case and a middle case scenario. Whereas the worst and best case represent extreme values within a plausible range of parameters, the middle case is an educated guess on the tipping point during an extreme precipitation event.

### 5.3.1. Similarities in scenarios

Similarities between the scenarios are associated with depression storage and the operation of the stormwater sewer system (Table 5.1). The available depression storage ($z_{depression}$ in Table 5.1) is based on a detailed ground level analysis of the Dutch Digital Elevation Model AHN3 and is therefore neither associated with variation, nor a range of uncertainty. Despite incomplete information on the sewer layout, an educated guess on the sewer layout could be made with the help of As-Built drawings, ArcMap, a detailed ground level analysis of the Dutch Digital Elevation Model AHN3 and a field visit (section 3.4.2). Therefore a similar sewer layout is apprehended in all scenarios.

Table 5.1: Similarities between parameter values in all scenarios

| | $z_{depression}$ [m] | D [mm] | $z_{weir}$ [m NAP] |
|---|---|---|---|
| *119.1* | 0.054 | 250 | 2.15 |
| *11.95* | 0.079 | 160-400 | 1.85 |

### 5.3.2. Differences between scenarios

Differences between the scenarios are related to interception by porous asphalt and infiltration (Table 5.2). To start with, Bles et al. (2012) and Blokland (2021) reveal that pollution such as rubber residue from tires drastically reduces the interception capacity of the porous asphalt. In the thesis by Blokland (2021) it is stated that at the end of its service life the asphalt layer is almost sealed by pollution, implying an almost complete loss of interception storage. Information on the exact speed of pollution and the condition of the porous asphalt in the case area, however, is lacking. Thereafter, the interception capacity is believed to vary between 0 and 23.8 mm (Table 5.2), despite the large vertical hydraulic conductivity of porous asphalt (Appendix B.1.2). It is simply assumed that in the middle case scenario, the interception capacity is equal to half the maximum interception capacity.

Uncertainty in parameter values arises in the infiltration model. To start with, Chapter 4 revealed that the FLEX model was not able to accurately estimate rainfall-runoff parameters. Next, measurements (Zwart, 2020) revealed a range in saturated hydraulic conductivities. The little amount of measurements that was generated, soil heterogeneities in the case area (section 3.2) and the use of a falling head method to measure the saturated hydraulic conductivity impose parameter uncertainties. As a result of the uncertainties, literature values were apprehended to define plausible infiltration parameters for the scenarios. Green and Ampt infiltration parameters for soil classification corresponding with the soil classification of case area (section 3.2) from research by Rawls et al. (1983) were used for the best and worst case scenarios. Rawls et al. (1983) derived Green-Ampt parameters for 5000 soil horizons in the USA and classified them according to soil texture class. As Rawls et al. (1983) is the most cited and known contribution on Green-Ampt parameters (Tügel et al., 2021), it can be considered an appropriate source for the scenarios. The middle case scenario is based on the hydraulic conductivity measurements by Zwart (2020).

Variation in boundary conditions arises in the infiltration model. Groundwater dynamics are encapsulated by the MHGL and MLGL groundwater statistics (Chapter 4). The MHGL and MLGL imply that the depth of the water table varies throughout time ($l_{wt}$ in Table 5.2) and therefore varying boundary conditions must be used to represent plausible scenarios. The worst case scenario corresponds with the MHGL computed in Chapter 4) and the best case and middle case scenarios correspond with the MLGL. The reason for using MLGL in the middle case scenario is that extreme precipitation events are most likely to occur during dry summer months, which are characterized by low groundwater heads.

Table 5.2: Differences in parameter values between scenarios (n = porosity, $\theta_i$ = initial moisture, K = effective hydraulic conductivity, $S_f$ = suction, $l_{wt}$ = depth of water table below ground level). Blue = cross-section 119.1, Red = cross-section 119.95.

| **Scenario** | **ZOABTW** | **infiltration** | | | | | |
|---|---|---|---|---|---|---|---|
| | **available storage [mm]** | **n [-]** | $\theta_i$ **[-]** | **K [m/d]** | $S_f$ **[m]** | $l_{wt}$ **[m]** | $l_{wt}$ **[m]** |
| *best case* | 23.8 | 0.45 | 0.083 | 2.8 | 0.0495 | 0.82 | 1.29 |
| *middle case* | 11.9 | 0.39 | 0.128 | 0.25<br>1 | 0.084 | 0.82 | 1.29 |
| *worst case* | 0 | 0.34 | 0.173 | 0.1 | 0.12 | 0.46 | 0.87 |

### 5.3.3. Plausibility of initial conditions in scenarios

No extremely wet initial conditions have been apprehended in the bucket models (Table 5.2), because the chance that two extreme precipitation events occur quickly after each other is very small. According to the requirements with respect to the stormwater sewer capacity (will be discussed in Chapter 7), the catchment of the road should be able to drain a design storm of 38 mm/h. For the hypothetical case that the buckets of cross-section 119.1 are full after an extreme precipitation event of 38 mm/d, emptying of the system can be facilitated through evaporation and drainage. Despite the blinds spots on evaporation and discharge processes in the case area, a combined drainage and evaporation capacity of 7 mm/d is plausible (Van De Ven, 2009). In the hypothetical case it takes approximately 6 days (38/7) to empty the system in order to be prepared for a new precipitation event of 38 mm/h. Analysis on precipitation data of the past 45 years of the Gilze-Rijen automatic weather station reveals that during the measurement period a precipitation event of 38 mm/h has not occurred (Figure 5.3). Additionally, Figure 5.3 reveals that a daily precipitation amount of 38 mm/h was exceeded 21 times throughout the past 45 years. High daily precipitation values mostly occurred throughout the past 15 years during summer. Therefore, the chance that two extreme precipitation events occur quickly after each other is largest in summer. Although the future increase in precipitation extremes due to global warming will increase the chance of occurrence of the hypothetical event (Lenderink et al., 2017; Beersma et al., 2018a), the probability of experiencing two T=10 event in a period of six days is small. The chance on the occurrence, i.e. the probability, of a T=10 event is 10% every year.

Using the binomial distribution it can be calculated what the probability of experiencing two T=10 precipitation events in ten years, i.e. the hydrological failure risk, is. The binomial distribution is as follows;

$$R = \binom{n}{k} P^k (1-P)^{n-k} = \frac{n!}{k!(n-k)!} \frac{1}{T}^k (1-\frac{1}{T})^{n-k} \tag{5.1}$$

in which P represents the probability of an event [$T^{-1}$], T represents the return period [T], n stands for the period under consideration [T] and k stands for the amount of events within the period under consideration [-]. According to the binomial distribution, the probability of k = 2 events with a return period of T=10 years within n = 10 years is R = 19%. Additionally, the likelihood of a 10-year precipitation event occurring at least once in six days can be quantified according to a simplified binomial distribution;

$$R_{simplified} = 1 - (1-P)^n \tag{5.2}$$

The chance of one or more T=10 events (P=1/10) in six days (n=6/365) according to the simplified binomial distribution is 1.7%. The statistics reveal that the chance that two extreme precipitation events occur quickly after each other is very small and that the chosen initial conditions based on the research by Rawls et al. (1983) are plausible.

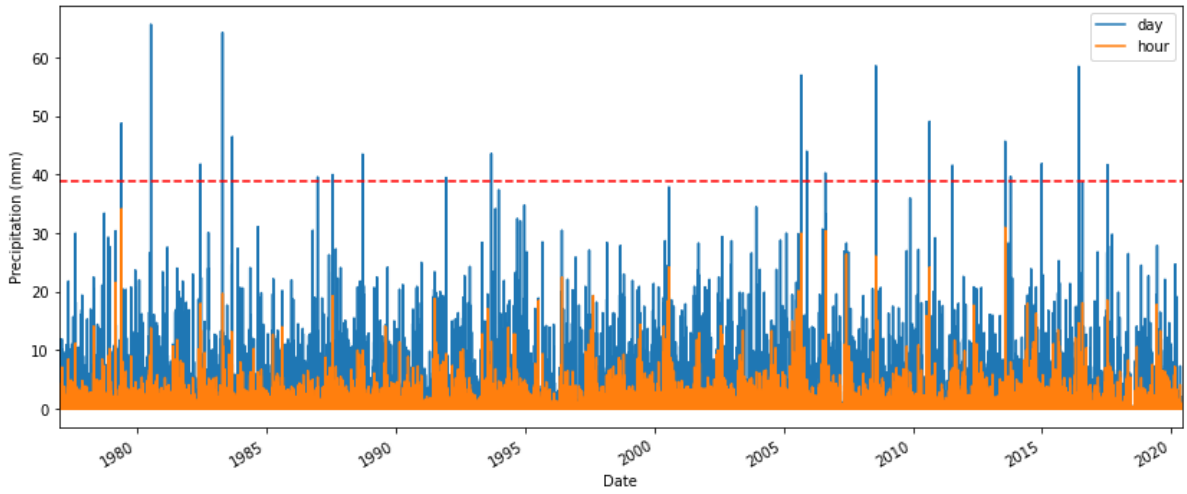


Figure 5.3: Hourly and daily precipitation sums for the Gilze-Rijen automatic weather station. The red, dashed line indicates an extreme precipitation event of 38 mm/hr.

## 5.4. Results bucket approach

### 5.4.1. Tipping points

Adaptation tipping points, i.e. the hourly precipitation intensity at which water exceeds the edge line of the road for a precipitation event with a maximum return period of 10 years, are determined by implementing the scenarios into the model structure. Table 5.3 reveals a range in adaptation tipping points from 6 to 60 mm/hr, dependent on the scenario.

### 5.4.2. Sensitivity of buckets, fluxes and parameters to flooding

The model structure allows quantification of the absolute and relative contribution of all buckets and fluxes to the delay of the tipping point. Table 5.3 reveals that in the case area especially the porous asphalt contributes largely to the delay of the tipping point (both absolute and relative). This makes sense, because the porous asphalt constitutes a large surface and therefore has a large water buffering potential. Therefore, pollution of porous asphalt plays an important role in flooding. The largest difference between the tipping points of the cross-sections is induced by the presence of a sewer system. Table 5.3 reveals that the presence of a stormwater sewer with open manholes causes a significant delay of the tipping point. Whereas the sewer has a limited storage capacity, its discharge capacity is high and therefore the sewer can result in a contribute significantly to the delay of the tipping point in case of extreme precipitation events with short concentration times, i.e. less than an hour. Next, the depression storage in the verge can be regarded of moderate influence

on the delay of the tipping point. To end with, the process of infiltration is least influential to the delay in flooding. In the case area infiltration excess overflow occurs quickly after runoff from the porous asphalt occurs and ends up in the verge. The Green-Ampt model is the most sensitive to the effective hydraulic conductivity, followed by the initial moisture content and the suction head (Parnas, 2018).

Table 5.3: Adaptation tipping points and contribution of buckets and fluxes to the delay of the tipping point. Blue = cross-section 119.1, Red = cross-section 119.95.

| **Scenario** | **Tipping point [mm/h]** | **Contribution to delay of tipping point** | | | |
|---|---|---|---|---|---|
| | | **ZOABTW [mm]** | **Verge [mm]** | **Infiltration [mm]** | **Sewer [mm]** |
| *Best case* | 38 | 23.8 (63%) | 4.2 (11%) | 10 (26%) | 0 (0%) |
| | 60 | 23.8 (40%) | 6.2 (10%) | 10 (17%) | 20 (33%) |
| *Middle case* | 21 | 11.9 (57%) | 4.2 (20%) | 4.9 (23%) | 0 (0%) |
| | 39 | 11.9 (31%) | 6.2 (16%) | 0.9 (2%) | 20 (51%) |
| *Worst case* | 6 | 0 (0%) | 4.2 (70%) | 1.8 (30%) | 0 (0%) |
| | 27 | 0 (0%) | 6.2 (23%) | 0.8 (3%) | 20 (74%) |

The contribution of the buckets and fluxes on the southern lane of cross-section 119.1 is illustrated in Figure 5.4 by revealing the interaction between the interception buckets and infiltration. In Rectangle 1 the porous asphalt bucket has not been filled yet and infiltration in the verge solely consists of precipitation in the verge. As soon as the porous asphalt bucket is full, runoff from the asphalt towards the verge occurs. This results in Rectangle 2, which represents a relatively fast increase in infiltration due to the contribution of both runoff from the porous asphalt as well as precipitation in the verge. At a rain intensity of approximately 20 mm/hr, the cumulative infiltration remains constant and one can speak of infiltration excess overland flow. At that point, the excess water depth in the verge (Rectangle 3) starts increasing until the depression storage of 54 mm is filled. At this point the adaptation tipping point is reached.

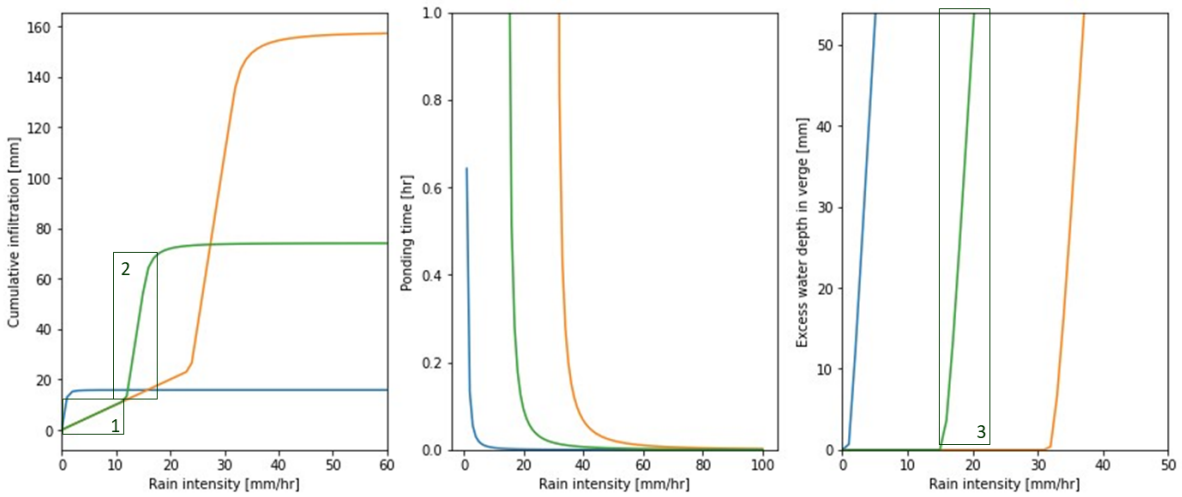


Figure 5.4: The contribution of the buckets and fluxes on the southern lane of cross-section 119.1. In blue, green and orange, the worst, middle and best case are represented respectively. The numbered rectangles are discussed in the text above.

# 6

# Focus group

A focus group aimed at exploring the societal robustness of measures against flooding of the A2 due to extreme precipitation. Supervisor Ing. J.B.M. Gerritsen and I facilitated the online focus group with a duration of 2 hours on the 17th of May 2021 in Dutch and translated it to English afterwards using the recording of the session and handwritten notes. The focus group consisted of three parts; the collection of objectives and constraints of stakeholders, a brainstorm for measures against local flooding of the A2 due to extreme precipitation in small groups and a discussion on the impact and effort of the gathered measures during the brainstorm. The focus group was prepared with help of expert judgement by a process and transition manager and a site manager. The inclusion of a brainstorm part was chosen to fulfil the pragmatic consideration to create willingness among participants to participate and to facilitate the design of societal robust Adaptation Pathways.

In order to prepare the focus group and the attendees, an online platform was prepared for each part and an instruction on the use of the online platform was sent to the participants in advance of the online session. Moreover, the attendees were sent information on the functions of the case area (section 3.1) and the hydrological processes involved in local flooding of the highway (section 5.4.2). Thereafter, the introduction of the topic could be done concisely during the focus group, leaving time for an open discussion. Additionally, attendees were asked for permission for recording and quoting, informed about the use of the results (publication on repository TU Delft) and anonymisation of results.

Six stakeholders of four different organisations joined the session. Unfortunately, no attendees from Staatsbosbeheer and Brabants Landschap were found. The stakeholders fulfil the following roles in their organisations;

1. Rijkswaterstaat: asset manager and advisor integral water management
2. Waterboard Aa and Maas: advisor water system and area administrator
3. Waterboard De Dommel: planner
4. Province: policy officer

## 6.1. Objectives and constraints

At the start of the focus group the case area and the functions of the area were concisely introduced using a map. Next, a cross-section of the road indicating hydrological processes relevant to local flooding of the highway was presented. Thereafter, the participants were asked to write down all their objectives and constraints that could possibly be related to flooding due to extreme precipitation, both in general as well as for the case area. Outcomes are presented in Table 6.1.

Table 6.1: Flooding related objectives and constraints of stakeholders

| Stakeholder | Objectives | Constraints |
|---|---|---|
| *Rijkswaterstaat* | Optimal traffic flow and road safety<br>Good agreements with adjacent water managers<br>Conditions for management and maintenance<br>Optimal groundwater levels | Flooding of the road surface<br>Limited availability of space for measures<br>Deterioration of water quality<br>Frost damage on road surface |
| *Waterboard Aa en Maas* | Balanced water quantity in surroundings of the road<br>Expansion of water storage in Bossche Broek to fulfill HoWaBo[a]<br>Improve water quality of surface water | Limited availability of space for water storage of water from the road<br>Poor quality stormwater runoff reaches Dungense ditch<br>Extra load on the Dungense ditch by discharge of the A2 |
| *Waterboard De Dommel* | Realisation of desired groundwater levels for the benefits of nature in Bossche Broek<br>Conservation of controlled water storage and expansion of water storage in Bossche Broek to fulfill HoWaBo<br>Meeting regional flooding standards<br>Discussion on acceptable flooding standards for the A2 | Loss of water storage<br>Negative effects on groundwater levels in Bossche Broek<br>Poor quality stormwater runoff reaches Dungense ditch<br>Extra load on the Dungense ditch by discharge of the A2<br>Decrease in drainage depth A2<br>Future climate; more and more intense precipitation and more frequent occurrence of simultaneous flood peaks of the river Meuse and the river Dommel |
| *Province* | Not directly known to participant | Local situations are not of direct provincial interest |

[a]HoWaBo is a flood protection program to generate water storage in the Bossche Broek.

## 6.2. Brainstorm

Next, a brainstorm for measures against flooding of the A2 due to extreme precipitation was held in two groups to stimulate interaction and discussion. An unguided brainstorm was apprehended to allow participants to generate their own ideas, frames and concepts (Kitzinger, 2005) . Whereas group 1 focused on technical solutions, group 2 focused on a system approach. During the brainstorm, the role of the facilitators was to answer questions related to flooding or the case area. After the brainstorm, both groups presented their findings to each other.

### 6.2.1. Results of brainstorm group 1

Brainstorm group 1 consisted of the advisor water system and area administrator of Waterboard Aa and Maas and the asset manager of Rijkswaterstaat. Overall, the group focused on technical solutions to counteract flooding. Whereas the asset manager of Rijkswaterstaat preferred measures facilitating quick discharge of water from the catchment of the road, the participants from waterboard Aa en Maas focused on retaining water near the road. Since these objectives conflict, it was found difficult to satisfy each others interests. Thereafter, no ideal solution was found that satisfies all interests. The following measures against flooding of the A2 were proposed;

- The asset manager of Rijkswaterstaat proposed the installation of manholes with holes to facilitate quick drainage of precipitation.
- The area administrator of the waterboard mentioned the installation of an underground, waterproof water buffer near the highway for extreme precipitation events. A waterproof storage was proposed to facilitate underground storage space despite the presence of high groundwater levels underneath the A2.
- The advisor water system of the waterboard proposed storage of stormwater runoff of the road elsewhere (not on the Dungense ditch) by pumping water away from highway.
- The asset manager of Rijkswaterstaat introduced the idea of raising the road to create extra space for the storage of water between the groundwater and the groundlevel.

- The advisor water system of the waterboard proposed infiltration trenches to improve the infiltration capacity of the verges.
- The asset manager of Rijkswaterstaat mentioned enlarging the sewer pipes to increase the sewer capacity and to facilitate drainage of precipitation. He remarked that a lack of adequate sewer maintenance of Rijkswaterstaat regularly results in a limited sewer capacity.

### 6.2.2. Results of brainstorm group 2

Brainstorm group 2 consisted of the planner of Waterboard De Dommel, the advisor integral water management from Rijkswaterstaat and the policy officer of the province. Overall, the group focused on a system approach to counteract flooding. All participants in the focus group agreed on the idea that it is of great importance to regard climate change and the occurrence of more wet and dry periods and to use water whenever possible. Therefore, measures which facilitate useful water retention were regarded effective. The following measures were proposed;

- Set up a water storage elsewhere in order to split the stormwater sewer system between the northern and southern lanes of the A2. This leads to a decrease of the load on the Dungese ditch. The water is preferably stored without the use of pumps, as these are sensitive to maintenance and management.
- Store stormwater from the A2 in the southern Bossche Broek to enhance ecological development. This corresponds with the plans for nature development in the southern Bossche Broek by Brabants Landschap (section 3.1). The feasibility of this measure is, however, questioned due to the issue of water quality.
- Monitor the hydrological functioning of the system more to facilitate a discussion between stakeholders on the acceptable flooding standards for the A2, regarding the various goals in the case area, such as mobility, HoWaBo 2.0 and Natura 2000.

## 6.3. Impact-Effort Matrix

After the brainstorm the participant from the province had to leave the online session. Thereafter, the final part of the focus group session was continued with participants from Rijkswaterstaat and the two waterboards. The third part of the focus group focused on a discussion on the impact and effort of the gathered measures during the brainstorm. To start with, the participants were asked to rank the measures on impact and effort in a matrix (Figure 6.1). The impact-effort matrix is a tool to to identify potential solutions (Andrássyová et al., 2013) by grouping them into four quadrants. Whereas *Quick wins* are most desirable, as they require little effort but create the most impact to counteract flooding, *Thankless* tasks are least desirable, as they require a lot of effort and have little impact. In between the two extremes are small, incremental measures, *Fill in jobs*, and *Major projects*. It is important to note that figure 6.1 reveals that impact and effort are ranked in general as assessed by representatives from Rijkswaterstaat and the two waterboards. Therefore, the effort a measure requires for the waterboards and Rijkswaterstaat in particular is not revealed in Figure 6.1.

To start the discussion it was first remarked by a facilitator that the participants regard the majority of measures as *Major Projects*. Next, it was remarked that all participants regard monitoring as a measure that involves little effort and has a significant impact. At this point all participants were asked to elaborate on potential measures.

To start with, the asset manager from Rijkswaterstaat pointed out that he finds enlarging the discharge capacity the best solution to counteract flooding, as it enables quick drainage of precipitation out of the catchment of the road and therefore ensures an optimal traffic flow and safety of the A2 highway. The advisor integral water management of Rijkswaterstaat added to this that the storage of water can have a large impact, but that pumping brings along a lot of management and maintenance effort. Thereafter, buffering water elsewhere through pumping (measure 3 in Figure 6.1) is regarded a *Thankless task*. In contrast to Rijkswaterstaat, the planner from Waterboard De Dommel mentioned experiencing difficulties in prioritizing measures already, in relation to other goals, such as HoWaBo and Natura 2000, and in relation to uncertainties in the hydrological behaviour of the system. However, the planner finds it interesting to consider a measure in case it is possible to sustainably use stormwater runoff from the A2 for other other goals in the case area, such as

ecological development. The advisor water system from waterboard Aa en Maas reacted to this by agreeing with the planner from Waterboard De Dommel and stating that reuse of stormwater runoff is a potentially successful measure. The area administrator from waterboard Aa en Maas concluded by mentioning that a measure that increases the buffering capacity and allows for infiltration after an extreme precipitation is preferred.

In order to derive information on the commitment and interest of stakeholders to realise measures to prevent flooding due to extreme precipitation, the participants were asked to give their view on responsibility for realising a measure. The planner from waterboard De Dommel reacted to this by stating that the the person who takes the initiative is responsible for all the consequences. However, suppose a measure is suggested that allows stormwater runoff to be applied in a useful manner, other parties such as the waterboard will be interested in contributing to the realisation of it. Thereafter, the planner from waterboard De Dommel stresses that if ones desires another party to contribute to a measure, the measure must contribute to the goals of the party to be involved. The advisor water system from waterboard Aa en Maas agrees by mentioning the potential of matching solutions to increase the willingness of stakeholders to commit themselves and contribute to a measure. As a consequence, the planner from waterboard De Dommel thought of another matching solution. The matching solution is to store runoff from other road sections in the southern Bossche Broek for the benefits of nature, in case of road widening of the A2. On the one hand, this matching solution neutralizes the extra discharge from the new paved surface. On the other hand, the stormwater is reused for the benefits of nature.

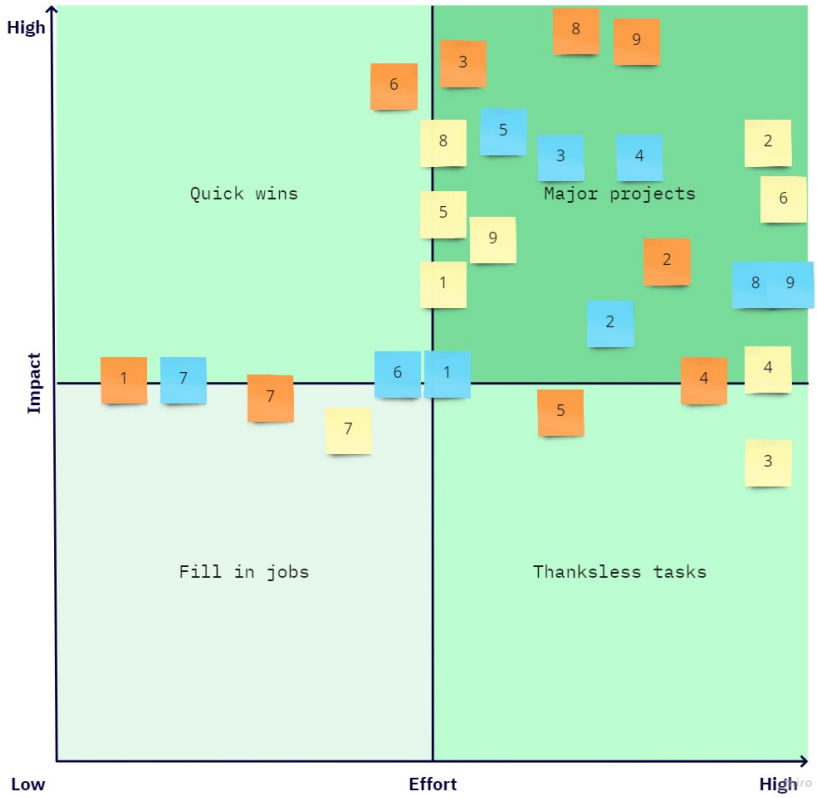


Figure 6.1: Impact Effort Matrix of measures gathered during brainstorm. The colours represent the various stakeholders; blue = waterboard De Dommel, orange = waterboard Aa en Maas, yellow = Rijkswaterstaat. The numbers represent the measures; 1 = install manholes with holes, 2 = install waterproof underground water buffer, 3 = buffer water elsewhere through pumping, 4 = raise the road, 5 = infiltration trench, 6 = increase sewer capacity, 7 = monitor and decide on challenges, 8 = use water elsewhere, 9 = buffer water without pumping.

# 7

# Adaptation Pathways

## 7.1. Objectives and constraints

Most of the objectives and constraints of stakeholders that were gathered during the focus group (Chapter 6) can be categorized according to several criteria; traffic flow, water buffering capacity, water quality, ecological value, costs and maintenance. The criteria reflect objectives and constraints relevant to the stakeholders and therefore provide information on the societal robustness of an adaptation measure. A societal robust adaptation measure meets multiple objectives of the relevant stakeholders and therefore provides a better trade-off than other potential adaptation measures in the Adaptation Pathways map (section 1.2.2).

### 7.1.1. Traffic flow

During the focus group the asset manager of Rijkswaterstaat revealed a clear preference for adaptation measures which are most suitable to ensure an optimal traffic flow of the A2 highway (Chapter 6). Section 1.1.2 reveals that impacts on traffic flow include reductions in capacity of the road network, travel speed, demand effects and loss of driving safety. In order to adequately fulfill their role as asset manager, guidelines with respect to the design of verges and stormwater drainage exist.

Rijkswaterstaat has formulated a guideline with respect to the design of verges (Rijkswaterstaat, 2019). According to the guidelines, verges must enable a safe return of vehicles that divert from the road into the verge. (Adaptation measures to) extreme precipitation can endanger this role by influencing the carrying capacity of the verge and the height difference between the road surface and the verge. Firstly, saturation of the verge as a result of extreme precipitation or high groundwater levels can negatively influence the carrying capacity of the verge (Rijkswaterstaat, 2019). Secondly, a large, abrupt height difference between the road surface and the verge as a result of adaptation measures can result in roadside accidents. According to the guidelines a safe verge is characterized by a maximum height difference between the road surface and the verge of 70 mm. However, in case of porous asphalt with a thickness exceeding 70 mm, this maximum height difference can be bridged step by step, to enable the porous asphalt to drain out to the side.

Additionally, requirements with respect to the stormwater drainage are defined by Rijkswaterstaat. These requirements are based on rainfall duration lines of T=10 year design storms according to the climate scenarios from the Dutch meteorological institute (Beersma et al., 2018a) and are presented in Table 7.1. In this thesis, thereafter, the tipping points indicate at which hourly precipitation intensity the consequences of flooding exceed the flooding standards, i.e. the hourly precipitation intensity water exceeds the edge line of the road for a precipitation event with a maximum return period of 10 years. According to Rijkswaterstaat (2020b), the current system for stormwater discharge should be able to accommodate a T=10 year design storm that occurs in 2050 according to the Dutch climate scenarios (Table 7.1). The system for stormwater discharge comprises stormwater discharge through the verge (e.g. through infiltration and drainage pipes) and through a stormwater sewer. Additionally, the crown of stormwater sewer pipes should be located at least 1 meter below the road surface to avoid pipe settlement due to traffic loads and the system for stormwater discharge must have a life service of 50 years (Rijkswaterstaat, 2020b).

Table 7.1: Rainfall duration lines of T=10 design storms according to the Dutch climate scenarios (Beersma et al., 2018a).

| Time [min] | Precipitation depth after 1 hour [mm] | | | |
|---|---|---|---|---|
| | 2018 | 2030 | 2050 | 2085 |
| *5* | 12 | 13 | 15 | 17 |
| *10* | 18 | 19 | 21 | 25 |
| *15* | 20 | 22 | 24 | 28 |
| *30* | 25 | 27 | 31 | 36 |
| *60* | 31 | 33 | 38 | 44 |
| *120* | 37 | 40 | 45 | 52 |
| *240* | 43 | 46 | 51 | 59 |
| *480* | 49 | 53 | 58 | 66 |
| *720* | 53 | 56 | 62 | 71 |

### 7.1.2. Water buffering capacity

During the focus group the participants from the waterboards revealed a clear preference for adaptation measures which enhance the continued functioning of the case area surrounding the catchment of the road after an extreme precipitation event (Chapter 6). Moreover, the constraint of a limited availability of space for water buffering was quoted by Rijkswaterstaat as well as by waterboard Aa en Maas. Retaining water near the road and expansion of water storage in the Bossche Broek are related to this.

The Dutch Water Act states that the provincial regulation must state standards prescribing a frequency of regional flooding. Regional flooding can in this case be interpreted as the flooding of small rivers (e.g. the rivers Dommel and Aa), surface water and ditches such as the Dungense ditch. The provincial regulation of the Province of Noord-Brabant has for example assigned a desired safety standard for flooding of once in a 100 years for main infrastructure and the built environment. For some areas a different standard than stated by the Dutch Water law is defined. For these areas, an administrative assessment of costs and benefits has taken place. The case area is an exception, as for 's-Hertogenbosch a protection level against flooding from the regional water system of the rivers Dommel and Aa of once in a 150 years applies. The standards can be regarded a good care obligation. In practice, a T = 150 flood can still occur and an extra water storage of 4.5 million cubic meters is necessary need to be stored to meet the regional flooding standard (HoWaBo Story Map, 2021).

The Decision of the Executive Board from waterboards De Dommel and Aa en Maas states that an increase and disconnection of paved surface must be carried out as hydrologically neutral as possible. The purpose of this principle is to prevent rainwater from being discharged into the water system more quickly as a result of expansion or disconnection of the paved surface. For discharges into surface water, the water board therefore requires a replacement storage facility, which neutralizes the extra discharge from the new paved surface. Regarding stormwater from paved surface, the water boards advocate the following order of preference, with option 1 being the most desirable and option 5 the least desirable;

1. Reuse of stormwater
2. Infiltration of stormwater
3. Retention and discharge
4. Discharge to surface water
5. Discharge to sewer system

### 7.1.3. Water quality

During the focus group all participants showed their concern of deterioration of water quality as a result of pollutants from vehicles in runoff water from roads (Chapter 6). A decision of the Council of State (200704332/1, 18 June 2008) reveals that the rainwater runoff is regarded as waste, independent of whether and to what extent this water is polluted or not. A decree for stormwater runoff exists (Van Grinsven and Van Muiswinkel, 2010; Rijkswaterstaat, 2014), which is based on the Environmental Management Act, the Soil Protection Act

and the Water Act. The decree provides a practical interpretation of the legal framework, with the aim of providing a sober and effective approach to dealing with stormwater runoff from highways, bridges, viaducts and tunnels (Van Grinsven and Van Muiswinkel, 2010). In short, the decree for runoff comprises a general obligation to care for the environment, which is implemented by "Good Housekeeping". Next to the source measure to counteract pollution in stormwater runoff, i.e. the implementation of porous asphalt (Van Grinsven and Van Muiswinkel, 2010), the decree indicates a preferential order with regard to deal with stormwater runoff. Stormwater runoff is preferably infiltrated in the verge, which ensures pollution is contained in the top layer near the road and can be easily removed when necessary. In case infiltration in the verge is not reasonably possible the runoff can be discharged in surface water. Whereas no rules on runoff water treatment exist, Rijkswaterstaat is expected to discharge runoff water to surface water in good harmony and according to the general obligation to care for the environment.

### 7.1.4. Ecological value

During the focus group the planner of waterboard the Dommel revealed a preference for adaptation measures which facilitate the realisation of the desired groundwater levels for the benefits of nature in the Bossche Broek (Chapter 6). The realisation of the desired groundwater levels can be related to the framework of the Integrated Approach to Nitrogen. This framework is a national plan of the Netherlands that connects economy and ecology (De Heer et al., 2017). In the case area, this connection is established by combining ecological restoration with ecological development. Raising the water level in the Zuiderplas is an example of this. Raising the Zuiderplas is intended at avoiding regional seepage to end up in the Zuiderplas and thereby increasing regional seepage of deep, calcareous groundwater in the Bossche Broek. As a result, groundwater levels in the Bossche Broek rise and favour abiotic conditions for valuable Natura 2000 vegetation such as the burnet blue (H1059), the large loach (1145), and wet meadows (H6410) (Zwart, 2020). The Bossche Broek is thus part of the European Natura 2000 network. Natura 2000 areas are the main instrument to achieve the Birds and Habitats Directives of the European Union, which are aimed at stopping the loss of biodiversity in the European union (De Heer et al., 2017).

### 7.1.5. Costs and maintenance

During the brainstorm and discussion part, the advisor integral water management from Rijkswaterstaat showed his interest in minimizing costs and maintenance (Chapter 6).

In order to adequately fulfill management and maintenance of the HWN, the Ministry of Infrastructure and Water Management has made performance agreements which are laid down in a Service Level Agreement (SLA). Flooding due to extreme precipitation events is expected to affect several performance indicators associated with the maximization of the availability and the safety functions of the road network. The performance indicator associated with maximizing the availability of the road network states that 90% of the time, the available road capacity must be sufficient to meet the expected capacity need for passenger and goods transport (Rijksbegroting, 2018). The performance indicators associated with safety state that roughness and rutting standards must be met 99.7% and 95% of the time respectively (Rijksbegroting, 2018). No local differences exists in the standards and therefore the performance indicators aim to provide insight into whether Rijkswaterstaat is fulfilling its role as asset manager manager in the field of road safety management in a timely manner.

The decree for runoff comprises a general obligation to care for the environment, which is implemented by "Good Housekeeping". The measures associated with "Good Housekeeping" are mostly part of the Rijkswaterstaat procedures from the viewpoint of traffic safety and preventive maintenance. According to Van Grinsven and Van Muiswinkel (2010) "Good Housekeeping" comprises cleaning porous asphalt of the emergency lane twice a year to fulfil its capacity to contain pollution and to elongate its lifetime. VBW (2010) states that cleaning of the other lanes is not necessary as a result of the self-cleaning capacity of the porous asphalt. This is in contrast to the findings by Blokland (2021) (section 5.3.2). Moreover, "Good Housekeeping" includes scraping of the top layer of the verge every five years, in order to ensure discharge from porous asphalt, and cleaning of runoff facilities. Figure 7.1 reveals deferred maintenance of a gutter in the case area. According to Rijkswaterstaat (2010) this is not an exception. The report mentions €7 million overdue maintenance of the HWN. According to Rijksbegroting (2018) the maintenance of pavements comprises 33% of total management and maintenance of the HWN.

Figure 7.1: Dirty open manhole near 119.0 (Van Den Biggelaar, 2021).

## 7.2. Adaptation measures against local flooding

The results of Chapter 5 imply that two types of adaptation measures are effective against local flooding; measures with a focus on increasing the discharge capacity and measures with a focus on increasing the storage capacity. Next to addressing the specific issue of delaying the tipping point as a result of flooding due to extreme precipitation, the results of section 7.1 imply that adaptation measures can influence other objectives and constraints. By rating potential adaptation measures according to the defined criteria (section 7.1), synergies with co-benefits and potential pitfalls can be defined (Table 7.2). Both the brainstorm of the focus group (Appendix 6), focusing on gathering societal robust adaptation measures, and limited literature research contribute to a list of possible adaptation measures. Information on the implementation of measures in the bucket approach can be found in Appendix B.2.

### 7.2.1. Adaptation measures related to increasing discharge

In the focus group three potentially successful adaptation measures related to increasing discharge were suggested (Chapter 6); installing manholes with holes, increasing the sewer capacity and using the water elsewhere without pumping;

- **Install manholes with holes:** As a result of opening the manholes of the road segment corresponding with typical cross-section 119.1, the existing sewer layout comes into play (section 3.4.2). As the manholes of cross-section 119.95 have holes already, this measure does not have any consequences for delaying the tipping point at cross-section 119.95.

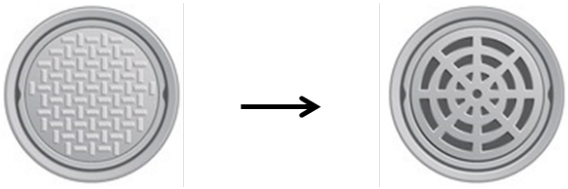

Figure 7.2: Schematic representation of installing manholes with holes

- **Increase in sewer capacity:** Increasing the sewer capacity of the existing sewer lay-out is established in the model by an increase in pipe diameters. From a cost-point of view, the smallest pipe that is able to transport the total discharge through a pipe segment must be selected. Therefore, an increase towards the successive commercially available diameter was chosen (Butler et al., 2018).

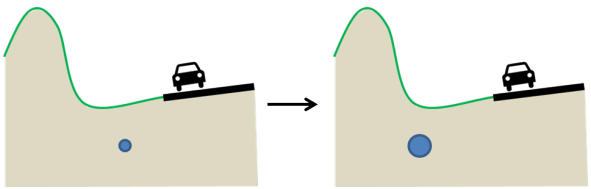

Figure 7.3: Schematic representation of increasing the sewer capacity

- **New sewer layout:** The new sewer layout is designed for transporting a T=10 year design storm that occurs in 2050 according to the Dutch climate scenarios (Table 7.1) and discharges it into the southern Bossche Broek. A re-iteration process was executed according to the rational method and hydraulic calculations in order to choose the most cost-effective solution to meet the requirement of no flooding for the design storm.

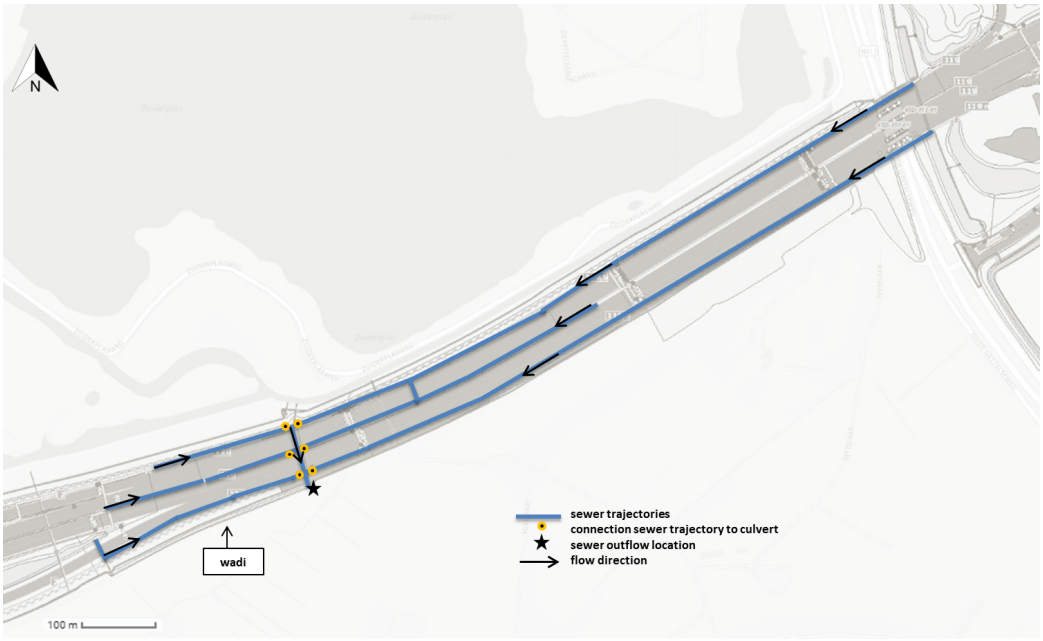


Figure 7.4: Schematic representation of new sewer layout; all sewer trajectories are directed towards the main culvert and discharge takes place on the southern side of the A2.

Installing manholes with holes can be regarded a straight-forward measure, as it makes use of the existing fabric. Enlarging the sewer capacity by installing thicker pipes is a measure which can follow the installation of manholes with holes to further delay the tipping point. Whereas both measures enhance the traffic flow during an extreme precipitation event, both measures can result in an extra load of stormwater on the Dungense ditch during a precipitation event compared to the current situation, and therefore do not benefit the criteria of water quality and water buffering capacity (Table 7.2).

The use of water elsewhere without pumping can be facilitated through a change in sewer design (Figure 7.4). The new sewer layout is designed for transporting an T=10 year Rijkswaterstaat design storm that occurs in 2050. The new sewer design collects all water from the sewer trajectories in the main culvert, which discharges the runoff into the wadi south of the A2. This allows for water storage in the southern Bossche Broek and can potentially result in a rise of the current groundwater heads in the Bossche Broek. This contributes to the ecological value of the case area. Thereafter, a matching solution is generated. However, some potential pitfalls should be considered concerning the new sewer design. To start with, the stormwater runoff quality may be insufficient to foster ecological development of the protected species in the Bossche Broek (Table 7.2). However, the quality of the stormwater runoff has not been tested. Secondly, the technical implementation of the adaptation measure brings along some difficulties, due to a limited amount of space between the ground and groundwater levels, and therefore does not fulfil the requirement which is related to pipe settlement as a result of traffic loads. The new sewer layout requires the need of relatively long pipes, which brings along relatively high investment costs and large pressure losses (equation B.16). Thereafter, large pipe diameters are required in order to prevent flooding at manholes. Next, the outflow location of the weir must be located above groundwater level, in order to prevent groundwater from flooding into the sewer system. Due to the limited amount of space between the groundwater level at the wadi south of the A2 and the groundlevel of the A2, crown levels of the pipes are therefore prone to be located less than 1 meter below the surface. On the other hand, it is possible for the stormsewer to discharge below groundwater level through a non-return valve. A disadvantage of this is the absence of mounting walls, which enable the settlement of contaminants from the A2 in the stormsewer system.

### 7.2.2. Adaptation measures related to increasing storage

Several potentially successful adaptation measures related to increasing storage in the catchment of the road can be suggested. The adaptation measures related to increasing storage on the road are as follows;;

- **Clean ZOABTW:** After cleaning ZOABTW the entire storage capacity of the porous asphalt bucket is available for precipitation in any scenario.

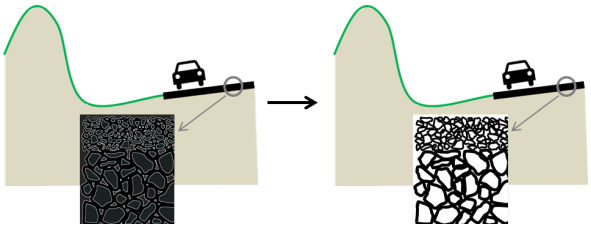

Figure 7.5: Schematic representation of cleaning the porous asphalt

- **Increase storage ZOABTW:** After cleaning the porous asphalt, an extra layer of porous asphalt can be added on top of the existing road surface. As a result of the addition of porous asphalt, the depression storage bucket in the verge is enlarged.

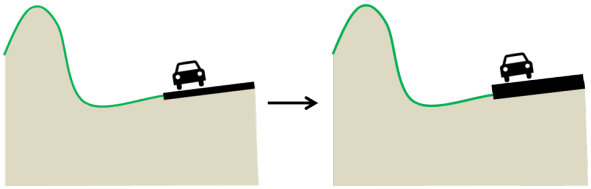

Figure 7.6: Schematic representation of increasing the storage capacity of ZOABTW

- **Plastic Road:** A new product by Koudstaal and Jorritsma (2015) is the Plastic Road. The Plastic Road consists of lightweight, modular elements that provide ample water storage, can easily be installed and have an expected life service of 50 years. The product can be used to collect rainwater, filter it and to let it gradually infiltrate into the local subsoil after a precipitation event. The modular elements can be positioned directly on a sand bed, thereby overcoming the need to construct a conventional foundation first. As the Plastic Road is produced of 100% recycled plastic it is circular product. Most processes in the current economy are linear in nature (Steens and De Vries Chairman, 2019). An example of a linear process is the production of an asphalt road, which fulfills its service to road users and is discarded afterwards. The circular economy is focused on a closed loop, by reusing materials in order to minimize the production of waste (Steens and De Vries Chairman, 2019). At the moment, the Plastic Road has been applied on footpaths, parking spaces and schoolyards. The innovation is promising, but a lot of research is required before Plastic Roads are applicable to highways (Williams, 2018).

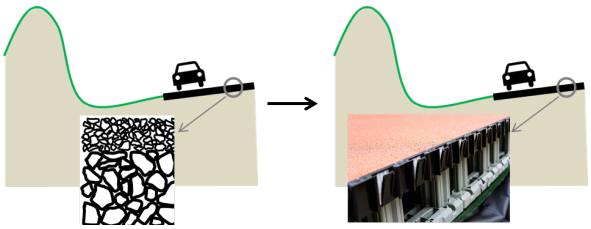

Figure 7.7: Schematic representation of a Plastic Road

The adaptation measures related to increasing storage in the verge are as follows;

- **Remove top layer verge:** The removal of the top layer of the verge increases the depression storage in the verge.

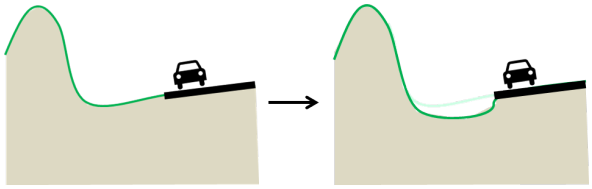

Figure 7.8: Schematic representation of the removal of the top layer of the verge

- **Infiltration verge:** The infiltration trench design with its corresponding parameters is based on Van De Ven (2009).

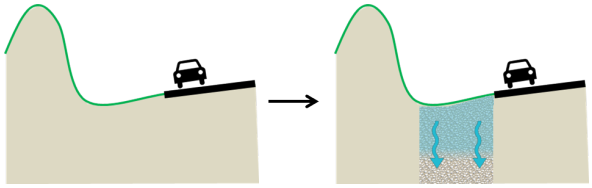

Figure 7.9: Schematic representation of the installation of infiltration trenches towards the surface

- **Raise the road:** In this case it is assumed that no porous asphalt will be added, but that the entire road will simply be raised by 10 cm.

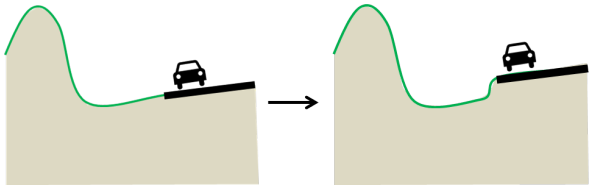

Figure 7.10: Schematic representation of raising the road

- **Descending verge:** Similar to removal of the top layer of the verge, the descending verge gives rise to an extra depression storage in the verge.

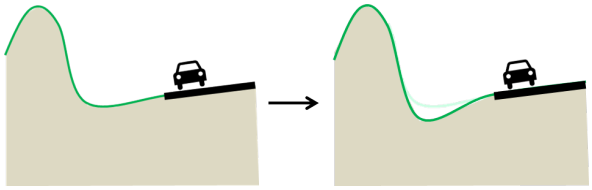

Figure 7.11: Schematic representation of the descending verge

To start with, several potential adaptation measures related to increasing the storage capacity of the road itself exist; cleaning the porous asphalt, increasing the storage capacity of the porous asphalt and a Plastic Road. Cleaning the porous asphalt and increasing the storage capacity of the porous asphalt allow an increase in stormwater runoff quality (section 7.1.3) and increase the water buffering capacity of the catchment of the road, by retaining water during an extreme precipitation event. Moreover, the increase of porous asphalt can be bridged step by step, to enable the porous asphalt to drain out to the side to satisfy the safety requirement from the ROA (section 7.1.1). The Plastic Road consists of lightweight, modular elements that provide ample

water storage, can easily be installed and have an expected life service of 50 years. The innovation is promising, but a lot of research is required before Plastic Roads are applicable to highways (Williams, 2018).

Moreover, several potential adaptation measures related to creating the storage capacity of the verge exist; removing the top layer of the verge, elongating the infiltration trenches towards the surface, raising the road and creating a descending verge. An infiltration trench is a compact instrument made up of course stones, to enhance the infiltration capacity and to create a reservoir (Van De Ven, 2009). All measures support the water buffering capacity of the road. Overall, the infiltration trench, the removal of the top layer and creating a descending verge perform in a similar manner regarding the criteria (Table 7.2). For all four measures the increase of porous asphalt can be bridged step by step, to satisfy the safety requirement of the verge (section 7.1.1). On the one hand, pollution is removed by removing the top soil of the highway verges to implement the adaptation measure. On the other hand, by removing soil and increasing the infiltration capacity, the filtering capacity of the soil decreases. Thereafter, the effect of the adaptation measure on the water quality is uncertain (Table 7.2). Raising the road does not effect the verge directly and therefore has no impact on the water quality, compared to the current situation (Table 7.2).

Table 7.2: Scorecard of measures; + indicates that the measure has a positive impact on that criterium, while – and – (more significant) indicate that that option has a negative impact. +/- indicates that the effect of the design option could go either way (uncertain). 0 indicates the option has no impact compared to the current situation. WBC = water buffering capacity, TF = traffic flow, WQ = water quality, EV = ecological value, CM = costs and maintenance

| **Measure** | **WBC** | **TF** | **WQ** | **EV** | **CM** |
|---|---|---|---|---|---|
| *New sewer layout* | + | + | +/- | +/- | - - |
| *Increase sewer capacity* | - | + | - | 0 | - - |
| *Install manholes with holes* | - | + | - | 0 | - |
| *Clean ZOABTW* | + | + | + | 0 | - |
| *Increase storage ZOABTW* | + | + | + | 0 | - - |
| *Plastic Road* | + | + | + | 0 | - - |
| *Remove top layer verge* | + | + | +/- | 0 | - |
| *Infiltration verge* | + | + | +/- | 0 | - - |
| *Raise the road* | + | + | 0 | 0 | - |
| *Descending verge* | + | + | +/- | 0 | - - |

## 7.3. Discarded adaptation measures

Several adaptation measures from in the focus group and literature were discarded as a potential measure to counteract flooding due extreme precipitation;

- Widening the roadside verges by either removing a lane or by moving the quays along the highway in order to create more storage has not been implemented. To start with, the measure is in contrast to the former expansion towards a ten-lane road in 2013, due to the economic importance and increase in traffic congestions of the A2 (section 3.1). Moreover, moving the quays towards the Bossche Broek results in a loss of Natura 2000 parts. Additionally, it results in a decrease in the water buffering capacity of the southern and northern Bossche Broek in case of high water levels in the river Dommel (HoWaBo). This is in contradictory to the extra water storage demand of 4.5 million cubic meters in order to meet the regional flooding standard (HoWaBo Story Map, 2021).
- A waterproof underground water buffer (Appendix 6) is aimed at creating more storage in the verge. Compared to the potentially successful adaptation measures in the verge, the underground water buffer results in a relatively poor score on water buffering capacity and water quality. Unlike the other measures, water is not allowed to infiltrate into the ground and thereafter no purification of stormwater runoff takes place. Thereafter, the waterproof underground water buffer was not chosen to be implemented in the Pathway map.
- Installing ditches along the verges is contradictory to the compensatory measures against drought in the Bossche Broek that have been executed in 2000 (section 3.1). Installing ditches results in the capture and relatively fast discharge of rainwater and seepage water between the quays. On the one hand

this results in a delay of the tipping point due to an increase in discharge capacity. On the other hand, this can result in a decrease in the seepage flux in the Bossche Broek and therefore in lower groundwater heads for the Natura 2000 species. The potentially successful measures against flooding provide a higher score on ecological value. Moreover, the installation of ditches along the A2 requires space, which is limited in the catchment of the road. A ditch which is close to the highway imposes extra risks to the traffic flow, in case cars divert from the road into the ditch (RAO). Thereafter it is assumed that increasing the drainage capacity of the A2 is preferably done by a stormwater sewer system instead of a ditch.

- In the focus group pumping the water away from the catchment of the road and using it elsewhere was suggested but it was ranked as a *Thanksless task* by the advisor integral water management, because pumping brings along a lot of management and maintenance effort (Appendix 6). According to RIONED (2015) increasing the dewatering capacity of a system that is dimensioned on storage by installing a pump has little effect on the prevention of local flooding during an extreme precipitation event. In the research a common pumping capacity of 1 mm/h is assumed, which is negligible in comparison to the load on the catchment as a result of an extreme precipitation event. Thereafter, a pump is regarded an ineffective measure during an extreme precipitation event. However, in case of flooding of the A2 a pump can temporarily be installed to remove water out of the catchment of the road.

- Drilling holes in the road to enhance infiltration of water underneath the road has been discarded as a result of expert knowledge. According to the advisor of the department of roads and geotechnics, the bearing capacity of loose-grained materials such as stabilisation sand underneath asphalt is strongly dependent on the moisture content of the soil. Infiltration increases the moisture content of the soil underneath the porous asphalt, which imposes a risk on the bearing capacity of the stabilisation sand underneath the asphalt road.

- The matching solution of storing runoff from other road sections in the southern Bossche Broek for the benefits of nature (Appendix 6) has not been implemented, as the technical implementation of the adaptation measure brings along some difficulties. The transport requires very long pipes, which bring along relatively high investment costs and large pressure losses. Therefore, the requirement which is related to pipe settlement as a result of traffic loads cannot be fulfilled. However, in case of an increase and disconnection of paved surface due to a future road widening of other A2 sections, water can be directed towards other locations in the southern Bossche Broek to be applied usefully. It is also an possible to create additional storage in the form of water tanks, from which water can be pumped towards vulnerable nature when necessary.

## 7.4. Adaptation Pathways maps

### 7.4.1. Reading the Adaptation Pathways maps

Figures 7.12 and 7.13 reveal the Adaptation Pathways for both cross-sections. Each figure contains three Adaptation Pathway maps, one for each scenario. Each map provides an overview of (combinations of) the aforementioned adaptation measures to show routes to a desired state of the catchment of the road. The horizontal axis shows the possible change of the climatic condition, i.e. the precipitation intensity. On the left hand side of the maps, the adaptation measures are listed. The set of actions are divided into actions regarding discharge and storage. These measures have been identified as effective, yet one measure is more effective than the other. In between the listed actions, a grey line indicating the current situation is present. Starting from the current situation, the effectiveness of the various adaptation measures is indicated by associated horizontal lines. For example, in the middle case scenario of Figure 7.12, cleaning the porous asphalt leads to a delay in the tipping point to 32 mm/h. The vertical lines that run from and to a circle indicate how one may switch from one measure to the other. One may for example change from installing manholes with holes to increasing the sewer capacity (Figure 7.12). Sometimes measures can be carried out simultaneously and are effective together. In those cases, this is shown by means of a dotted line. In the example this is amongst others illustrated by the combination of cleaning porous asphalt with removing the top layer of the verge. In the bottom of the graph, the T=10 year design storms according to the climate scenarios from the Dutch meteorological institute are indicated in red. Thereafter, the condition-based pathways can be related to time.

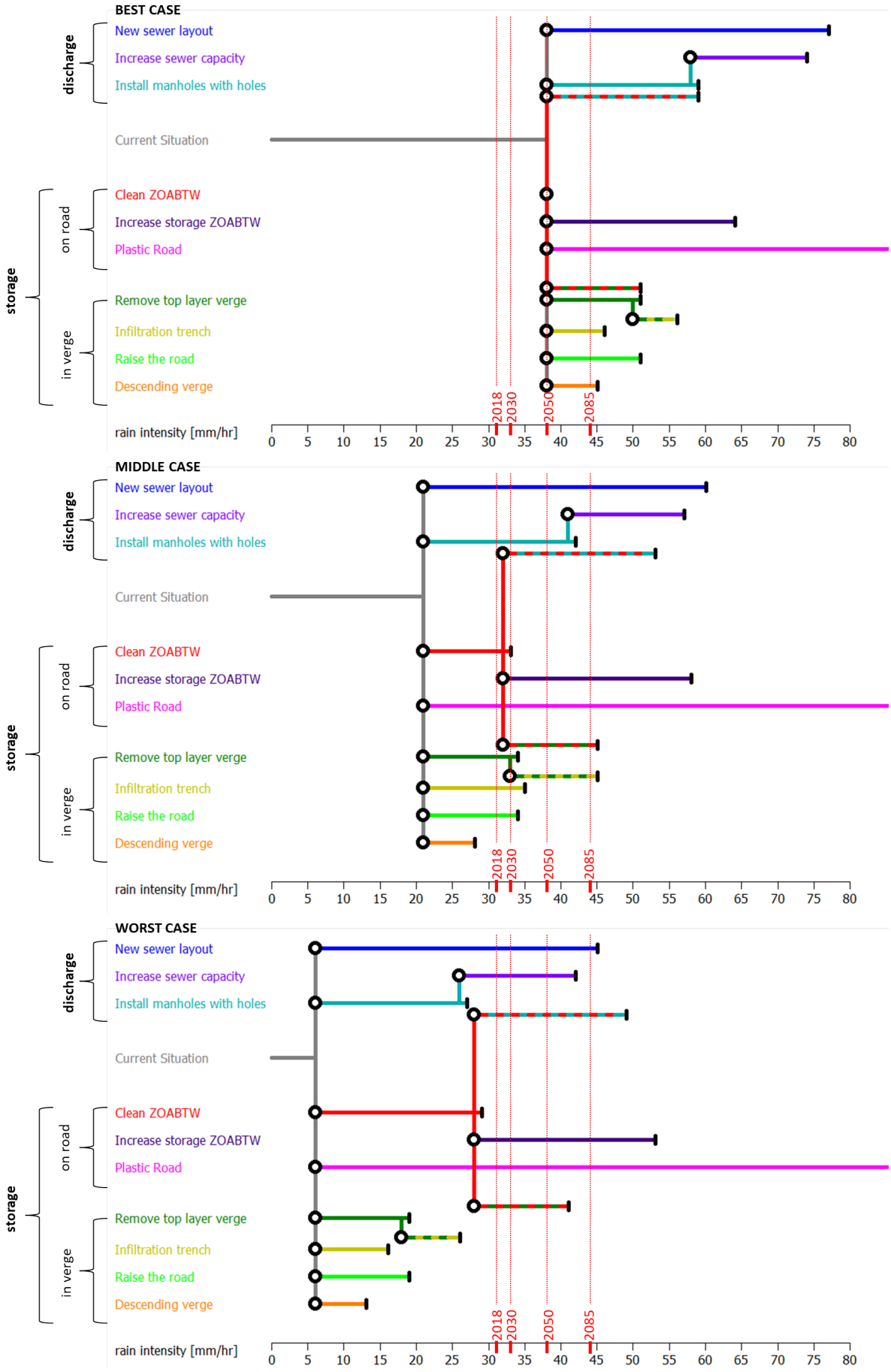


Figure 7.12: Adaptation Pathways for cross-section 119.1

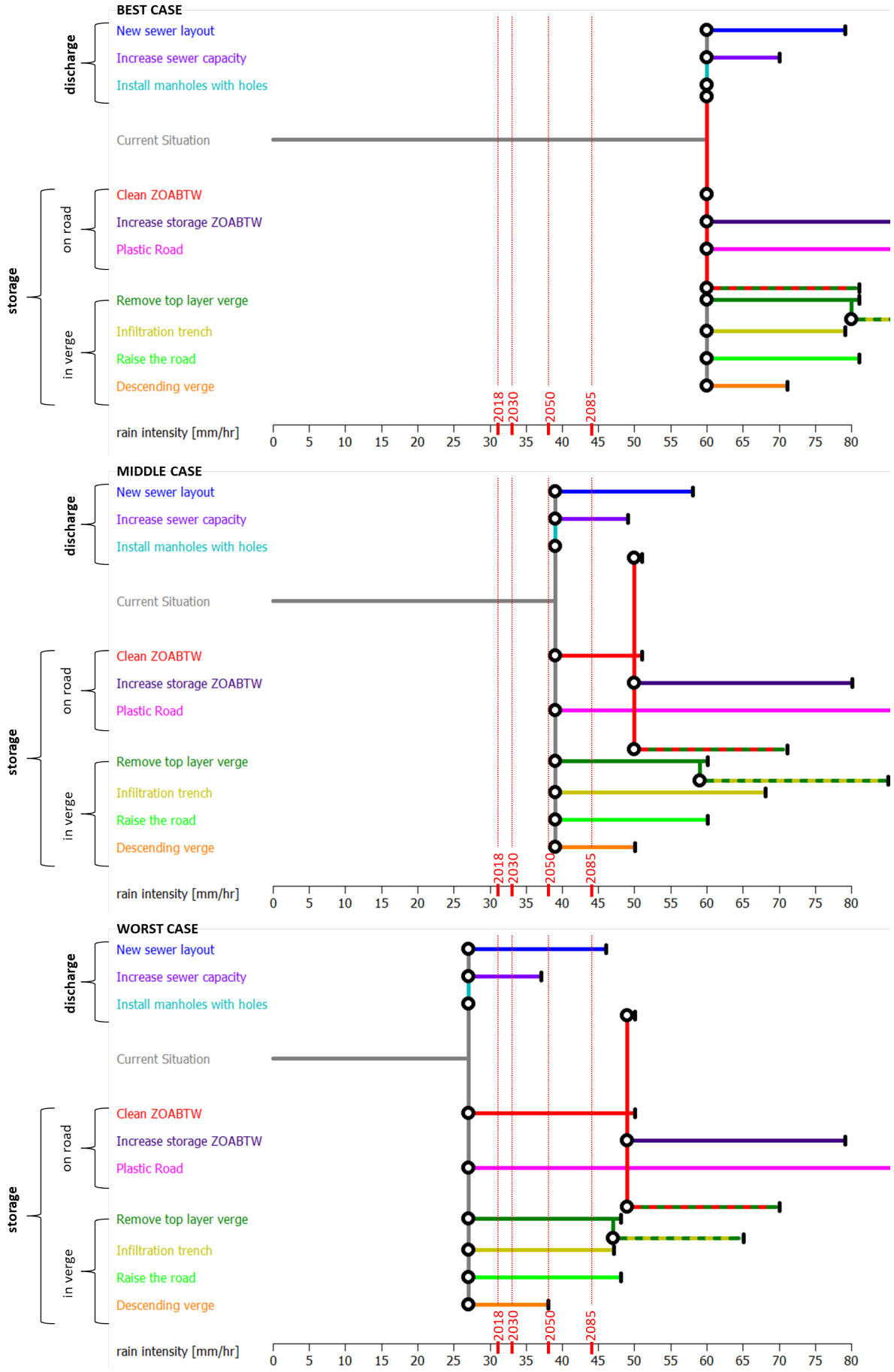


Figure 7.13: Adaptation Pathways for cross-section 119.95

### 7.4.2. Findings from the pathway maps

Figures 7.12 and 7.13 reveal that the overall set of pathways creates a wide range of possible futures. An overview of effectiveness of the individual Adaptation Pathway maps are illustrated in Figure 7.14. Figure 7.14 reveals that the middle case scenario of cross-section 119.95 and the best case scenario of cross-section 119.1 are able to withstand a T=10 year design storm that corresponds with 2050 (Rijkswaterstaat, 2020b). Moreover, the figure reveals that for each cross-section and all scenarios adaptation measures enable the fulfillment of the T=10 design storm that corresponds with 2050 and even the fulfillment of a T=10 design storm that corresponds with 2085.

Regarding Figures 7.12 and 7.13, various observations regarding the effectiveness of types of adaptation measures can be made. To start with, installing manholes with holes at cross-section 119.1 delays the tipping point to values which correspond with the current situation of cross-section 119.95. As aforementioned (section 5.4.2), the presence of a sewer system is thus very influential to the tipping point (Figure 7.14). Thereafter, increasing the discharge capacity of the catchment of the road can be considered an effective measure.

Next, Figures 7.12 and 7.13 show that the storage capacity of porous asphalt largely influences the tipping point. This corresponds with findings from Leijstra et al. (2018).

A difference can be observed in the effectiveness of adaptation measures to increase storage in the verge between Figures 7.12 and 7.13. To start with, the removal of the top layer of the verge leads to a relatively large delay of the tipping point at cross-section 119.95, compared to cross-section 119.1. This difference in delay can be owed to the area ratios of the buckets. Since the available surface area in the verge near 119.95 is larger than the available surface area in the verge near 119.1, the removal of the verge is more effective at cross-section 119.95. The same holds for adaptation measures raising the road and descending verge. Secondly, the application of an infiltration trench leads to a relatively large delay of the tipping point at cross-section 119.95, compared to cross-section 119.1. This difference in delay can be owed to the shallow groundwater heads in the case area. As the installation of an infiltration trench changes the infiltration parameters, it results in saturation excess overland flow in case of an extreme precipitation event (instead of infiltration overland flow in the current situation). Thereafter, the infiltration capacity is dependent on the amount of available storage in the unsaturated zone and thus on the groundwater head. Cross-section 119.1 is characterized by relatively high groundwate heads, in comparison to cross-section 119.95. As a consequence of the availability of space the installation of infiltration trenches is more effective at cross-section 119.95.

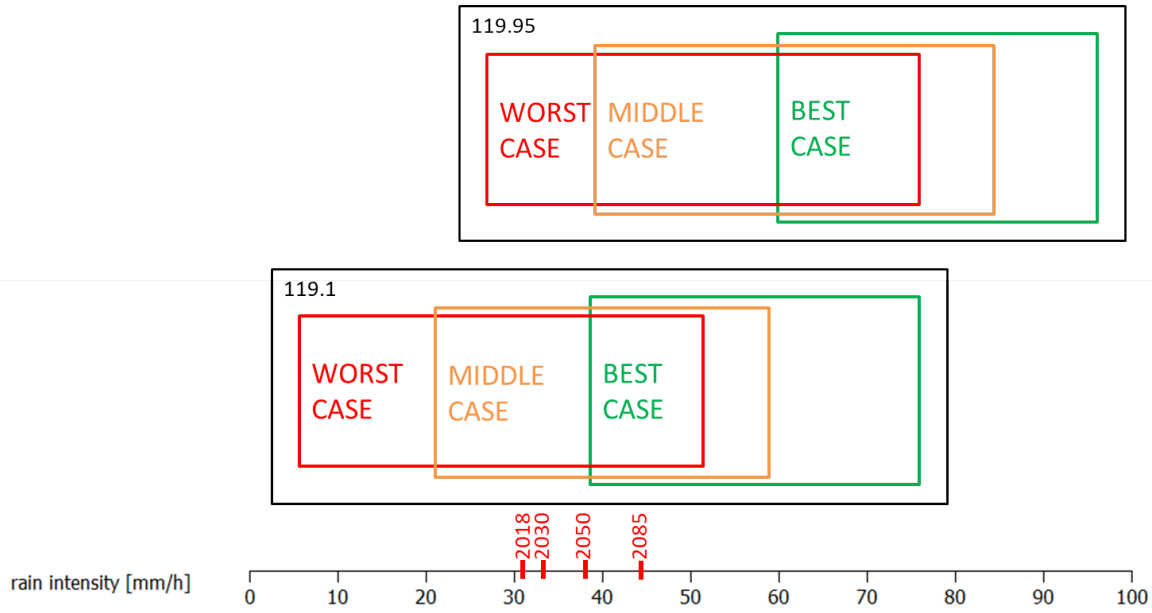


Figure 7.14: Overview Adaptation Pathways

# 8

# Discussion

## 8.1. Comparison with results of other research

### 8.1.1. Plausibility of tipping points

The model structure and associated scenarios result in a broad range of adaptation tipping points; the hourly precipitation intensity at which water exceeds the edge line of the road for a precipitation event with a maximum return period of 10 years varies between 6 and 60 mm/hr for the current situation. Dependent on the scenario, the cross-section which is characterized by manholes without holes has tipping points ranging between 6 and 38 mm/hr, whereas the cross-section characterized by manholes with holes has tipping points ranging between 27 and 60 mm/hr.

Information on the actual occurrence of local flooding and comparison with other research results does not provide clear guidance on assessing the plausibility of the range of tipping points. According to Van Der Biggelaar (2021) the case area is an overall wet area due to high groundwater levels, but local flooding of the road has not occurred so far. This can be supported by consultation of the office for functional traffic systems, which have no record of notifications related to local flooding for the case highway in their Uniform Dry Logging System (UDLS system). On the other hand, the actual occurrence of local flooding of the highway can be considered probable, as the UDLS system solely includes notifications and therefore the occurrence of flooding is not always reported (office for functional traffic systems, 14-5-2021). This hypothesis can be supported by Figure 8.1, which shows washout of the soil next to a manhole near 119.1. Figure 8.1 suggests that in the past accumulation of water as a result of heavy rainfall occurred, thereby washing away the soil. Additionally, regarding the historic precipitation dataset of the automatic Gilze-Rijen weather station (Figure 5.3), it is likely that an extreme precipitation event of 38 mm/h has never taken place at the highway. Such an event is a T=10 design storm for which the system should be designed according to the guidelines of Rijkswaterstaat (Chapter 7).

Next to information on the actual occurrence of local flooding of the highway, the research results by Leijstra et al. (2018) provide no clear guidance on assessing the plausibility of the range of tipping points. Leijstra et al. (2018) designed Adaptation Pathways for the A58 highway as a result of pluvial flooding (section 1.2.2), i.e. overland flow after precipitation in case the water system around the road is not capable for discharge of water (Table 1.2). The Adaptation Pathways reveal a tipping point of the current system after a precipitation amount of 44 mm in 2 hours. According to the rainfall duration lines by Beersma et al. (2018a) a precipitation event of 44 mm in 2 hours corresponds with a precipitation amount of approximately 36 mm in 1 hour. A tipping point of 36 mm/hr is within the tipping point range of this research. However, since the exact definition of the tipping point, information on the hydrological model and input such as case area characteristics are not elaborated on by Leijstra et al. (2018), assessing the plausibility of the broad range of tipping points in this research remains difficult.

Figure 8.1: Wash-out of the soil near a closed manhole near 119.1 (Van Den Biggelaar, 2021).

### 8.1.2. Addressing local flooding of the Dutch national highway network

Overall, this research can be regarded an improvement compared to previous research, i.e. the Climate Effect Atlas and Stresstest (section 1.2.1), as it provides tipping points; this research provides the hourly precipitation intensity at which water exceeds the edge line of the road for a precipitation event with a maximum return period of 10 years. Comparison of this research to the Climate Effect Atlas and Stresstest separately reveals insight on improvements of previous research and on the complementary of this research to previous research.

To start with, various differences between the research results and the Stresstest can be observed. Section 1.2.1 states that the Stresstest provides insight into the vulnerability of the highway network to waterfilm formation at an extreme precipitation event on a grid resolution of 100m, by categorizing the entire HWN (Figure 1.3a). The Stresstest identifies a sensitivity due to the absence of the stormwater sewer on the northern lane corresponding with cross-section 119.1 of the catchment of the road (Figure 1.3a). However, this research reveals that a stormwater sewer is present, but that manholes without holes do not result in discharge through the stormwater system. Whereas the Stresstest only marks the northern lane as sensitive to flooding, this research reveals the presence of closed manholes on the southern lane corresponding with cross-section 119.1 as well. This offers room for improvement of the Stresstest (section 9.2).

This research complements to the Stresstest by addressing the limitation of the lack of analysing the actual impact of flooding by quantifying the impact of a stormwater sewer on local flooding of the highway. Chapter 7 illustrates that the presence of a sewer system is very influential to the tipping point, i.e. the sewer system contributes to a tipping point delay of 20 mm/hr. Thereafter, it can be stated that the Stresstest rightfully identifies the absence of a stormwater sewer as a sensitivity to waterfilm formation.

This research complements to the Climate Effect Atlas by addressing the sensitivity of processes and the influence of local conditions. Section 1.2.1 states that the Climate Effect Atlas provides an indication of the water depth that can occur as a consequence of extreme precipitation events (Figure 1.3b). Limitations of the Climate Effect Atlas are the assumption that all sewer systems function optimally with a uniform sewer discharge capacity of 20 mm/hour, the use of a spatial resolution of 2 by 2 metres based a digital elevation map from 2007 and 2012 and the use of a simplified soil classification (Slager, 2018).

The assumption that all sewer systems function optimally with a uniform sewer discharge capacity of 20 mm/hr corresponds with the sewer calculations from the rational method and hydraulic calculations. Therefore, the assumptions are correct for the case area. In a study by Slager (2018) it was found that under- and overestimations of the sewer system capacity by 50% have significant consequences for the quantification of water depths due to an extreme precipitation event (in the range of 25 to 40%). Moreover, this research reveals that the transport capacity of the sewer system is very influential to the tipping point (Table 5.3). Therefore, adding knowledge on the local operation of the sewer system throughout the HWN can result in significantly different flooding impacts of the Climate Effect Atlas.

Improvements of the research results compared to the Climate Effect Atlas are the use of a spatial resolution of 0.5 by 0.5 metres in determining the depression storage, the use of a detailed soil classification and providing insight into the sensitivity of buckets, fluxes and parameters to flooding. To start with, higher spatial resolution yields depression storage results with a higher accuracy on the spatial scale of local flooding. Table 5.3 stresses the need to improve the Climate Effect Atlas by implementing local knowledge, as the sensitivity to flooding is largely influenced by local conditions such as the interception capacity of the porous asphalt and the infiltration capacity of the soil.

### 8.1.3. Addressing climate adaptation measures for road infrastructure

A similar methodology for addressing climate adaptation measures for road infrastructure was used in the InnovA58 project by Leijstra et al. (2018), i.e. the design of Adaptation Pathways to prevent local flooding of a Dutch highway. The research by Leijstra et al. (2018) corresponds to this research by revealing that an increase in the storage capacity of the catchment of the road or the discharge capacity can facilitate a delay of the tipping point during an extreme precipitation event. For example, an increase in the interception capacity of porous asphalt as well as an increase in the sewer capacity are measures that occur in both studies.

Unlike the study by Leijstra et al. (2018) this thesis contributes to the scientific challenge of societal robustness of local Adaptation Pathways by the use of a scorecard (Table 7.2). In the InnovA58 project it was proved difficult to integrate information from stakeholders with information of the road itself, because the possible measures mainly focus on the functionality of the road and not on making integral solutions to create matching solutions with other goals (section 1.2.2). The combination of the Adaptation Pathways map together with the scorecard provides an assessment of the climate resilience of the A2 as an integral part of the surrounding environment, because it reveals information on effectiveness, as well as societal robustness of adaption measures. The use of a scorecard is that it provides a ranking of measures that can be used in further discussions and decisions regarding adaptation (De Bruin et al., 2009). Since decisions on adaptation at a local scale rely heavily on local constitutes, because of differences in responsibilities and preferences (Barnett et al., 2014), exploring societal robustness through a scorecard can be considered an improvement of the research by Leijstra et al. (2018). As an example, despite its effectiveness (Figures 7.13 and 7.12), increasing the sewer capacity shows a negative score on water quality and water buffering capacity , whereas a new sewer layout could provide matching solutions with other goals such as water quality and ecological value (Table 7.2). Whereas the scorecard provides a ranking of measures, the scores generated in this research do not evaluate the costs and benefits of the various adaptation measures specifically. Solely and indication of the impact is provided. For example, all adaptation measures are expected to have a positive impact on the traffic flow by diminishing local flooding and therefore reducing the impacts of extreme precipitation on the traffic flow (section 1.1.2). Further analysis on the initial and recurrent costs for any actions, but also the costs associated with transferring from one action to another and further analysis on other criteria (Table 7.2) is necessary in order to prioritise adaptation measures (Marchau et al., 2019).

Besides the study by Leijstra et al. (2018), Knott et al. (2019) introduce a hybrid Adaptation Pathways approach to pavement adaptation with climate-change-induced temperature and groundwater rise for a specific case area, i.e. coastal New Hampshire. The hybrid approach is similar to the bottom-up and top-down framework of this research (sections 2.2.2 and 2.3) and showed promising by providing information on both the observed environmental change (top-down) as well as on the asset-specific performance through a vulnerability assessment (bottom-up). Moreover, Heeres (2017) states that integrated planning approaches are increasingly applied internationally such as area-oriented planning in the Netherlands, context-sensitive design in the United States and Infrastruktur in der Landschaft in Germany. The combined use of a scorecard with Adaptation Pathways for climate adaptation of road infrastructure, however, has not been explored before.

Whereas the concepts of resilience, adaptive planning and area-oriented approaches to foster climate resilient infrastructure are frequent in literature, concrete information on climate adaptation is scarce and climate change is not structurally addressed in road infrastructure projects (Picketts et al., 2016; Barten et al., 2017; Leijstra et al., 2018). Barten et al. (2017) illustrates the latter for concrete road infrastructure projects. The study reveals that at the current project of upgrading the provincial highway N65 to four-lane highway climate aspects were not included in the scope of the strategic environmental assessment. Additionally, it illustrates a lack of including all relevant climate effects in road infrastructure projects by discussing the cur-

rent project of adding extra lanes to the A27 highway. In the project the impact of the expansion on the risk of flooding as a result of sea level rise was considered, but other water-related risks due to e.g. extreme precipitation events (Table 1.2) and other climate effects are left out.

Reasons for the relatively slow uptake of climate adaptation planning in road infrastructure are the lack of public priority, legislative reasons, a lack of knowledge and expertise and a difference in the time scale of climate change effects and road infrastructure planning (Picketts et al., 2016; Barten et al., 2017). According to Picketts et al. (2016) a lack of public priority arises from other infrastructure deficits related to asset management, which cause public agencies to be hesitant to consider adaptation actions that increase costs in the short term. Regarding legislative reasons, there are no legislative risks in terms of project rejection in case climate change is not accounted for. Moreover, a lack of knowledge on and uncertainty on climate change risks can be reason for the slow uptake of climate adaptation planning. Finally, climate change is well beyond the planning horizon of infrastructure projects (Barten et al., 2017).

## 8.2. Reflection on the methodology

### 8.2.1. Time series analysis

Section 4.2.1 reveals that the linear groundwater recharge model is performing well with a timestep of $\Delta t = 1$ day. Therefore section 4.2 reveals that the use of TFN models in the case area allows a geohydrologist

1. to understand that overall the precipitation and evaporation stresses are able to explain most of the groundwater head time series.

2. to acknowledge sufficient quality of the available data.

3. to quantify trends in the groundwater system and to forecast the output signal at non-observed periods by generating groundwater statistics, despite the presence of anthropogenic elements such as a stormsewer.

Despite the good fit and lack of trends in the residuals, it is important to note that the length of the time series, inaccurate stresses, groundwater base level d and evaporation factor f can still cause inaccuracies in the TFN simulations (Bakker and Schaars, 2019);

- PASM0001 can be used to illustrate the issue of the length of the time series through the step response (Figures A.1 and A.2). The step response shows the groundwater head response to a continuous rainfall event of 1 mm/d (Collenteur et al., 2019). At a certain point in time the head reaches a constant value, i.e. the gain (Pezij et al., 2020). The gain corresponds with shape parameter A (Table 4.2) and thus reveals how much the groundwater head has risen as a result of the continuous rainfall event of 1 mm/d. The time after which the gain is reached corresponds to the memory of the system. For all groundwater series, but especially for PASM0001, the memory of the system is large compared to the length of the available time series. According to the Pastas simulation of PASM0001, for example, the memory of the system is approximately 600 days, whereas the length of the available groundwater head series is 495 days (Figure A.2). Thereafter, the aforementioned preferred length of several times the memory is not met. Regarding PASM0001, peaks such as the one in March 2020 are underestimated, and lows are overestimated (Figure A.2). PASM0002 and PASM0003, which are characterized by a shorter system memories and a similar observation length compared to PASM0001, perform better at the simulation of peaks and lows. It can be hypothesized that this can be related to the length of the available time series. To reinforce this statement, focus can be put on the base groundwater level. Whereas the calibrated base groundwater levels seem plausible (table 4.2), the calibrated Menyanthes base groundwater level b of PASM0001 is significantly lower than the Pastas base groundwater level of PASM0001. Thereafter, the length of the available time series can be regarded a pitfall for inaccurate TFN modelling.

- The fact that the precipitation and evaporation series are measured at a distance of 28.81 kilometres from the case area can induce inaccurate stresses (Bakker and Schaars, 2019). Especially extreme rainfall events, characterized by little spatial and temporal correlations, that overpassed the case area but did not overpass the automatic weather station of Gilze-rijen or the other way around might not have been covered accurately in the TFN model. This may also be a reason for the poor simulation with a timestep of $\Delta t = 1$ hour.

- Whereas the Pastas groundwater base level d seems physically plausible for all piezometers under consideration, it is prone to hide stresses that do not vary throughout time significantly, such as seepage (Bakker and Schaars, 2019). Thereafter, it can be regarded important to gain insight into the strength of the seepage flux.
- Evaporation factor f can be regarded an uncertainty in time series analysis. The evaporation factor can vary between zero and twice the potential reference evaporation factor. Regarding the results, the value of f is relatively high for PASM0002 and PASM0003 (higher than 1), but relatively low for PASM00001 (lower than 1). At locations PASM0002 and PASM0003, therefore, the potential evaporation is exceeded. This might be an indication for a hidden loss, such as sewer and drainage losses at PASM00002. If sewer discharge were measured, it would therefore be recommended to add the time series to the model as a stress and check whether the addition of the sewer stress improves the model simulation.

Despite the aforementioned potential errors of time series analysis the generated statistics, based on the linear groundwater recharge TFN models, provide an indication of the groundwater dynamics at the three measurement locations in in the case area. Table 4.3 reveals that the different statistic computation methods reveal relatively similar groundwater statistics for a linear groundwater recharge model with a timestep of $\Delta$t = 1 day. Consequently, it can be stated that the generated statistics were rightfully implemented in Chapter 5.

As a result of the large standard errors of the parameters the FLEX model results for non-linear recharge were not apprehended in the bucket approach. Section 4.2.2 used the FLEX recharge model to study soil water dynamics in the unsaturated zone and to test the new development in TFN modelling of calibrating parameters associated with rainfall-runoff models using groundwater levels without the necessity of adding much data. The results of the TFN modelling with the non-linear groundwater recharge revealed large standard errors and significant differences between the parameters values of the three piezometers in the case area (Table 4.4). According to Collenteur et al. (2020) physical interpretation of the calibrated parameters using the FLEX recharge model must be done with caution, since the TFN models do not consider the physical lower and upper limits of soil moisture and are prone to the aforementioned uncertainties. Possible causes for the large differences between the parameter values and large standard errors in the research results are an insufficient warm-up period due to a limited length of the time series head observations, feedback between the groundwater and the root-zone, missing or incomplete stresses (e.g. sewer discharge), missing processes (e.g. the fast reservoir in the FLEX model), inaccurate fixation of the $S_{i,max}$ and $l_p$ and a change in the system behaviour (Bakker and Schaars, 2019; Collenteur et al., 2020).

### 8.2.2. Bucket approach

Several assumptions and simplifications were made in the model structure which impact the legitimacy of the results. To start with, the assumptions on a homogeneous precipitation and no routing in the case area imply that the model is applicable at the neighbourhood scale. Moreover, the assumptions on an unlimited storage and discharge capacity of the Dungense ditch and on leaving out processes such as evaporation, horizontal runoff through porous asphalt and discharge by drainage pipes imply that the model is suitable for the short time scale. As a consequence of the aforementioned assumptions on spatial and temporal scale, the bucket model is suitable for simulating local flooding, but not for modelling other climate effects. For example, the duration and geographic extent of the climate effect flooding as a result of the failure of a flood defence is a climate effect with a spatial extent of numerous square kilometres and a duration of weeks to months (Table 1.2, Figure 8.2). Another example is the climate effect of drought, which must be studied for a larger spatial and temporal scale compared to flooding (Figure 8.2).

Whereas the use of two different cross-sections accounts for heterogeneities such as differences in cross-slope of the highway and the type of manhole, i.e. with or without holes, the use of two typical cross-sections for quantifying the tipping point leaves no room for heterogeneity within the cross-sections. According to Nijzink et al. (2016) it becomes increasingly problematic in hydrological modelling to treat catchments as a group of homogeneous buckets when the catchment size increases, as a result of heterogeneities within the catchment. Heterogeneity in the subsurface of the cross-sections is likely due to the soil composition (section 3.2). The three scenarios embed parameter uncertainties, amongst others induced by soil heterogeneity, and therefore represent a plausible range of parameters in which heterogeneity can occur. Spatial heterogeneity along the A2 was embedded in the depression storage calculations, by using the Dutch Digital Elevation Model AHN3 with a grid resolution of 0.5 by 0.5 metres. Herein, it is assumed that the depression storage is

filled in case water starts exceeding the edge line of the road somewhere in a grid cell of 0.5 by 0.5 metres along the cross-section under consideration. Therefore, the tipping point for the cross-section is associated with a critical location along the cross-section where the edge line is exceeded first during an extreme precipitation event. In reality spatial heterogeneity in the verge results in different tipping points for each grid cell along the edge line. However, since local flooding has cascading effects on the traffic flow throughout road networks, e.g. congestions (Snelder and Calvert, 2016), the assumption of choosing the critical location which is most sensitive to flooding can be regarded acceptable.

Additionally, interaction between cross-sections within the case area is not represented by the bucket approach. By determining the tipping points for cross-sections, one can easily overlook the interaction between the cross-sections, i.e. the transitions between road sections. As aforementioned, transitions between road sections with opposite slopes are prone to hydroplaning accidents due to the accumulation of runoff at the zero slope in the centre of the transition (Bles et al., 2012).

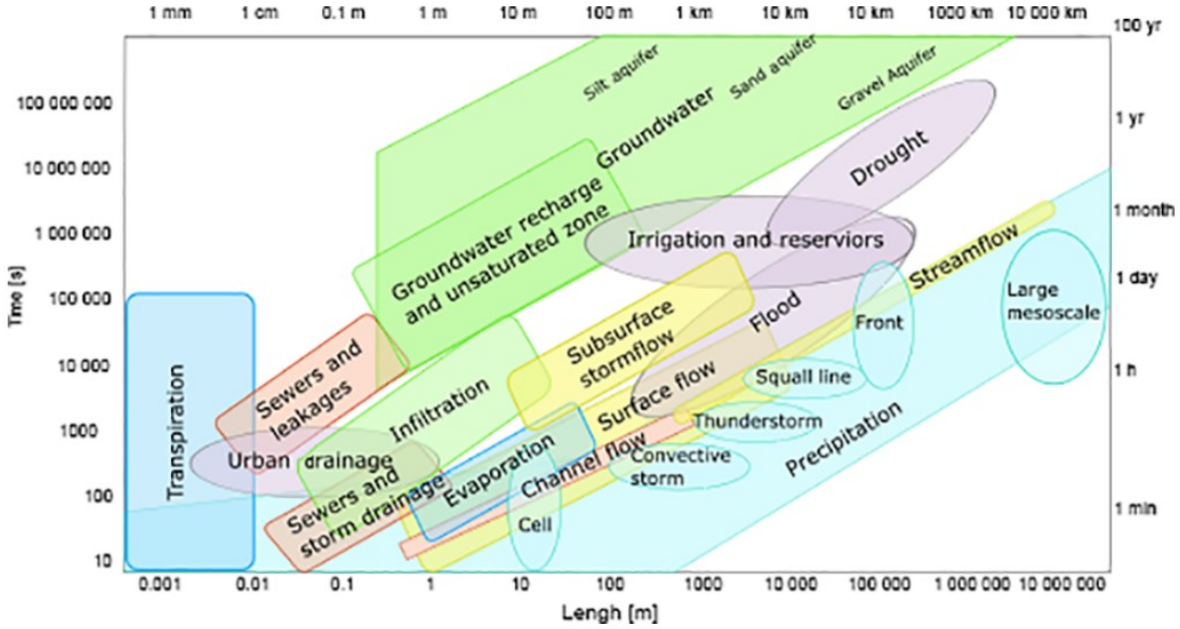


Figure 8.2: Spatial and temporal scale variability of hydrological processes with processes related to the atmosphere (in blue), the surface (in yellow), the underground (in green) and urban areas (in red). Grey circles reveal problems for society that can be caused by hydrological processes, e.g. flood and drought (Cristiano et al., 2017).

### 8.2.3. Complementarity of a bucket approach with time series analysis

A computational model can serve as a fast, integrated model and is therefore preferred over time-consuming, computationally expensive, complex models in case of exploratory research such as designing Adaptation Pathways (Haasnoot et al., 2013; Manocha and Babovic, 2017). The bucket model structure therefore can be regarded satisfactory for the main purpose of this research. However, the model results should be handled with care as a result of the simplifications in e.g. time, space and processes and require rigorous testing and calibration (if used in decision-making) (section 8.1.1). According to Gharari et al. (2014) and Nijzink et al. (2018) constraining a model with multiple information sources can enhance hydrological modelling. In order to improve the predictive potential of bucket models, complementary use of data-based time series analysis with a bucket approach was thereafter explored.

In this thesis the data-based approach of time series analysis and the conceptual bucket approach were made compatible by implementing groundwater dynamics, generated with time series analysis, as boundary conditions in the bucket approach. Both Obergfell et al. (2019) and Collenteur et al. (2020) recommend the complementary use of the synergies of conceptual hydrological models with time series analysis. Whereas the conceptual model allows simulation of catchments in a schematic fashion, time series analysis was used to constrain groundwater dynamics. Despite the complementary use of a bucket approach with time series analysis the model structure and associated scenarios resulted in a broad range of adaptation tipping points.

A reason for this is the limitation of insufficient data to constrain parameters and to calibrate and validate the bucket approach.

As the sensitivity to flooding is largely influenced by local conditions it can be argued that distributed modelling is preferable over lumped modelling to simulate local flooding. Whereas lumped models consider the catchment as an entity, distributed models can be regarded as lumped models that are implemented at finer grid scale by breaking up the system in small compartments. The level of complexity and detail of a distributed model remains under debate (Gharari et al., 2014; Hrachowitz and Clark; 2017). This thesis contains a distributed modelling element, i.e. quantification of the depression storage by using a grid resolution of 0.5 by 0.5 metres to understand how overland low runs spatially. Whereas spatial variability on ground level is available, high-resolution data of infiltration, storm-sewer discharge and interception by porous asphalt are not available. Next to being computationally expensive and complex a distributed model will in this thesis likely neither improve understanding of the hydrological processes, nor will it improve the plausibility of the tipping points. According to Cristiano et al. (2017) and Hrachowitz and Clark (2017) the spatial scale of observations can be related to this. For example, two soil core samples were used to determine the soil hydraulic conductivity (section 3.2). By assuming that the samples represent the much larger modelling unit the heterogeneities such as macropores and other soil matrix features are not warranted for. Moreover, prediction the hydrological behaviour of a non-linear system by increasing complexity through distributed modelling is problematic because of the combined effects of limited observation accuracy and representativeness.

### 8.2.4. Focus group

The use of a focus group impacts the collection of qualitative data. A focus group can be regarded a suitable method to explore complex issues than other forms of survey research, because it facilitates discussion between participants (Kitzinger, 2005; Bhattacherjee, 2012). Therefore, responses or ideas that participants did not think about before can be triggered. However, potential disadvantages of focus groups are domination by a dominant personality and reluctance to voice opinions, especially when dealing with a sensitive issue such as politics (Kitzinger, 2005; Bhattacherjee, 2012). Next to these potential disadvantages, the focus group in this research did not include stakeholders from Staatsbosbeheer, Brabants Landschap, inhabitants in the case area and road users. Thereafter, objectives and constraints regarding flooding due to extreme precipitation might not have been identified. Due to the limitations of the focus group in the research, the objectives and constraints of (missing) stakeholders must further be explored further before preferred pathways can be selected. Nevertheless, the focus group encouraged the participants to explore societal robust measures against flooding of the A2 due to extreme precipitation.

### 8.2.5. Adaptation Pathways

The use of Adaptation Pathways for measures to prevent local flooding on the Dutch national highway network allows clear visualization of effectiveness of measures and provides the means of motivating decision-makers to accommodate for future developments (section 1.2.2). However, this sections reveals several limitations of Adaptation Pathways and reflects on the use of Adaptation Pathways.

Whereas the Adaptation Pathway maps (Figures 7.12 and 7.13) reveal a wide range of plausible futures, no information on responsibility and no decision moments are provided and non-quantifiable adaptation measures are not included. In the focus group two non-quantifiable measures were suggested; monitoring and a discussion between stakeholders on the acceptable flooding standards for the A2, regarding the various goals in the case area, such as mobility, HoWaBo 2.0 and Natura 2000 (Chapter 6).

Adaptation Pathways maps do not provide an indication on responsibility and provide no decision moments. According to De Bruin et al. (2009), it is crucial to create transparency on the responsibilities of the various stakeholders in order to deal with the impacts of climate change. Whereas no responsibilities are illustrated on the map, Adaptation Pathways maps can serve as a starting point for the discussion on responsibilities in climate adaptation. Additionally, the Adaptation Pathways can facilitate a discussion on urgency, in order to establish the decision moment on the implementation of measures.

A non-quantifiable adaptation measure is monitoring, since it does not directly influence the delay of the tipping point, nor does it influence the criteria. However, despite not being present in the Adaptation Pathways map, monitoring is considered an important step towards choosing preferred pathways and designing

an adaptive plan. Monitoring the system can for example enhance the understanding of the hydrological system by improving the modelling results and can thus result in a more narrow, plausible range of the tipping points for the various scenarios. Thereafter, decision-makers can be better informed on the effectiveness of adaptation measures.

Another non-quantifiable adaptation measure that is not presented on the Adaptation Pathways map is the discussion between stakeholders on the acceptability of flooding standards for the A2, regarding the various goals in the case area, such as mobility, HoWaBo 2.0 and Natura 2000 (Chapter 6). Discussion can be regarded important to make decisions on the urgency of the various objectives and constraints related to different goals. For example, the flooding of the highway in 1995 provided enough sense of urgency to change the current water management strategies and to create room for storage in the southern and northern Bossche Broek. However, the current plans to raise the surface water level of the Zuiderplas and groundwater levels in the Bossche Broek to favour Natura 2000 areas results in a loss of storage for HoWaBo. Moreover, the urgency of extreme precipitation events on the A2 in relation to flood peaks of the river Dommel is another consideration. The latter can be elaborated on by relating the occurrence of an extreme precipitation event to the occurrence of simultaneous flood peaks. According to Geertsema et al. (2018) a strong seasonality in the occurrence of discharge peaks can be observed, with peaks only occurring in the period November to March. The most extreme precipitation events occur during summer. As a result, the timing of the nine highest discharge peaks in the Meuse and Dommel does not match with the nine highest precipitation peaks (Geertsema et al., 2018). Whereas the timing of the events is different, adaptation measures that contribute to the water buffering capacity of the catchment of the road or the case area can influence the hydrological system throughout the year and thereby can influence the availability of storage in the Bossche Broek in times when storing a discharge peak of the river Dommel is required.

Further elaborating on the acceptability of flooding, the definition of tipping points in Adaptation Pathways can be discussed. In this thesis the definition of the tipping point is based on the deep uncertainty of climate change in extreme precipitation. Therefore, the tipping point is defined as the hourly precipitation intensity at which water exceeds the edge line of the road for a precipitation event with a maximum return period of 10 years. This definition is based on the requirements with respect to the stormwater drainage as defined by Rijkswaterstaat. Under the current policy local flooding due to precipitation events exceeding 38 mm/hr is acceptable, i.e. the hourly precipitation intensity with a maximum return period of 10 years of the 2050 rainfall duration line (Table 7.1). From this viewpoint failing to meet the objective rather than climate adaptation is the driver for taking action against climate change (Kwadijk et al., 2010). Thus, different flooding standards directly influence the tipping points. The tipping points of Figures 7.12 and 7.13 reveal the hourly precipitation intensity at which water exceeds the edge line of the road for a precipitation event with a maximum return period of 10 years. The figures thus do not directly indicate the acceptability of local flooding. The advantage of this is that significant deviations from the expected rate of increase in extreme precipitation intensities will inform decision-makers about the necessity to delay or accelerate the program (Bloemen et al., 2018). For example, a change in the stormwater drainage requirement to a 2085 rainfall duration line, the Adaptation Pathways map can still be used. In case of a change in rainfall duration lines of design storms (Table 7.1) the red lines of Figures 7.12 and 7.13 can simply be moved.

Next to climate change, deep uncertainty in infrastructure arises from technological breakthroughs, economic developments, shifts in preferences and objectives of stakeholders related to traffic flow (Marchau et al., 2010; Haasnoot et al., 2013). Milakis et al. (2017) illustrate an example of deep uncertainty, i.e. the emergence of automated driving technology. Deep uncertainty in this example arises from the lack of knowledge on to what extent automated vehicles will emerge on the market and on how automated driving technology will affect traffic flow. Another example of deep uncertainty in infrastructure arises from the COVID-19 pandemic. As a consequence of the pandemic a shift in preferences and objectives of stakeholders related to traffic flow is observed, but the future development of the shift is deeply uncertain (Corker et al., 2021). For example, on the one hand a continuation of working at home might result in a decrease of road use. On the other hand the individual use of private cars as a mode of transport might regain importance, due to the protection it offers compared to public transport. Uncertainty has been considered in transport policy and planning since the 1990s as a result of unfavourable impacts of policy measures, large budget overruns and incorrect forecasts of future transport demand. Traffic flow is subject to uncertainty in many ways, e.g. by stakeholder dynamics, and therefore ways uncertainty can or should be taken into account in traffic policy-

making are still developing (Marchau et al., 2010; Van Geenhuizen et al., 2016). Thus, whereas this thesis focuses on local flooding as a result an increase of extreme precipitation due to climate change, tipping points might have ecological, technical, political, economic and societal causes (Kwadijk et al., 2010; Marchau et al., 2010; Haasnoot et al., 2013; Manocha and Babovic, 2017).

Another limitation of Adaptation Pathways is that practice shows that the selected pathways often lead to short-term, reactive incremental measures, instead of pro-active, anticipating transformative measures (Kates et al., 2012; Roggema et al., 2012; Bloemen et al., 2018). As infrastructure is characterized by long lifespans, tends to be capital-intensive and inflexible, incremental measures in infrastructure are characterized by path dependency. Path dependency can be defined as a decreased flexibility which leads to inefficacy as the environment, climate and socio-economic conditions change over time. Consequences of path-dependencies are unused assets, costly retrofitting and large costs for the implementation of alternatives (Haasnoot et al., 2019). An example of a path-dependency is the Dutch Maeslant barrier, a €450 million investment originating from the 1990s in order to improve the Maeslant barrier. However, it is expected that appropriate functioning of the barrier will stop approximately 25 years before the design life time as a result of sea level rise. In case the functional lifespan of the barrier ends, the barrier must close and will thereby impede a major global trade hub. The costs associated with replacing and dismantling the barrier account to €966 million (Haasnoot et al., 2019).

The Adaptation Pathways designed in this research reveal incremental measures too. Figures 7.13 and 7.12 reveal that adaptation measures related to increasing discharge of the road and cleaning porous asphalt are incremental measures to effectively delay the tipping point. However, the scorecard reveals that by increasing the capacity of the sewer system, negative impacts regarding water buffer capacity and water quality occur (Table 7.2). Additionally, cleaning porous asphalt is a weak link in the system, as the current HWN is already faced by deferred maintenance. Incremental measures related to existing omnipresent infrastructure throughout the HWN, such as sewers and porous asphalt, therefore impose path-dependencies.

According to Kates et al. (2012) reasons to not implement anticipatory transformational adaptation measures are uncertainties about climate change risks and adaptation benefits, costs of transformational actions and the habit of maintaining existing policies. However, as a result of climate change, transformational measures of drastic interventions, altering the system in a fundamental way are required (Bloemen et al., 2018). Initiating transformational adaptation requires supportive social contexts by maximizing broad commitment and fostering free thinking space for the consideration of actions that do not seem politically or financially acceptable in the short term (Kates et al., 2012).

The Adaptation Pathways designed in this research reveal transformational measures too. In order to create matching solutions to enhance societal robustness of adaptation measures, the combination of the Adaptation Pathways map with the scorecard reveals that one should focus on achieving hydrologic neutrality (Figures 7.13 and 7.12 and Table 7.2). This can be achieved by mimicking pre-development hydrological conditions in the case area, either by storing precipitation in the catchment of the road or by discharging precipitation to a nearby location outside the catchment of the road, where it is used. Thereafter, one could put forward a transformational change to measures that make the highway hydrologically neutral (section 8.3.3). Aditionally, the Plastic Road is an example of a transformational measure that could provide the road to an innovative, circular alternative for the weak link porous asphalt. The PlasticRoad has advantages such as direct placement on the sandbed, a long life time and creating a hydraulicaly neutral highway by temporary storage followed by infiltration into the subsurface.

## 8.3. Reflection on possibilities for generalization

This study provides an innovative approach for designing Adaptation Pathways of measures to prevent flooding as a result of extreme precipitation on the Dutch national highway network, by combining the synergies of a bucket approach and time series analysis with Adaptation Pathways with a scorecard. The research results and methodology offer opportunities for generalizability of the study.

### 8.3.1. Generalization of adaptation measures against local flooding to the HWN

This research can be generalized to other locations along the HWN, by creating clusters of potentially successful adaptation measures regarding soil characteristics and land use. Creating clusters can be serve as a starting point to fulfil the second ambitions of the Climate-proof Networks project, i.e. creating an overview of how to act in order to the HWN set up in a water-resilient manner by 2050 (section 1.2.1). Tables 8.1 and 8.2 define several soil and landuse types and their main characteristics relevant to local flooding of the HWN and adaptation measures. The case area is located on the transition between the relatively high sandy soils and the fluviatile soils and is surrounded by nature, i.e. the Bossche Broek.

Potentially successful adaptation measures against local flooding of the HWN on peat and clay grounds are related to storage of precipitation on the road and to discharging water out of the catchment (section 7.2). As a result of a low infiltration capacity and a limited availability of space in the verges between the groundwater head and ground level, creating infiltration facilities in the verge is not considered effective here. In sandy grounds, on the other hand, the high infiltration capacity and large availability of space with respect to the groundwater head enable the application of infiltration and storage facilities in the verge (section 7.2). Fluviatile and anthropogenic soil types show varying characteristics. Thereafter, local conditions should be studied in order to decide on suitable adaptation measures.

Table 8.1: Soil types and its main characteristics relevant to local flooding of the HWN (Veld and Zwaan, 2021).

| **Soil type** | **extent of HWN on soil type [km]** | **infiltration capacity** | **elevation with respect to NAP** |
|---|---|---|---|
| *Sand* | 3425 | high | high |
| *Clay* | 2314 | low | low |
| *Peat* | 603 | low | low |
| *Fluviatile* | 1074 | varying | varying |
| *Anthropogenic* | 737 | varying | varying |

As a result of the limited availability of space in case an urban area surrounds the HWN, potentially successful adaptation measures against local flooding of the HWN are related to storage on the road and in the verge. In rural and nature areas, successful adaptation measures against local flooding can be related to increasing storage in the catchment and discharge.

Table 8.2: Land use surrounding HWN and its main implications for climate adaptation measures against extreme precipitation (Veld and Zwaan, 2021).

| **Land use** | **extent of HWN on land use type [km]** | **main implication for climate adaptation measures** |
|---|---|---|
| *Urban* | 1296 | limited availability of space<br>high concentration of paved surface |
| *Rural* | 4625 | much available space |
| *Nature* | 1904 | much available space<br>matching solutions for nature |

Whereas soil type and land use help to cluster potentially successful adaptation measures, it can be noted that adaptation measures related to storage of precipitation on the road are successful regardless of soil type and land use.

### 8.3.2. Generalization of methodology for addressing climate adaptation of road infrastructure

Firstly, the conceptual bucket approach can be generalized to the design of Adaptation Pathways for other highways, both nationally as well as internationally as well as for a variety of climate effects. A reason for this is that a bucket model serves as a fast, integrated model, fit for the exploratory design of Adaptation Pathways (Haasnoot et al., 2013; Manocha and Babovic, 2017). Another reason for the possibility for generalization of the bucket approach is its model structure. According to Hrachowitz and Clark (2017) all models need to have the same fundamental model structure to reflect our conceptual understanding on the partitioning of fluxes in a hydrological system. Figure 5.1 reflects a similar fundamental model structure in the partitioning of all relevant water fluxes for two cross-sections, which can form the basis bucket models at other highways.

Parametrization and assumptions on the relative importance of fluxes related to the spatial and temporal extent of a climate effect can thereafter tailor the bucket model to any case highway and climate effect.

Secondly, the approach of Adaptation Pathways with a scorecard can be generalized to climate adaptation of road infrastructure. The combination of Adaptation Pathways with a scorecard provides an assessment of the climate resilience of a highway as an integral part of the surrounding environment, because it reveals information on effectiveness, as well as societal robustness of adaption measures. This facilitates the decision making by offering intuitively understandable visualizations of policy options, by stimulating planners to include adaptation over time and to raising awareness about the challenges of adaptation (Marchau et al., 2019; De Bruin et al., 2009). Heeres (2017) state that paying appropriate attention to inter-relatedness between infrastructure and its surrounding environment can lead to synergies between road network development and local improvements in an area. Integrated planning approaches are increasingly applied internationally, such as area-oriented planning in the Netherlands, context-sensitive design in the United States and Infrastruktur in der Landschaft in Germany (Heeres, 2017). It can be argued that the approach of Adaptation Pathways with a scorecard can be generalized internationally to provide an effective method for integrated planning approaches to assess climate change vulnerability and potential measures for road infrastructure and to increase adaptive design of road infrastructure.

### 8.3.3. Generalization of a paradigm shift towards water neutral highways

In this study the combination of the Adaptation Pathways map with the scorecard reveals that one should focus on achieving a hydrologically neutral highway in order to create matching solutions to enhance societal robustness of adaptation measures (Figures 7.13 and 7.12) and Table 7.2). This can either be done by storing precipitation in the catchment of the road or by discharging precipitation to a nearby location outside the catchment of the road, where it is used. Thereafter, one could put forward a transformational change to measures that make the highway hydrologically neutral. Since initiating transformational adaptation requires supportive social contexts by maximizing broad commitment, it can argued that a paradigm shift towards storing water locally is successful for this case (Kates et al., 2012).

Making the highway hydrologically neutral complies with the principles of systematic water management of the $21^{st}$ century and low impact development. The principle of systematic water management of the $21^{st}$ century is based the Dutch National Policy on Water Management for the $21^{st}$ Century and was established in 2000 as a result of the need for a new water management paradigm (Jiggins et al., 2007; Verdonschot and Verdonschot, 2020). In the 1990s water managers started understanding that the water system, efficient as it might be, lacked resilience in the face of extreme events (Jiggins et al., 2007). Therefore, a paradigm shift towards "living" with water, in which the order of preference for water management consists of four steps: 1) direct utilization of precipitation, 2) infiltration 3), water retention and 4) runoff to surface water (Figure 8.3).

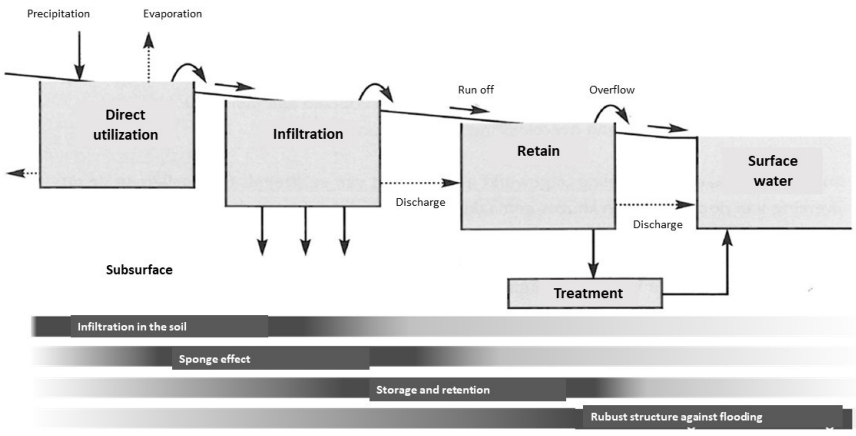


Figure 8.3: Schematic overview of the four steps of the systematic water management of the 21st century (Veld and Zwaan, 2021).

Low impact development (LID) describes an approach that aims at achieving hydrologic neutrality in managing stormwater water management. (Eckart et al., 2017). According to Eckart et al. (2017) and Pour et al. (2020), major cities around the the world incorporate LID measures into their stormwater management plans and regulatory bodies. Examples of measures are storage for runoff volumes and infiltration improvements. As the transformational adaptation measures comply with the systematic water management of the $21^{st}$ century and low impact development, one could argue for generalization of a transformation towards hydrologically neutral highways. Whereas Adaptation Pathways promote incremental changes such as cleaning asphalt and enlarging the sewer capacity which enhance path-dependency (section 8.2.5), the combination of Adaptation Pathways with a scorecard provides insight on transformational adaptation measures. The use of Adaptation Pathways with a scorecard fosters free thinking space for the consideration of actions that do not seem politically or financially acceptable in the short term. As the transformational adaptation measures comply with the systematic water management of the $21^{st}$ century and low impact development, one could argue for generalization towards hydrologically neutral highways. This implies that perhaps we should drop the sewer networks (internationally) on the long-term, and find alternatives for the weak link of porous asphalt to mimic the natural water cycle, for example by the Plastic Road.

# 9

# Conclusion and recommendations

## 9.1. Conclusion

This main objective of this research was: **to design Adaptation Pathways of measures to prevent flooding as a result of extreme precipitation on the Dutch national highway network.** In the attempt to achieve this objective, five research questions were defined that focus on quantifying local flooding of the Dutch national highway network with respect to scenarios, identifying possible measures to control flooding, identifying the interests of stakeholders, designing Adaptation Pathways and generalization of the research. Hereto, two typical cross-sections of the case area, i.e. the A2 between the Vught and Sint-Michielsgestel junctions, were defined.

Hydrological modelling through the complementarity of time series analysis with a bucket approach quantitatively describes local flooding of the A2. Time series analysis of the available groundwater head series with a net recharge based on a linear function of precipitation and evaporation proved complementary to the bucket approach as a tool to constrain groundwater dynamics as boundary conditions in the bucket approach to the mean high and low groundwater levels. It was found that calibrating rainfall-runoff parameters, such as the saturated hydraulic conductivity, through time series analysis of the available groundwater head series with a net groundwater recharge based on a non-linear response of recharge to precipitation using soil-water balance concepts of the FLEX model proofed unsuccessful. An insufficiently long length of the available time series of approximately 500 days and the exclusion of anthropogenic reservoirs such as a stormsewer are reasons for the latter. In the bucket approach three plausible scenarios that reflect the increase in extreme precipitation intensities due to climate change were generated to embed uncertainties in interception and infiltration parameters and variations in the boundary conditions of groundwater levels; a worst case, a best case and a middle case scenario. Whereas the worst and best case represent extreme values of parameters and boundary conditions, the middle case is an educated guess. The bucket approach, complemented by the groundwater dynamics of time series analysis, quantified a plausible range of tipping points between 6 and 60 mm/hr for the current situation, depending on the scenario and the cross-section. The tipping point refers to the hourly precipitation intensity at which water exceeds the edge line of the road for a precipitation event with a maximum return period of 10 years. Processes that influence local flooding are interception by porous asphalt and the verge, infiltration and sewer discharge. It was found that the processes of interception by porous asphalt and sewer discharge are most influential to delay the tipping point, whereas infiltration is the least influential to delay the tipping point. The broad range of tipping points reveals that the sensitivity to flooding is largely influenced by local conditions such as the interception capacity of the porous asphalt and the infiltration capacity of the soil.

Adaptation measures that result in (1) an increase in the storage capacity of the catchment of the road (either on the road itself or in the verge) or (2) an increase in the discharge capacity of the catchment of the road were identified as possible measures to prevent local flooding of the A2 between the Vught and Sint-Michielsgestel junctions, based on the processes that influence local flooding. Possible adaptation measures to increase the storage capacity on the road that were identified are cleaning porous asphalt, increasing the thickness of the porous asphalt and installing a Plastic Road. Possible adaptation measures to increase the storage capacity of

the verge that were gathered are removing the top layer of the verge, installing an infiltration trench, raising the road and creating a descending verge. Moreover, it was found that an increase in the discharge capacity of the catchment of the road can be established through a new sewer layout, increasing the sewer capacity and installing manholes with holes.

A focus group revealed the possible measures against local flooding of the A2 and interests of stakeholders with respect to flooding. (1) Traffic flow, (2) water buffering capacity, (3) water quality, (4) ecological value and (5) costs and maintenance reflect the criteria relevant to the stakeholders of the focus group and therefore provide information on the societal robustness of an adaptation measure. A societal robust adaptation measure meets multiple objectives of the relevant stakeholders over many scenarios and therefore provides a better trade-off than other potential adaptation measures in the Adaptation Pathways map. A scorecard provides the means to rank the potential adaptation measures according to the defined criteria. The scorecard revealed that measures related to storing precipitation in the catchment of the road or to discharging precipitation to a nearby location outside the catchment of the road where it is used are societally robust.

The design of Adaptation Pathways for measures to prevent local flooding on the Dutch national highway network revealed a wide range of possible futures for the defined measures, in which the fulfillment of the T=10 year design storm that is associated with 2050 requirement is either already met or possible through the implementation of adaptation measures. The combination of the Adaptation Pathways map together with the scorecard provided an assessment of the climate resilience of the A2 as an integral part of the surrounding environment, by revealing information on effectiveness, as well as societal robustness of adaption measures. It was found that the designed Adaptation Pathways promote incremental changes, such as cleaning porous asphalt and enlarging the sewer capacity, which enhance path-dependency. Moreover, it was discovered that using a combination of Adaptation Pathways with a scorecard provides insight on transformational adaptation measures that focus on achieving hydrologic neutrality. Hydrologic neutrality can be either be achieved by storing precipitation in the catchment of the road or by discharging precipitation to a nearby location outside the catchment of the road, where it is used.

It was found that the research results can be generalized in multiple ways. The applicability of adaptation measures at other locations along the HWN can be generalized through defining clusters of potentially successful adaptation measures regarding soil characteristics and land use. Overall, adaptation measures related to storage of precipitation on the road are successful, regardless of the soil characteristics and land use. Next, the conceptual bucket approach can be generalized to the design of Adaptation Pathways for other highways, both nationally as well as internationally as well as for a variety of climate effects. Reasons for this are its fundamental model structure and its fast, integrated modelling abilities which are preferable for exploratory research such as designing Adaptation Pathways. Additionally, it was found that the approach of Adaptation Pathways with a scorecard can be generalized internationally to other cases to provide an effective method for integrated planning approaches to assess climate change vulnerability and potential measures for road infrastructure and to increase adaptive design of road infrastructure. Finally, as the transformational change towards hydrologically neutral highways complies with the principles of systematic water management of the $21^{st}$ century and low impact development, one could argue for generalization towards hydrologically neutral highways. This implies that we should consider dropping the sewer networks on the long-term and find alternatives for the weak link of porous asphalt to mimic the natural water cycle, such as the Plastic Road.

Overall, this study contributes to the research of a highly relevant problem: climate adaptation of road infrastructure. Therefore, it is desirable that, building on this research, methods and approaches can be further developed and improved in the future. The results presented yield important insights for climate adaptation of highways in practice.

## 9.2. Recommendations

Adaptation Pathways can definitely play a role in road resiliency, although further research is needed. Below some recommendations are made on topics that require extra attention for future research with the aim of substantiating more insight in climate adaptation of highways, in practical implications of the research and in improvement of the methodologies.

### 9.2.1. Practical implications

- This research can be considered an improvement to the Climate Effect Atlas and Stresstest by providing tipping points. In order to increase the water-resilience of the Dutch national highway network, similar research approaches could be implemented to other cases throughout the HWN. By starting at the most vulnerable locations according to the Stresstest, the Climate Effect Atlas and the record of notifications related to local flooding, the vulnerable, critical locations are addressed first.

- Another practical implication of the research is to adopt a similar definition of the tipping point in other research related to local flooding of highways, to make the research more comparable and to ensure transparency and consistency. Moreover, the definition of a tipping point in this research can be regarded advantageous, because it does not directly indicate the acceptability of flooding. Therefore, under significant deviations from the expected rate of increase in extreme precipitation intensities, the Adaptation Pathways are still able to inform decision-makers about the necessity to delay or accelerate the program (Bloemen et al., 2018).

- It is also recommended to reconsider the design storm requirements, based on the length of a HWN segment (Fortuin, 2021) and to thereby create more locally tailored design requirements. Table 1.1 reveals that a relatively long segment of the HWN is more susceptible to extreme precipitation events than a short segment. In case of a long segment without the possibility to exit the road, e.g. the Afsluitdijk, flooding of the road segment has a large traffic impact. Therefore, a higher resilience against local flooding is advisable on long segments.

- This research stresses the need to improve the Climate Effect Atlas by implementing local knowledge, as it reveals the sensitivity to flooding is largely influenced by local conditions such as the interception capacity of the porous asphalt. Therefore, it is recommended to monitor the dynamical behaviour of stormwater runoff on highways and the influence of pollution in porous asphalt to flooding in more detail. Moreover, as a result of the potential of road storage timely cleaning of the porous asphalt is recommended as an effective measure against flooding. Moreover, monitoring time series on groundwater levels, precipitation and sewer discharge can enhance the predictive capacity of the hydrological model.

### 9.2.2. Recommendations to improve the research methodologies

- Research is needed on determination of the effect of the length of the used time series on the accuracy of groundwater head estimation through TFN modelling (Collenteur et al., 2020).

- In order to increase the compatibility of the bucket approach with time series analysis, additional hydrological processes (e.g. surface runoff and sewer discharge) may be included in the FLEX-model. According to Collenteur et al. (2020) improved groundwater level simulations by enhancing the model structure are the result of a better representation of the hydrological processes due to the use of physically-based impulse-response functions, rather than merely the result of added mathematical complexity. Even in case of a lack of insufficiently long time series, no constraints on parametrizations and no calibration, improving the structure of the FLEX-model for highways can strongly enhance the model performance (Gharari et al., 2014).

- The potential of the focus group results can be increased by a combination with questionnaires (Kitzinger, 2005) and by involving the currently missing stakeholders such as road users and Brabant Landschap. Questionnaires can simply be filled in by the participants of the focus group to gain extra background information on objectives and constraints and to offer participants the opportunity to reveal matters they would rather not say in a group.

- Further analysis on the initial and recurrent costs for any actions, but also the costs associated with transferring from one action to another and further analysis on other criteria is recommended in order to prioritise adaptation measures (Marchau et al., 2019).

### 9.2.3. Recommendations to gain more insight in climate adaptation of highways

- It is recommended that the slow uptake of climate adaptation planning in road infrastructure is studied. Thereafter, ways can be sought to reduce the lack of public priority to climate adaptation in road infrastructure, to better implement climate change in infrastructure-related legislation and to change the planning horizon of infrastructure projects.
- Whereas this study focuses on local flooding of the Dutch national highway network, it is interesting to consider the effect of adaptation measures on other climate effects such as droughts as well, when prioritizing measures for decision making. This research offers opportunities to generalise towards other climate effects.
- Finally, it may be worthwhile to compare experiences in area-oriented road design in different countries more in-depth to learn from each other, for example with respect to planning processes. Examples of such experiences are context-sensitive design in the United States and Infrastruktur in der Landschaft in Germany (Heeres et al., 2012).

# Bibliography


Alastal, K. and Ababou, R. (2019). Moving multi-front (mmf): A generalized green-ampt approach for vertical unsaturated flows. *Journal of Hydrology*, 579:124184.

Andrássyová, Z., Žarnovskỳ, J., Álló, Š., and Hrubec, J. (2013). Seven new quality management tools. In *Advanced Materials Research*, volume 801, pages 25–33. Trans Tech Publ.

Arcadis (2006). Waterberging 's-Hertogenbosch (HoWaBo) startnotitie M.E.R. *Waterboard Aa and Maas*.

Attema, J., Bakker, A., Beersma, J., Bessembinder, J., Boers, R., Brandsma, T., Van Een Brink, H., Drijfhout, S., Eskes, H., Haarsma, R., Hazeleger, W., Jilderda, R., Katsman, C., Lenderink, G., Loriaux, J., Van Meijgaard, E., Van Noije, T., Van Oldenburg, G. J., Selten, F., Siebesma, P., Sterl, A., De Vries, H., Van Weele, M., De Winter, R., and Van Zadelhoff, G.-J. (2014). KNMI'14: Climate Change scenarios for the 21st Century—A Netherlands perspective. *Scientific report WR2014-01, KNMI, De Bilt, The Netherlands*.

Axelsen, C., Grauert, M., Liljegren, E., Bowe, M., and Sladek, B. (2016). Implementing climate change adaptation for European road administrations. *Transportation Research Procedia*, 14:51–57.

Bakker, M. and Schaars, F. (2019). Solving groundwater flow problems with time series analysis: you may not even need another model. *Groundwater*, 57(6):826–833.

Barnett, J., Graham, S., Mortreux, C., Fincher, R., Waters, E., and Hurlimann, A. (2014). A local coastal adaptation pathway. *Nature Climate Change*, 4(12):1103–1108.

Barten, B., Van Muiswinkel, K., Fortuin, P., and Nuesink, J. (2017). Climate adaptation in impact assessments for Dutch road infrastructure. *IAIA Conference*.

Beersma, J., Lenderink, G., and Overeem, A. (2018a). Update neerslagstatistiek korte duren voor RWS-WVL o.b.v. STOWA. *RWS-WVL*, page 18.

Beersma, J., Versteeg, R., and Hakvoort, H. (2018b). Neerslagstatistieken voor korte duren. *STOWA*, (2019):58.

Berendrecht, W., Heemink, A., Van Geer, F. C., and Gehrels, J. (2006). A non-linear state space approach to model groundwater fluctuations. *Advances in water resources*, 29(7):959–973.

Bhattacherjee, A. (2012). Social science research: Principles, methods, and practices.

Bierkens, M. F. and Van Geer, F. C. (2007). Stochastic hydrology.

Bles, T., Van Leeuwen, E., Hommes, S., Woning, M., De Bel, M., Brolsma, R., Venmans, A., Klingen, L., Van Marle, M., Hendriksen, G., Stuurman, R., Otto, L., Aboufirass, A., and Van Kester, B. (2020). Gevoeligheid van het hoofdwegennet voor klimaatverandering. *Deltares*, page 188.

Bles, T. J., Van Der Droef, M., Van Buren, R., Buma, J., Brolsma, R., Venmans, A., and Van Meerten, J. (2012). Investigation of the blue spots in the Netherlands National Highway Network. *Deltares*.

Bloemen, P., Reeder, T., Zevenbergen, C., Rijke, J., and Kingsborough, A. (2018). Lessons learned from applying adaptation pathways in flood risk management and challenges for the further development of this approach. *Mitigation and Adaptation Strategies for Global Change*, 23(7):1083–1108.

Blokland, J. T. (2021). Verkenning naar klimaatadaptieve staat ZOAB-asfalt op de Nederlandse Rijkswegen. *Hogeschool Rotterdam*.

Booij, M. J. (2003). Determination and integration of appropriate spatial scales for river basin modelling. *Hydrological processes*, 17(13):2581–2598.

Brevnova, E. V. (2001). Green-ampt infiltration model parameter determination using SCS curve number (CN) and soil texture class, and application to the SCS runoff model.

Butler, D., Digman, C. J., Makropoulos, C., and Davies, J. W. (2018). *Urban drainage*. Crc Press.

Clark, M. P., Slater, A. G., Rupp, D. E., Woods, R. A., Vrugt, J. A., Gupta, H. V., Wagener, T., and Hay, L. E. (2008). Framework for Understanding Structural Errors (FUSE): A modular framework to diagnose differences between hydrological models. *Water Resources Research*, 44(12).

Collenteur, R. A., Bakker, M., Caljé, R., Klop, S. A., and Schaars, F. (2019). Pastas: open source software for the analysis of groundwater time series. *Groundwater*, 57(6):877–885.

Collenteur, R. A., Bakker, M., Calje, R., and Schaars, F. (2021). Pastas documentation release 0.17.0.

Collenteur, R. A., Bakker, M., Klammler, G., and Birk, S. (2020). Estimating groundwater recharge from groundwater levels using non-linear transfer function noise models and comparison to lysimeter data. *Hydrology and Earth System Sciences Discussions*, pages 1–30.

Corker, E., Mitev, K., Nilsson, A. K. K., Tamis, M., Bouman, T., Holmlid, S., Lambe, F., Michie, S., Osborne, M., Renes, R. J., et al. (2021). The impact of COVID-19 related regulations and restrictions on mobility and potential for sustained climate mitigation across the Netherlands, Sweden and the UK: A data-based commentary. *UCL Open: Environment Preprint*.

Cristiano, E., Veldhuis, M.-C. T., and Giesen, N. V. D. (2017). Spatial and temporal variability of rainfall and their effects on hydrological response in urban areas–a review. *Hydrology and Earth System Sciences*, 21(7):3859–3878.

Davoudi, S., Shaw, K., Haider, L. J., Quinlan, A. E., Peterson, G. D., Wilkinson, C., Fünfgeld, H., McEvoy, D., Porter, L., and Davoudi, S. (2012). Resilience: a bridging concept or a dead end? *Planning theory & practice*, 13(2):299–333.

De Bruin, K., Dellink, R., Ruijs, A., Bolwidt, L., Van Buuren, A., Graveland, J., De Groot, R., Kuikman, P., Reinhard, S., Roetter, R., et al. (2009). Adapting to climate change in The Netherlands: an inventory of climate adaptation options and ranking of alternatives. *Climatic change*, 95(1):23–45.

De Heer, M., Roozen, F., and Maas, R. (2017). The integrated approach to nitrogen in the netherlands: a preliminary review from a societal, scientific, juridical and practical perspective. *Journal for Nature Conservation*, 35:101–111.

De Monte, L. and Van De Vrede, E. (n.d.). De Moerasdraak: Een korte gebiedsbeschrijving van het bossche broek. *WUR E-depot*.

De Ridder, N., Zijlstra, G., et al. (1994). Seepage and groundwater flow. *Drainage principles and applications. The Netherlands, ILRI Publication*, (16).

Eckart, K., McPhee, Z., and Bolisetti, T. (2017). Performance and implementation of low impact development–a review. *Science of the Total Environment*, 607:413–432.

Evans, B., Chen, A. S., Djordjević, S., Webber, J., Gómez, A. G., and Stevens, J. (2020). Investigating the Effects of Pluvial Flooding and Climate Change on Traffic Flows in Barcelona and Bristol. *Sustainability*, 12(6):23–30.

Fang, X., Thompson, D. B., Cleveland, T. G., Pradhan, P., and Malla, R. (2008). Time of concentration estimated using watershed parameters determined by automated and manual methods. *Journal of Irrigation and Drainage Engineering*, 134(2):202–211.

Fenicia, F., Savenije, H., Matgen, P., and Pfister, L. (2006). Is the groundwater reservoir linear? learning from data in hydrological modelling. *Hydrology and Earth System Sciences*, 10(1):139–150.

Fortuin, P. (29-06-2021). Webinar extreem weer en weginfrastructuur. *Rijkswaterstaat*.

Geertsema, T. J., Teuling, A. J., Uijlenhoet, R., Torfs, P. J., and Hoitink, A. J. (2018). Anatomy of simultaneous flood peaks at a lowland confluence. *Hydrology and Earth System Sciences*, 22(10):5599–5613.

Gerrits, A. M. J. (2010). *The role of interception in the hydrological cycle*. VSSD.

Gerrits, M. (2009). Na regen komt interceptie. *Stromingen*, 15(1):37–40.

Gharari, S. (2016). On the role of model structure in hydrological modeling: Understanding models.

Gharari, S., Hrachowitz, M., Fenicia, F., Gao, H., and Savenije, H. (2014). Using expert knowledge to increase realism in environmental system models can dramatically reduce the need for calibration. *Hydrology and Earth System Sciences*, 18(12):4839–4859.

Gupta, H. V., Clark, M. P., Vrugt, J. A., Abramowitz, G., and Ye, M. (2012). Towards a comprehensive assessment of model structural adequacy. *Water Resources Research*, 48(8).

Haasnoot, M., Kwakkel, J. H., Walker, W. E., and ter Maat, J. (2013). Dynamic adaptive policy pathways: A method for crafting robust decisions for a deeply uncertain world. *Global environmental change*, 23(2):485–498.

Haasnoot, M., Van Aalst, M., Rozenberg, J., Dominique, K., Matthews, J., Bouwer, L. M., Kind, J., and Poff, N. L. (2019). Investments under non-stationarity: economic evaluation of adaptation pathways. *Climatic Change*, pages 1–13.

Heeres, N. (2017). Towards area-oriented approaches in infrastructure planning: Development of national highway networks in a local spatial context.

Heeres, N., Tillema, T., and Arts, J. (2012). Integration in Dutch planning of motorways: From "line" towards "area-oriented" approaches. *Transport policy*, 24:148–158.

Hendriks, M. (2010). *Introduction to physical hydrology*. Oxford University Press.

Hrachowitz, M. and Clark, M. P. (2017). Hess Opinions: The complementary merits of competing modelling philosophies in hydrology. *Hydrology and Earth System Sciences*, 21(8):3953–3973.

Hrachowitz, M., Fovet, O., Ruiz, L., Euser, T., Gharari, S., Nijzink, R., Freer, J., Savenije, H., and Gascuel-Odoux, C. (2014). Process consistency in models: The importance of system signatures, expert knowledge, and process complexity. *Water resources research*, 50(9):7445–7469.

Huveneers, N. (2018). Rapport Klimaatadaptatie in MIRT-projecten. *Rijkswaterstaat Zuid-Nederland*.

IVN (2012). Geologische (onder-) achtergrond en waterbeheersing. Accessed: 2021-01-20.

Jiggins, J., Van Slobbe, E., and Röling, N. (2007). The organisation of social learning in response to perceptions of crisis in the water sector of The Netherlands. *Environmental science & policy*, 10(6):526–536.

Johnson, R. B. and Onwuegbuzie, A. J. (2004). Mixed methods research: A research paradigm whose time has come. *Educational researcher*, 33(7):14–26.

Jotisankasa, A. and Sirirattanachat, T. (2017). Effects of grass roots on soil-water retention curve and permeability function. *Canadian Geotechnical Journal*, 54(11):1612–1622.

Kale, R. V. and Sahoo, B. (2011). Green-ampt infiltration models for varied field conditions: A revisit. *Water resources management*, 25(14):3505–3536.

Kates, R. W., Travis, W. R., and Wilbanks, T. J. (2012). Transformational adaptation when incremental adaptations to climate change are insufficient. *Proceedings of the National Academy of Sciences*, 109(19):7156–7161.

Kitzinger, J. (2005). Focus group research: using group dynamics. *Qualitative research in health care*, 56:70.

Klimaateffectatlas (2020). Kaartverhaal wateroverlast. *https://www.klimaateffectatlas.nl/nl/kaartverhaal-wateroverlast*, Retrieved 30 November 2020.

Knott, J. F., Jacobs, J. M., Sias, J. E., Kirshen, P., and Dave, E. V. (2019). A framework for Introducing climate-change adaptation in pavement management. *Sustainability*, 11(16):4382.

Koetse, M. J. and Rietveld, P. (2009). The impact of climate change and weather on transport: An overview of empirical findings. *Transportation Research Part D: Transport and Environment*, 14(3):205–221.

Kwadijk, J. C., Haasnoot, M., Mulder, J. P., Hoogvliet, M. M., Jeuken, A. B., Van Der Krogt, R. A., Van Oostrom, N. G., Schelfhout, H. A., Van Velzen, E. H., Van Waveren, H., et al. (2010). Using adaptation tipping points to prepare for climate change and sea level rise: a case study in the Netherlands. *Wiley interdisciplinary reviews: climate change*, 1(5):729–740.

Kwakkel, J. H., Haasnoot, M., and Walker, W. E. (2015). Developing dynamic adaptive policy pathways: a computer-assisted approach for developing adaptive strategies for a deeply uncertain world. *Climatic Change*, 132(3):373–386.

Leijstra, M., Van Muiswinkel, K., Leendertse, W., and Bles, T. (2018). Development of a Climate Adaptation Strategy for the InnovA58 highway in the Netherlands. *TRA2018*, April:16–19.

Lenderink, G., Barbero, R., Loriaux, J., and Fowler, H. (2017). Super-Clausius–Clapeyron scaling of extreme hourly convective precipitation and its relation to large-scale atmospheric conditions. *Journal of Climate*, 30(15):6037–6052.

Luxemburg, W. and Coenders, A. (2011). Cie4440-hydrological measurements. *TU Delft*.

Lázaro, C. P. (2020). A Systematic Methodology to Study Driving Adaptation Effects under Flooding Conditions. *MSc thesis Delft University of Technology*.

Ma, W., Norris, J., and Chen, G. (2020). Projected changes to extreme precipitation along North American west coast from the CESM large ensemble. *Geophysical Research Letters*, 47(1):e2019GL086038.

Manocha, N. and Babovic, V. (2017). Development and valuation of adaptation pathways for storm water management infrastructure. *Environmental Science & Policy*, 77:86–97.

Marchau, V. A., Walker, W. E., Bloemen, P. J., and Popper, S. W. (2019). *Decision making under deep uncertainty: from theory to practice*. Springer Nature.

Marchau, V. A., Walker, W. E., and Van Wee, G. (2010). Dynamic adaptive transport policies for handling deep uncertainty. *Technological forecasting and social change*, 77(6):940–950.

Mens, M. J., Klijn, F., De Bruijn, K. M., and Van Beek, E. (2011). The meaning of system robustness for flood risk management. *Environmental science & policy*, 14(8):1121–1131.

Milakis, D., Snelder, M., Van Arem, B., Van Wee, B., and De Almeida Correia, G. H. (2017). Development and transport implications of automated vehicles in the Netherlands: scenarios for 2030 and 2050. *European Journal of Transport and Infrastructure Research*, 17(1).

Ministry of Public Works and Water Management (2020). Factsheet klimaatbestendige netwerken RWS (2050) Hoofdwegen.

Mostert, E. (2018). An alternative approach for socio-hydrology: case study research. *Hydrology and Earth System Sciences*, 22(1):317–329.

Mostert, E. (2019). Open Textbook: Nederlands waterrecht voor niet-juristen.

Nijzink, R., Almeida, S., Pechlivanidis, I., Capell, R., Gustafssons, D., Arheimer, B., Parajka, J., Freer, J., Han, D., Wagener, T., et al. (2018). Constraining conceptual hydrological models with multiple information sources. *Water Resources Research*, 54(10):8332–8362.

Nijzink, R. C., Samaniego, L., Mai, J., Kumar, R., Thober, S., Zink, M., Schäfer, D., Savenije, H. H., and Hrachowitz, M. (2016). The importance of topography-controlled sub-grid process heterogeneity and semi-quantitative prior constraints in distributed hydrological models. *Hydrology and Earth System Sciences*, 20(3):1151–1176.

Obergfell, C., Bakker, M., and Maas, K. (2019). Estimation of average diffuse aquifer recharge using time series modeling of groundwater heads. *Water Resources Research*, 55(3):2194–2210.

Parnas, F. E. Å. (2018). Modelling runoff from permeable surfaces in urban areas. Master's thesis, NTNU.

Peterson, T. and Western, A. (2014). Nonlinear time-series modeling of unconfined groundwater head. *Water Resources Research*, 50(10):8330–8355.

Pezij, M., Augustijn, D. C., Hendriks, D. M., and Hulscher, S. J. (2020). Applying transfer function-noise modelling to characterize soil moisture dynamics: a data-driven approach using remote sensing data. *Environmental Modelling & Software*, 131:104756.

Picketts, I. M., Andrey, J., Matthews, L., Déry, S. J., and Tighe, S. (2016). Climate change adaptation strategies for transportation infrastructure in Prince George, Canada. *Regional Environmental Change*, 16(4):1109–1120.

Pour, S. H., Abd Wahab, A. K., Shahid, S., Asaduzzaman, M., and Dewan, A. (2020). Low impact development techniques to mitigate the impacts of climate-change-induced urban floods: Current trends, issues and challenges. *Sustainable Cities and Society*, 62:102373.

Rawls, W. J., Brakensiek, D. L., and Miller, N. (1983). Green-ampt infiltration parameters from soils data. *Journal of hydraulic engineering*, 109(1):62–70.

Rijksbegroting (2018). Rijksbegroting, Infrastructuurfonds 2018, Bijlage 4 Instandhouding.

Rijkswaterstaat (2010). Analyse Instandhoudingskosten Rijksinfrastructuur.

Rijkswaterstaat (2014). Kader afstromend wegwater.

Rijkswaterstaat (2019). Richtlijn Ontwerp Autosnelwegen.

Rijkswaterstaat (2020a). Eisen Bovenbouw versie 3.

Rijkswaterstaat (2020b). Eisen HWA op een aardebaan versie 4.

RIONED (2015). Regenwatersystemen op de testbank;Benchmark functioneren bij extreme neerslag.

Roggema, R., Vermeend, T., and Dobbelsteen, A. V. D. (2012). Incremental change, transition or transformation? optimising change pathways for climate adaptation in spatial planning. *Sustainability*, 4(10):2525–2549.

Roussel, M. C., Thompson, D. B., Fang, X., Cleveland, T. G., and Garcia, C. A. (2005). Time-parameter estimation for applicable Texas watersheds. *Texas Department of Transportation Research Report 0–4696–2, Lamar University, Beaumont, Texas*.

Savenije, H. H. G. (2006). Lecture notes CT5450 Hydrology of catchments, rivers and deltas. *TU Delft*, page 153.

Savenije, H. H. G. (2009). Hess Opinions: The art of hydrology. *Hydrology and Earth System Sciences*, 13(2):157–161.

Slager, K. (2018). Overstromingsrisico's door intense neerslag. *Deltares*, page 43.

Snelder, M. and Calvert, S. (2016). Quantifying the impact of adverse weather conditions on road network performance. *European Journal of Transport and Infrastructure Research*, 16(1).

Steens, A. and De Vries Chairman, B. (2019). Exploration for a successful transition to a circular civil engineering sector.

Sterk, A. (01-4-2021). Bossche Broek Noord en Zuid. *De Dommel, Waterboard*.

Tijhuis, S. and Beentjes, R. M. (2019). Mirt-verkenning A2 Deil-Vught; Gebiedsbeschrijving en probleemanalse. *Rijkswaterstaat*.

TNO (n.d.). Isohypsen Grondwatertools. Accessed: 2021-01-20.

Tügel, F., Hassan, A., Hou, J., and Hinkelmann, R. (2021). Applicability of literature values for Green-Ampt parameters to account for infiltration in hydrodynamic rainfall-runoff simulations in ungauged basins.

Van De Ven, F. H. (2009). Water management in urban areas. *Lecture Notes, TU Delft.[Online] Available at: ocw. tudelft. nl/courses/watermanagement/water-management-in-urban-areas/lectures/[Accessed 02 November 2009]*.

Van Der Biggelaar, C. (20-5-2021). Email and telephone calls with road inspector concerning the occurrence of local flooding in the case area. *Rijkswaterstaat*.

Van Der Hauw, K. (2012). Evaluatie Waterproject Ruinen - een praktijktoepassing van interventieanalyse met Menyanthes. *Stromingen*, 18(2):15–30.

Van Der Steen, A. (2005). Effecten gradering op de functionele eigenschappen van tweelaags ZOAB.

Van Geenhuizen, M., Rietveld, P., and Reggiani, A. (2016). New trends in policy making for transport and regional network integration. In *Policy Analysis of Transport Networks*, pages 17–32. Routledge.

Van Geer, F. (2012). Tijdreeksanalyse: Introductie en aandachtspunten. *Stromingen*, 18(2):5–13.

Van Grinsven, W. G. M. A. and Van Muiswinkel, C. (2010). Motorway runoff in the Netherlands, runoff and spray pollution, legislation and prevention measures.

Van Wijk, G. (19-4-2021). Email and telephone calls concerning seepage and return valve after field visit. *Waterboard De Dommel*.

VBW (2010). Richtlijn Tweelaags ZOAB. *Vakgroep Bitumineuze Werken*.

Veld, M. and Zwaan, J. (2021). Betekenis bodembuffers voor een klimaatbestendig hoofdwegennetwerk. *TAUW*.

Verdonschot, P. F. and Verdonschot, R. C. (2020). Factsheet KIWK: Stroming en waterbeweging. Technical report, Wageningen Environmental Research, Zoetwaterecosystemen.

Volkskrant (2014). Snelweg A10 onder water. `https://www.volkskrant.nl/nieuws-achtergrond/Voorpagina~qee531dc/`. Accessed: 2021-01-13.

Von Asmuth, J. R. (2012). Groundwater system identification through time series analysis.

Von Asmuth, J. R., Bierkens, M. F., and Maas, K. (2002). Transfer function-noise modeling in continuous time using predefined impulse response functions. *Water Resources Research*, 38(12):23–1.

Von Asmuth, J. R., Maas, K., Bakker, M., and Petersen, J. (2008). Modeling time series of ground water head fluctuations subjected to multiple stresses. *Groundwater*, 46(1):30–40.

Walker, W. E., Lempert, R. J., and Kwakkel, J. H. (2012). Deep uncertainty. *Delft University of Technology*, 1(2).

Werners, S. E., Wise, R. M., Butler, J. R., Totin, E., and Vincent, K. (2021). Adaptation pathways: A review of approaches and a learning framework. *Environmental Science & Policy*, 116:266–275.

Williams, L. (2018). End of the asphalt road? *Engineering & Technology*, 13(9):72–73.

Willway, T., Baldachin, L., Reeves, S., Harding, M., McHale, M., and Nunn, M. (2008). The effects of climate change on highway pavements and how to minimise them: Technical report. *The Effects of Climate Change on Highway Pavements and how to Minimise them: Technical Report*, 1(1):1–111.

Zaadnoordijk, W. J., Bus, S. A., Lourens, A., and Berendrecht, W. (2019). Automated time series modeling for piezometers in the national database of the netherlands. *Groundwater*, 57(6):834–843.

Zeisl, P., Mair, M., Kastlunger, U., Bach, P. M., Rauch, W., Sitzenfrei, R., and Kleidorfer, M. (2018). Conceptual urban water balance model for water policy testing: an approach for large scale investigation. *Sustainability*, 10(3):716.

Zwart, J. (2020). Onderzoek en maatregelen Rijksweg A2 Den Bosch-Zuid. *Wareco*.

# A

# Details on time series analysis

## A.1. Basic equations of TFN modelling

The basic model structure of TFN models can be defined as follows;

$$h(t) = \sum_{m=1}^{M} h_m(t) + d + r(t) \tag{A.1}$$

with observed groundwater heads h(t) [L], base groundwater level, i.e. the steady state groundwater head when all stresses are zero, d [L], contribution of stress m to the groundwater level $h_m(t)$ [L] and model residuals r [L] (Collenteur et al., 2019; Zaadnoordijk et al., 2019; Collenteur et al., 2020) (Figure 2.3).

A noise model with exponential decay of the residuals is applied for computing the residuals (Collenteur et al., 2019; Pezij et al., 2020);

$$r(t_i) = v(t_i) + r(t_{i-1})e^{-\Delta t_i/\alpha} \tag{A.2}$$

with white noise $v$ [L], decay parameter $\alpha$ [T] and time step $\Delta t_i$ [T] between observations at times $t_i$ and $t_{i-1}$.

The contribution of stress m ($h_m(t)$) is obtained through convolution, a mathematical approach to combine input signals to an output signal;

$$h_m(t) = \int_{-\infty}^{t} S_m(\tau)\Theta_m(t-\tau)d\tau \tag{A.3}$$

with time series $S_m$ and impulse response function $\Theta_m$. Time series $S_m$ can consist of a single stress or of the combined contribution of multiple stresses, for example a groundwater recharge function (see equations 2.1 and 2.2).

A frequently applied impulse response function for precipitation and evaporation for example is the scaled gamma distribution (Pezij et al., 2020).;

$$\Theta(t) = A\frac{t^{n-1}}{a^n\Gamma(n)}e^{-t/a} \qquad t \geq 0 \tag{A.4}$$

with scale factor A [L], shape factors a [T] and n [-] and the Gamma function $\Gamma$ [-]. Scale parameter A is related to the total change in output signal and shape factors a and n are related to the response time of the output signal due to a stress (Von Asmuth et al., 2002). In case of an (almost) instantaneous response of groundwater heads to stresses the scaled gamma distribution can be reduced to the exponential impulse response function (Collenteur et al., 2021);

$$\Theta_e(t) = Ae^{-t/a} \qquad t \geq 0 \tag{A.5}$$

## A.2. Results of time series analysis in Menyanthes

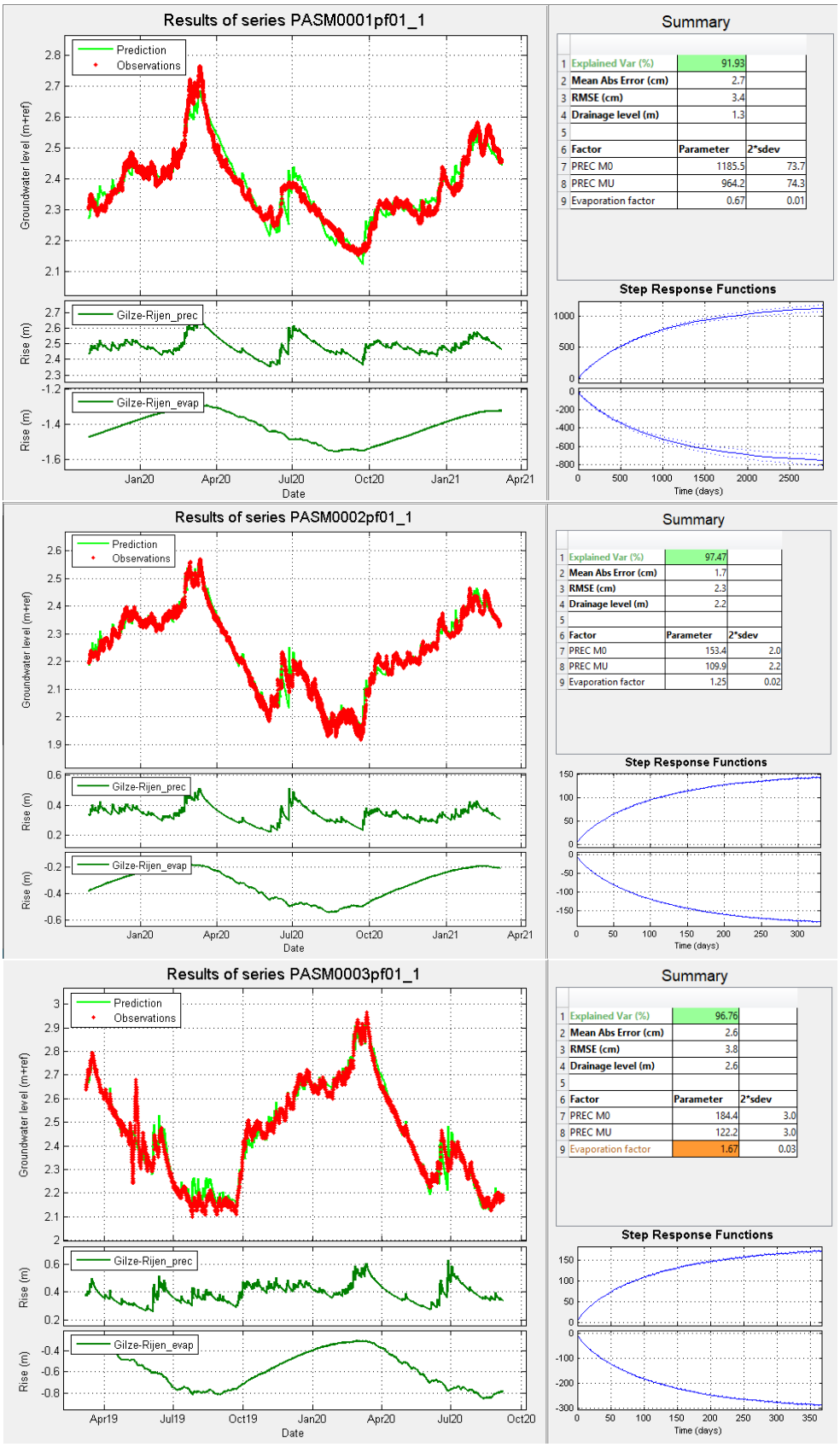


Figure A.1: Menyanthes simulation of groundwater head series, based on linear groundwater recharge from the available KNMI evaporation and precipitation measurements series. For each piezometer (PASM0001, PASM0002 and PASM0003) the simulated groundwater levels, the contribution of the precipitation and evaporation stresses to the groundwater recharge, the model parameters and the step response function are provided.

# A.3. Results of time series analysis in Pastas

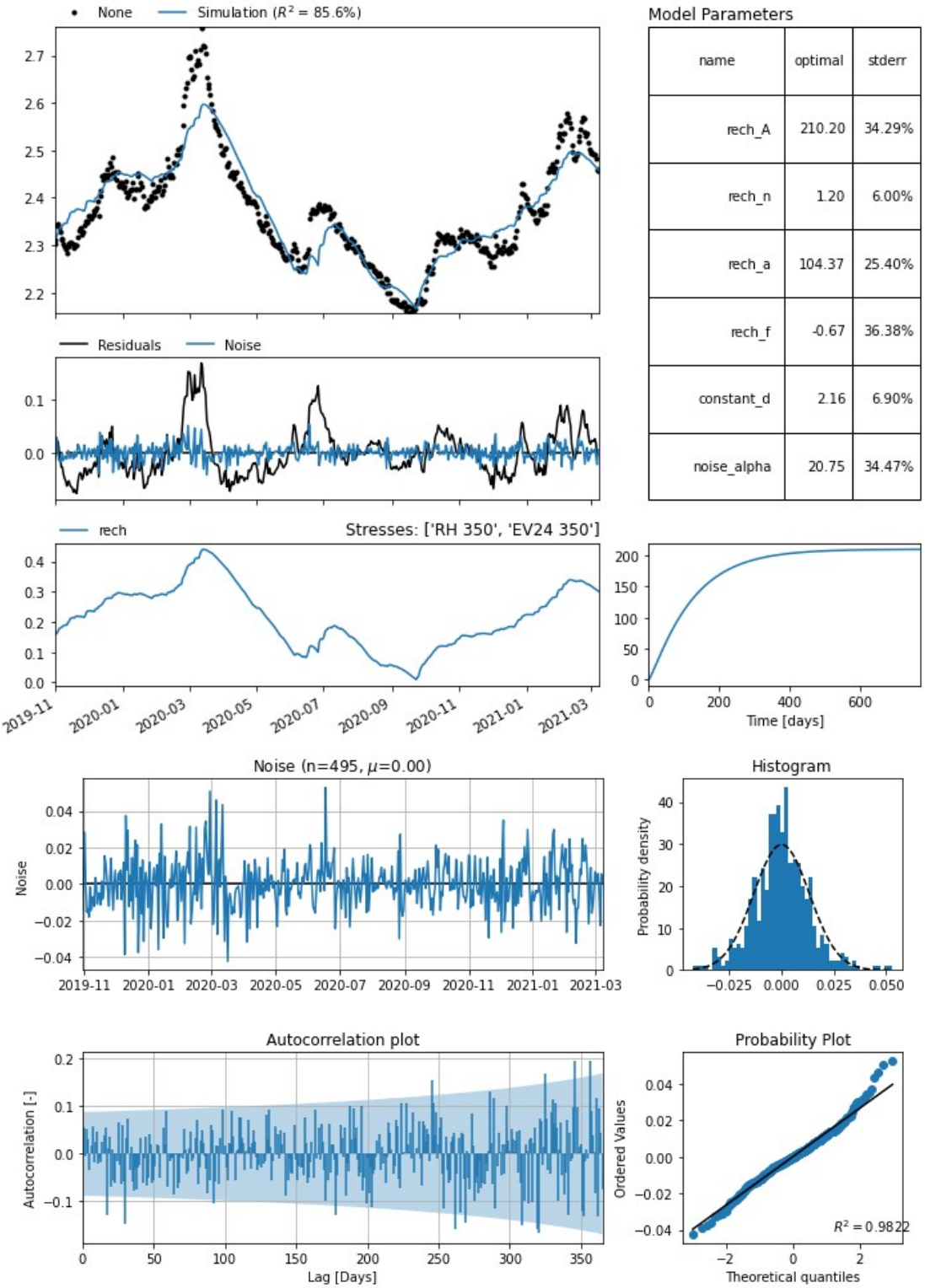


Figure A.2: Pastas simulation of groundwater head series PASM0001 (Δt=1 day), based on a scaled gamma distribution response function and linear groundwater recharge from the available KNMI evaporation and precipitation measurements series. The simulated groundwater levels, the model residuals and noise, the calibrated parameters values and their estimated standard errors, the step response function and information on the noise time series, such as the number of observations (n) and the mean value ($\mu$) of the modelled noise, are provided.

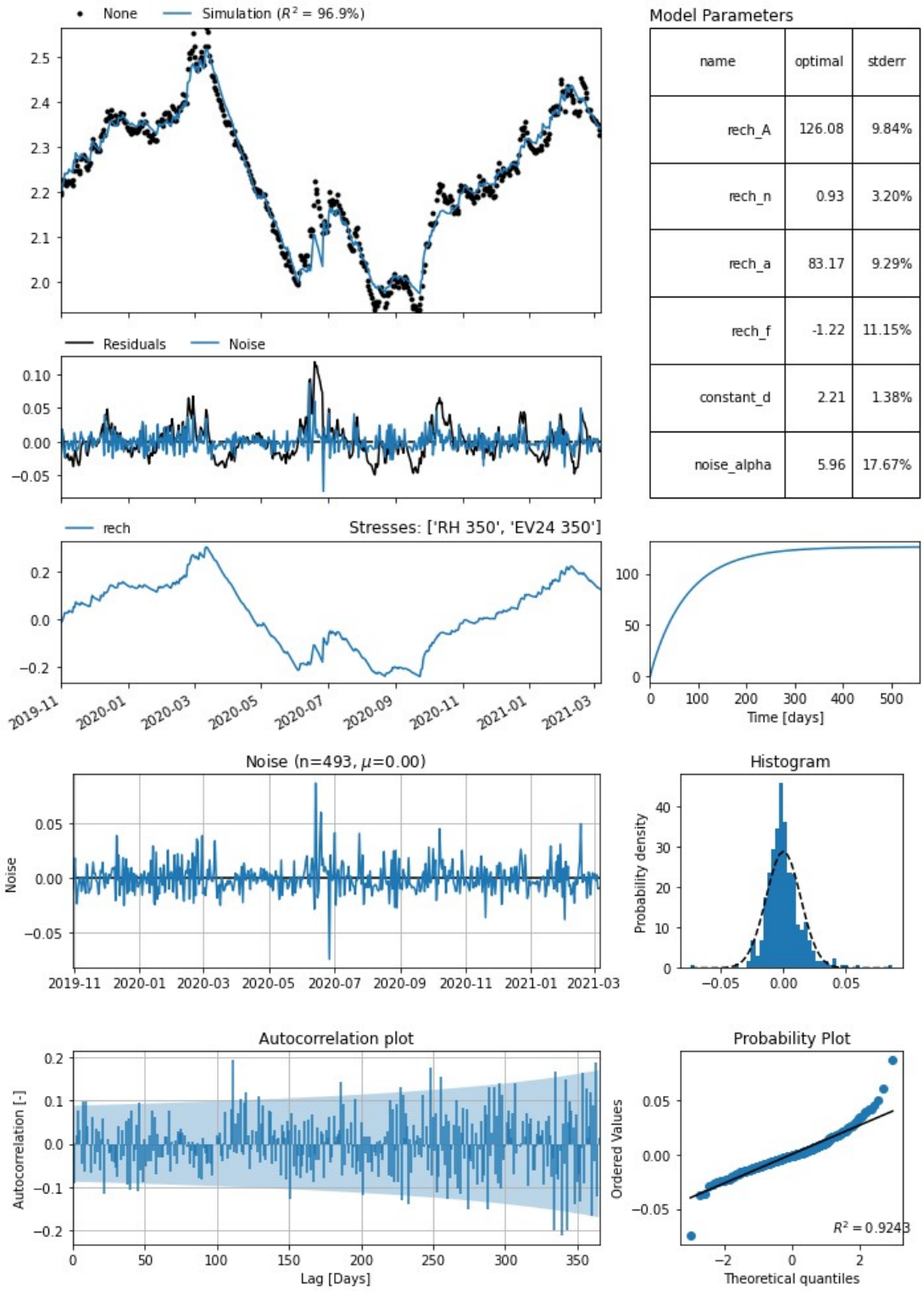


Figure A.3: Pastas simulation (Δt=1 day) of groundwater head series PASM0002, based on a scaled gamma distribution response function and linear groundwater recharge from the available KNMI evaporation and precipitation measurements series. The simulated groundwater levels, the model residuals and noise, the calibrated parameters values and their estimated standard errors, the step response function and information on the noise time series, such as the number of observations (n) and the mean value ($\mu$) of the modelled noise, are provided.

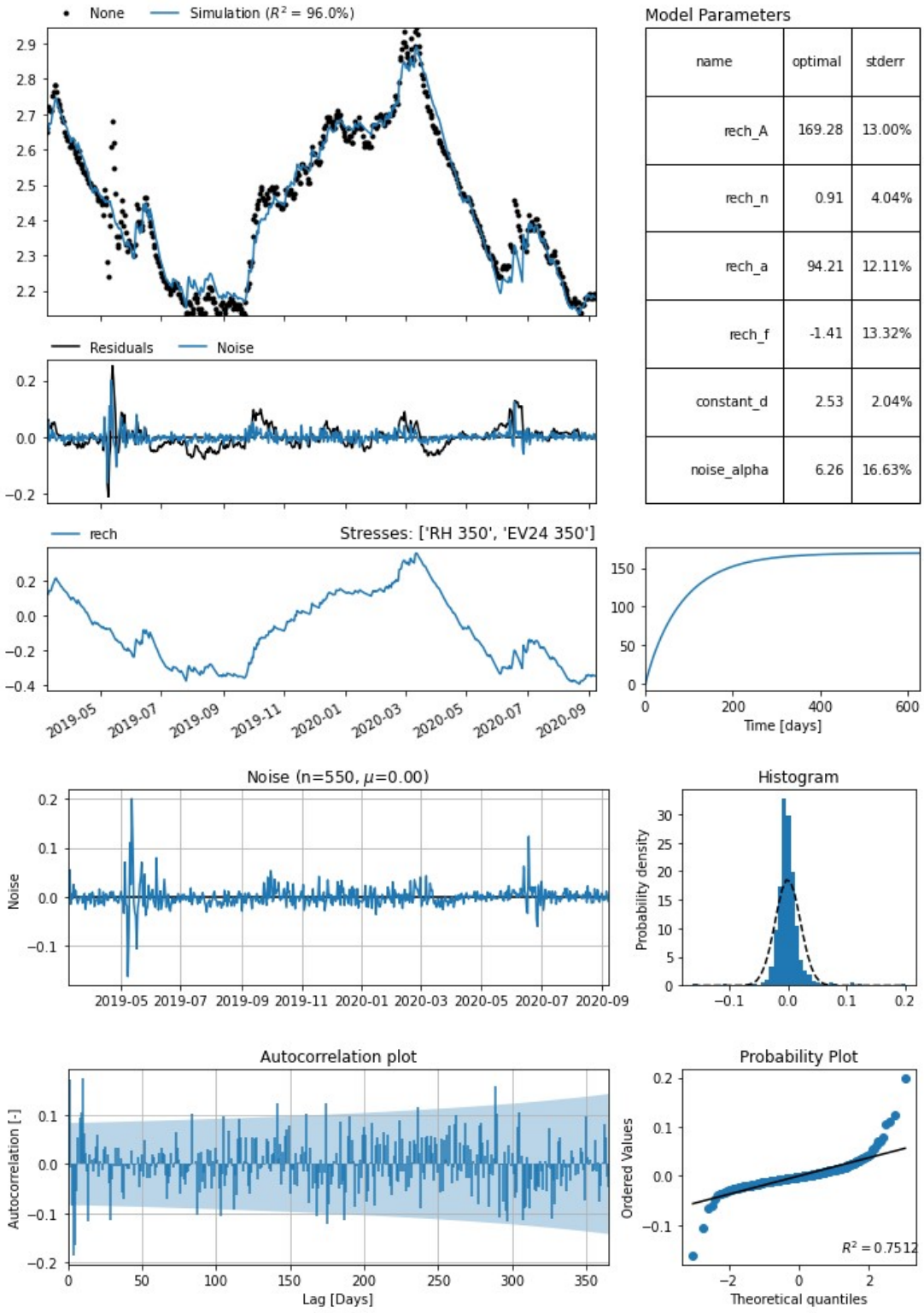


Figure A.4: Pastas simulation (Δt=1 day) of groundwater head series PASM0003, based on a scaled gamma distribution response function and linear groundwater recharge from the available KNMI evaporation and precipitation measurements series. The simulated groundwater levels, the model residuals and noise, the calibrated parameters values and their estimated standard errors, the step response function and information on the noise time series, such as the number of observations (n) and the mean value ($\mu$) of the modelled noise, are provided.

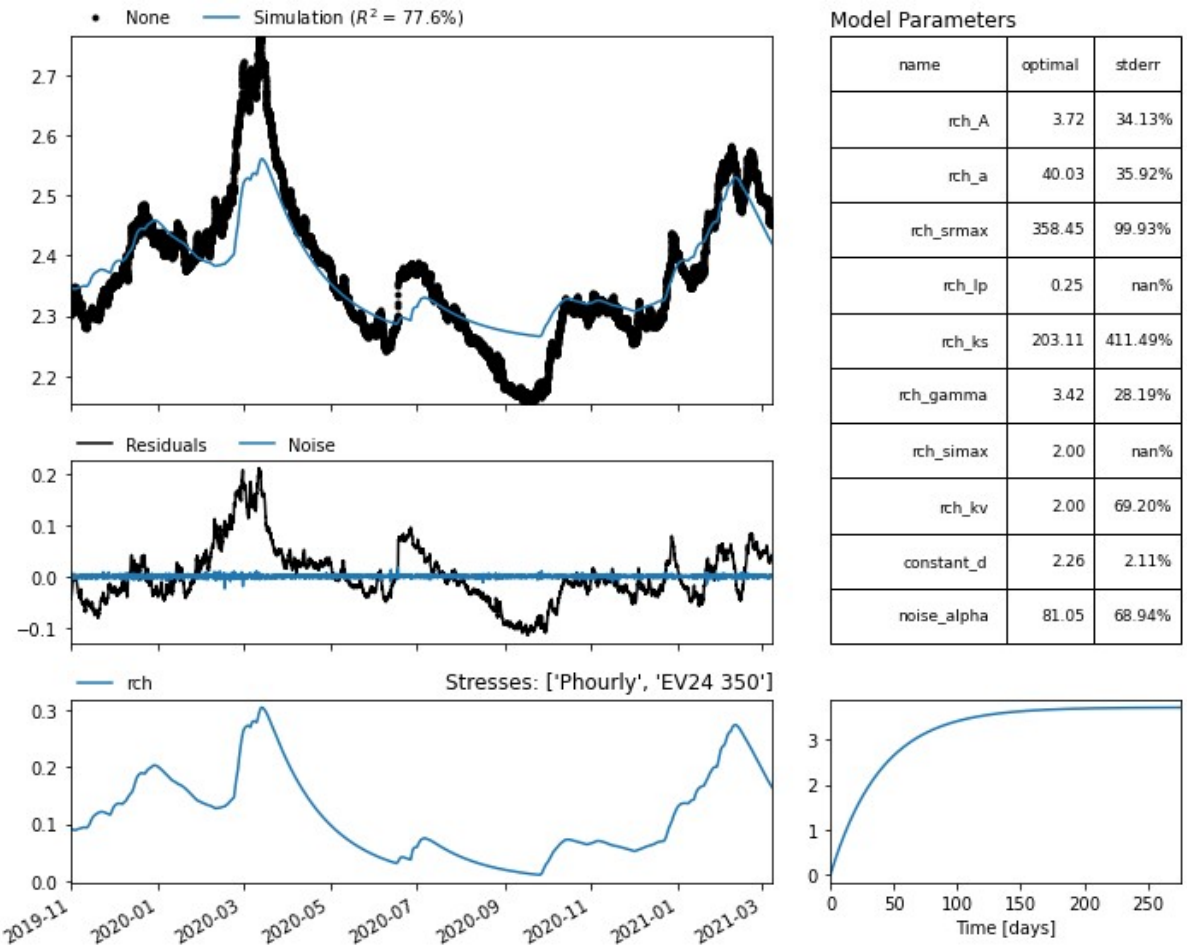


Model Parameters

| name | optimal | stderr |
|---|---|---|
| rch_A | 3.72 | 34.13% |
| rch_a | 40.03 | 35.92% |
| rch_srmax | 358.45 | 99.93% |
| rch_lp | 0.25 | nan% |
| rch_ks | 203.11 | 411.49% |
| rch_gamma | 3.42 | 28.19% |
| rch_simax | 2.00 | nan% |
| rch_kv | 2.00 | 69.20% |
| constant_d | 2.26 | 2.11% |
| noise_alpha | 81.05 | 68.94% |

Figure A.5: Pastas simulation (Δt=1 hour) of groundwater head series PASM0001, based on an exponential response function, the FLEX groundwater recharge model and potential evaporation and precipitation stresses. The simulated groundwater levels, the model residuals and noise, the calibrated parameters values and their estimated standard errors and the step response function are provided.

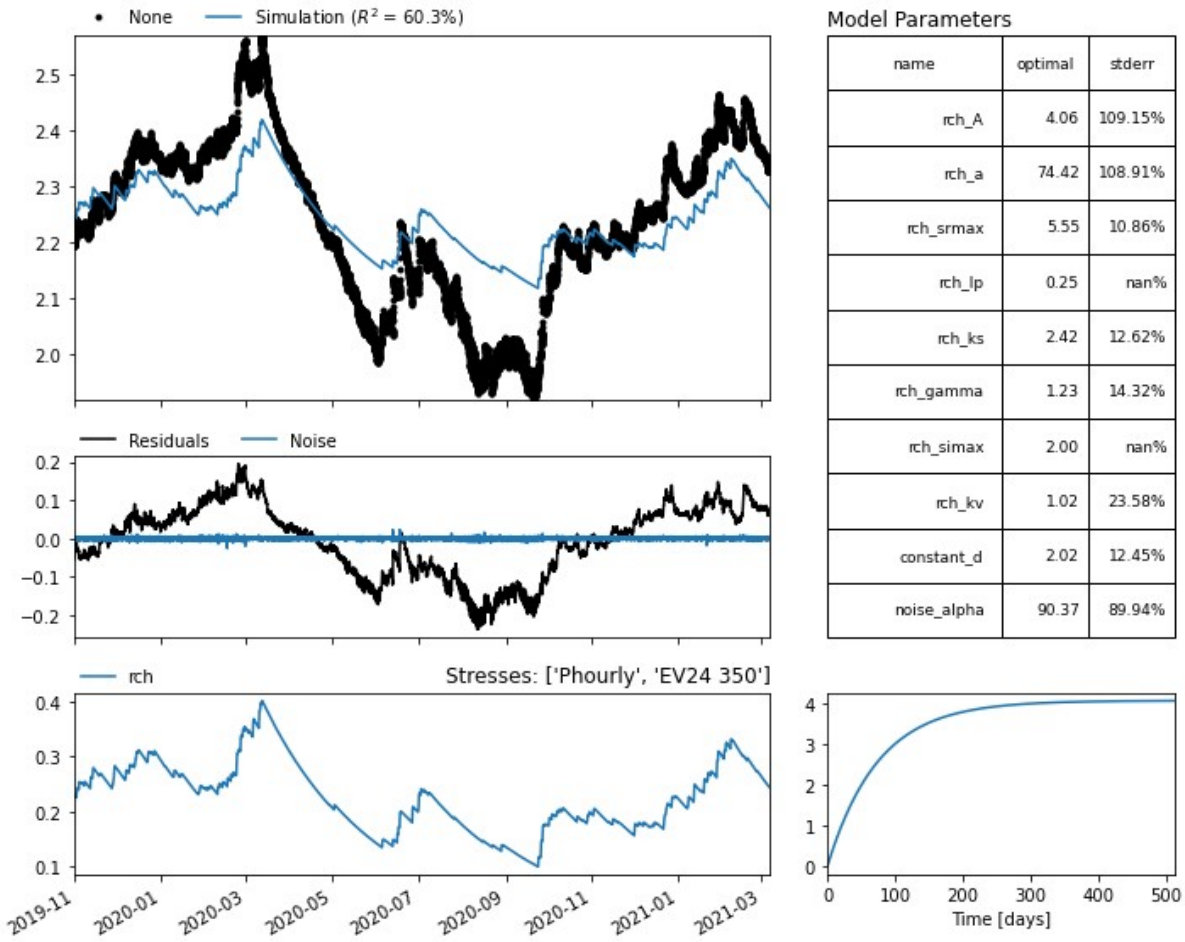


Model Parameters

| name | optimal | stderr |
|---|---|---|
| rch_A | 4.06 | 109.15% |
| rch_a | 74.42 | 108.91% |
| rch_srmax | 5.55 | 10.86% |
| rch_lp | 0.25 | nan% |
| rch_ks | 2.42 | 12.62% |
| rch_gamma | 1.23 | 14.32% |
| rch_simax | 2.00 | nan% |
| rch_kv | 1.02 | 23.58% |
| constant_d | 2.02 | 12.45% |
| noise_alpha | 90.37 | 89.94% |

Figure A.6: Pastas simulation (Δt=1 hour) of groundwater head series PASM0002, based on an exponential response function, the FLEX groundwater recharge model and potential evaporation and precipitation stresses. The simulated groundwater levels, the model residuals and noise, the calibrated parameters values and their estimated standard errors and the step response function are provided.

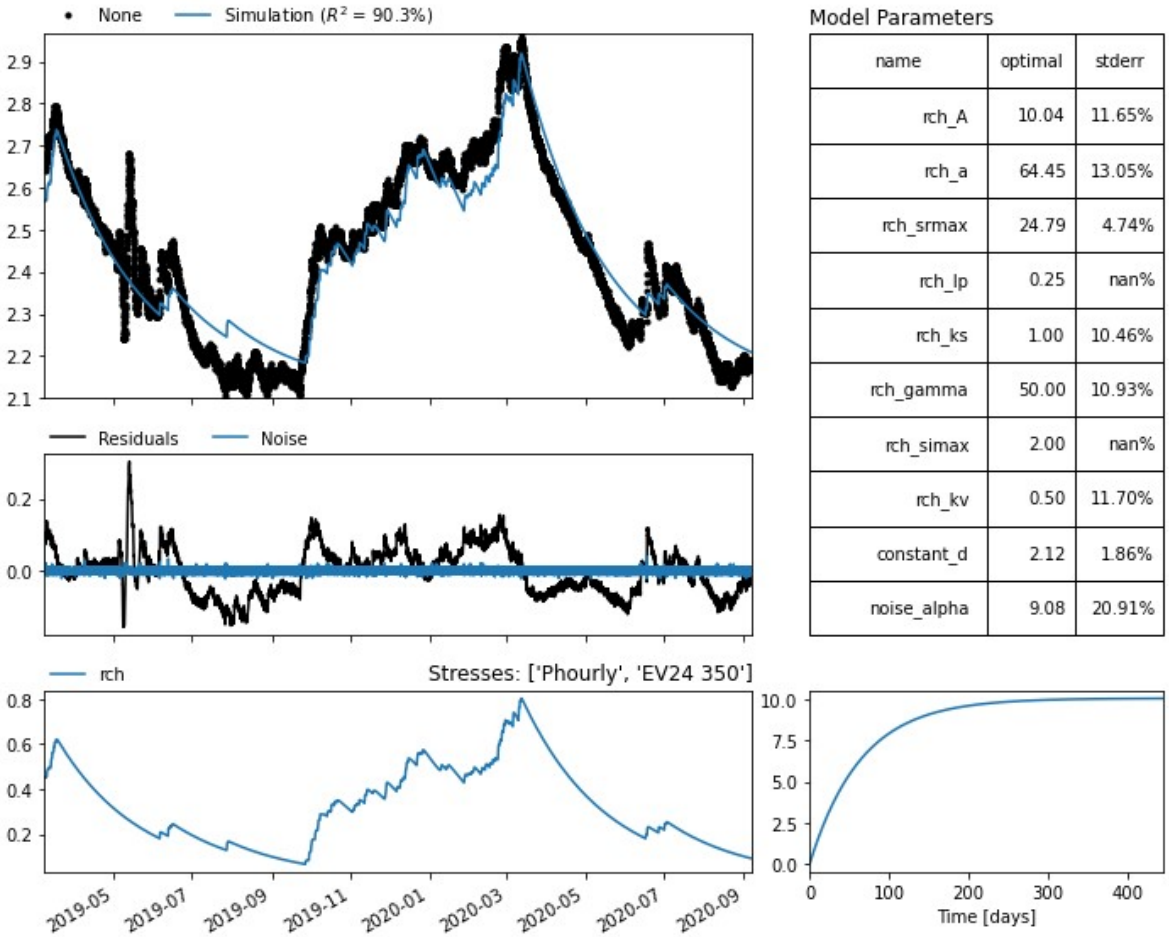


Model Parameters

| name | optimal | stderr |
|---|---|---|
| rch_A | 10.04 | 11.65% |
| rch_a | 64.45 | 13.05% |
| rch_srmax | 24.79 | 4.74% |
| rch_lp | 0.25 | nan% |
| rch_ks | 1.00 | 10.46% |
| rch_gamma | 50.00 | 10.93% |
| rch_simax | 2.00 | nan% |
| rch_kv | 0.50 | 11.70% |
| constant_d | 2.12 | 1.86% |
| noise_alpha | 9.08 | 20.91% |

Figure A.7: Pastas simulation (Δt=1 hour) of groundwater head series PASM0003, based on an exponential response function, the FLEX groundwater recharge model and potential evaporation and precipitation stresses. The simulated groundwater levels, the model residuals and noise, the calibrated parameters values and their estimated standard errors and the step response function are provided.

# B

# Details on bucket approach

## B.1. Model components

### B.1.1. Forcing

The forcing [$LT^{-1}$], i.e. precipitation and evaporation, are represented as follows in the model;

- **Precipitation:** The forcing by precipitation is represented by a uniform rainfall intensity and is systematically increased by 1 mm/hr to determine the tipping point.
- **Evaporation:** According to Van De Ven (2009) evaporation on paved terrain is a blind spot in hydrology. However, Van De Ven (2009) provides an indication for the magnitude of evaporation on asphalt during a thunderstorm on a sunny summer afternoon. The research reveals a computed evaporation value of 1 mm/h, which implies that the influence of evaporation throughout the extreme precipitation event can be regarded negligible. This is supported by Ma et al. (2020), who states that in case of extreme precipitation, evaporation can be ignored.

### B.1.2. Buckets

The porous asphalt, the verges, the unsaturated zone, the phreatic groundwater, the wadi, the regional confined groundwater, the infiltration trench, the drainage pipes and the stormwater sewer are the buckets [L] of the catchment of the road (Figure 5.1) and are represented as follows in the model;

- **Porous asphalt:** The maximum interception capacity of the porous asphalt (ZOABTW in Figure 5.1) is quantified by multiplication of the porosity (obtained from Bles et al. (2020)) with the thickness of the asphalt layer (see section 3.4). The results of the computation are presented in Table B.1.

Table B.1: Computed interception values by porous asphalt according to porosity values from Bles et al. (2020).

| ZOABTW | thickness [mm] | porosity [%] | storage [mm] |
|---|---|---|---|
| layer 1 | 30 | 18 | 5.4 |
| layer 2 | 80 | 23 | 18.4 |
| | | *total:* | *23.8* |

It is assumed that the entire storage capacity of the porous asphalt bucket is available for precipitation and that runoff from asphalt starts occurring in case the storage capacity of the porous asphalt bucket is exceeded. This assumption can be substantiated by studying the vertical hydraulic conductivity values obtained by Van Der Steen (2005). The vertical hydraulic conductivity represents the filling speed of the porous asphalt reservoir with precipitation and was found to range from 2.5 to 3.5 $\times 10^{-3}$ m/s. Compared to extreme rainfall intensities, the vertical hydraulic conductivity can be considered very large. Therefore, the assumption can be regarded appropriate.

- **Verge:** Interception by the verge is twofold, because it allows for both grass interception storage as well as depression storage. In this research it is assumed that the interception storage can be considered part of the depression storage (Butler et al., 2018). The depression storage in the verges along the A2 which are susceptible to runoff accumulation (Figure B.3), is computed using ArcMap. ArcMap enables ground level analysis of the Dutch Digital Elevation Model AHN3, which has a grid resolution of 0.5 by 0.5 metres (Δx, Δy). For each pixel, the depression puddle below a reference plane can be quantified by using the pixel area and the elevation difference between the reference plane and the elevation of the pixel (Δz) (Figure B.1). The reference plane corresponds with the elevation of the margin of the road, because the tipping point is reached when the puddle exceeds the margin of the road (Figure B.1). Using the Raster Calculator function of ArcMap, the total area ($A_{total}$), the total volume ($V_{total}$) and the weighted average of the water depth ($z_{depression}$) of the depression storage is calculated using the sum of all individual depression puddle pixels;

$$V_{depression} = \sum \Delta x \Delta y \Delta z \tag{B.1}$$

$$A_{depression} = \sum \Delta x \Delta y \tag{B.2}$$

$$z_{depression} = \frac{\sum \Delta z \times pixel\,amount}{\sum pixel\,amount} \tag{B.3}$$

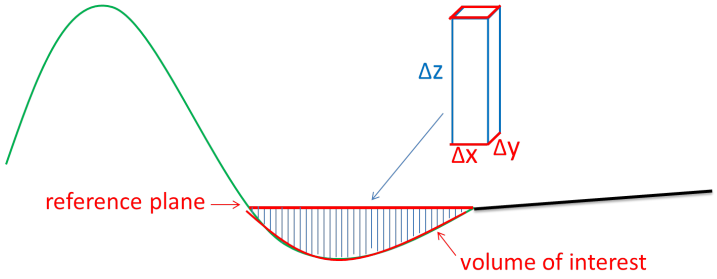


Figure B.1: Schematization of the depression storage volume calculation.

It is assumed that the depression depth increases linearly as the bucket fills according to;

$$z_{depression} = \frac{V_{1\,mm\,runoff}}{A_{depression}} \times (P - ZOABTW) \tag{B.4}$$

However, in case of a full verge bucket, the puddle spreads out over the highway and the depression depth follows a power relation (Figure B.2). This relation is not incorporated in the models, since the bucket models aim at determining the tipping point. However, it is important to note that the linear relation in the bucket approach is not valid after the tipping point has been reached.

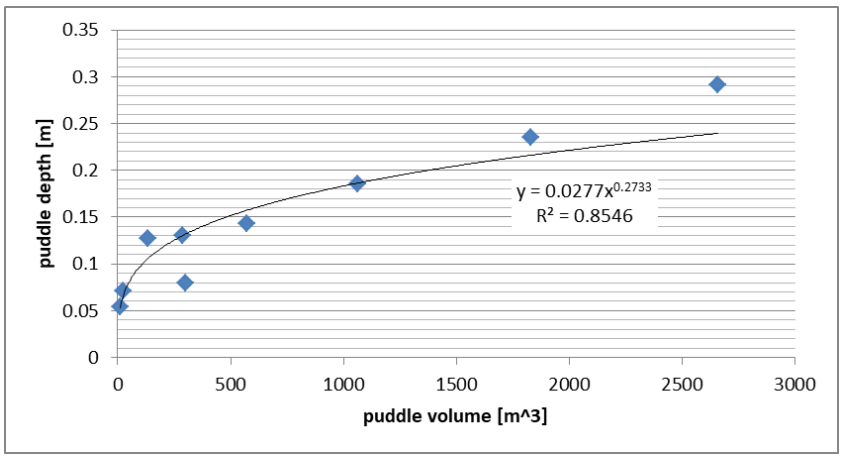


Figure B.2: The increase in puddle depth with increase in puddle volume follows a power relation. The blue rhombuses reflect various puddles that are quantified in ArcMap.

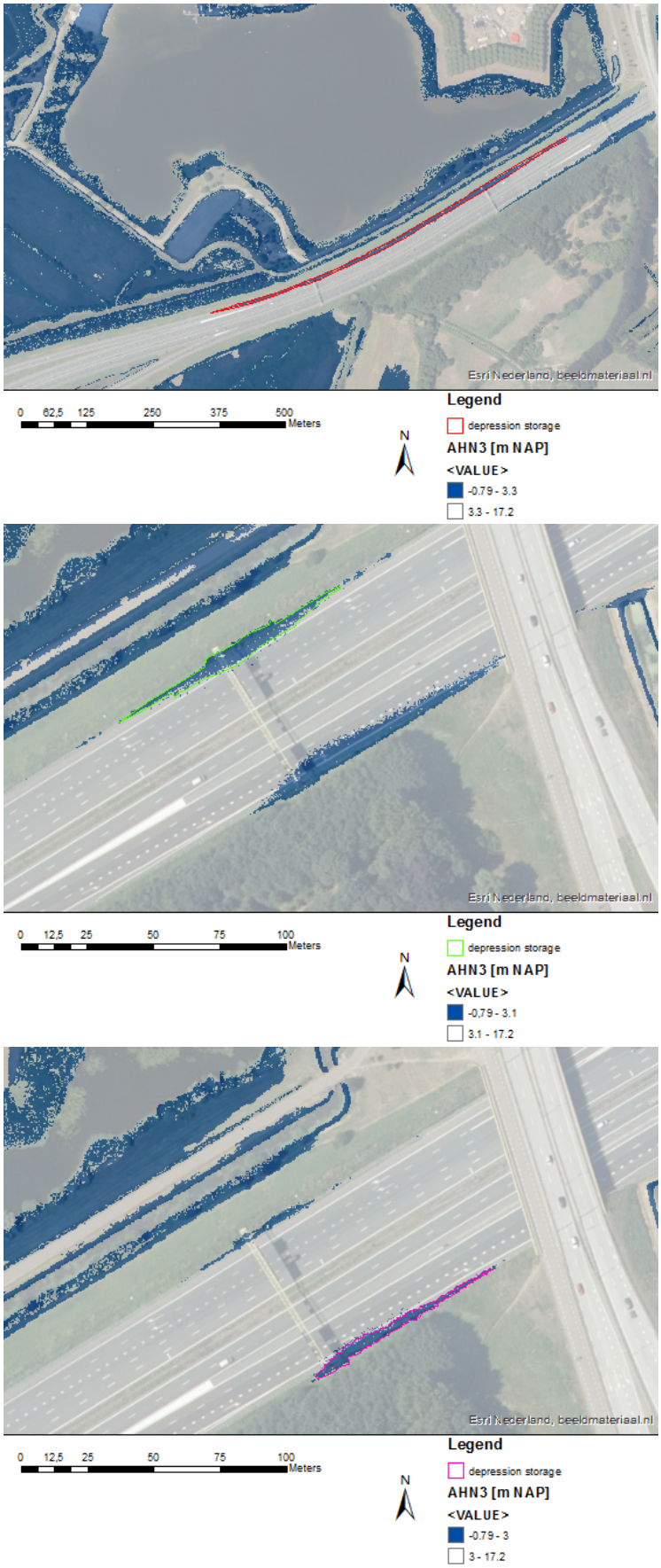


Figure B.3: Depression storages of verges susceptible to runoff accumulation. From top to bottom, the depression storages amount to 7.9, 7.1 and 5.4 centimetres.

- **Infiltration trench, unsaturated zone, phreatic groundwater, regional confined groundwater, wadi:** The capacity of the buckets associated with the soil below ground level depends on the initial available storage and on the boundary conditions, i.e. the MHGL and MLGL groundwater statistics. The buckets are incorporated in the infiltration models (section B.1.3).

- **Stormwater sewer system:** The volume of the conduits is calculated according to

$$V_{conduit} = \pi L R^2 \tag{B.5}$$

where R represents the radius of the conduit and L is the length of the conduit. Due to the aforementioned loss of capacity of the stormwater sewer system (section 3.4.2), the volume partially filled conduits was computed using a partially filled tilted tank volume formula:

$$V_{fill} = V_{conduit} - \frac{R^2}{2}\int_0^L \theta(x) - \sin\theta(x)\,dx \tag{B.6}$$

with

$$\theta = 2\arccos\frac{R - (x\tan\alpha + h_0)}{R} \tag{B.7}$$

where $\alpha$ refers to the tilt angle and $h_0$ illustrates the liquid level at the upper base of the conduit (Figure B.4). In the formula it is assumed that both bases are partially filled with water and that the liquid level $h_0$ is measured directly on the upper base. The lost storage the sewer at cross-section 119.95 equals 1.3mm, which corresponds with approximately 50% of the storage capacity of the sewer. Due to a lack of information on the sewer layout, it is assumed that the lost storage is 50% in the other sewer trajectories as well. As the lost storage is small, this assumption can be regarded acceptable.

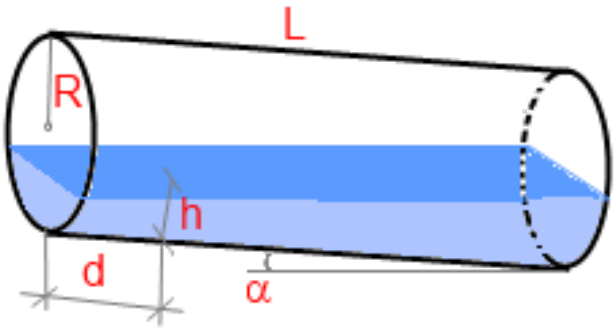


Figure B.4: Clarification of symbols in equations B.7 and B.6

### B.1.3. Fluxes

The fluxes $[LT^{-1}]$, i.e. runoff, infiltration, drainage, overflow, pumping, percolation, capillary rise, seepage and recharge are represented as follows in the model;

- **Runoff:** The amount of runoff is simply difference between the cumulative amount of precipitation within the simulation time and the storage capacity of the porous asphalt (Appendix B.1.2). This paragraph explains the assumptions regarding runoff, i.e. ignoring horizontal runoff through the porous asphalt and routing;

  1. By ignoring the effect of wind, assuming that the highway is free of ruts and applying a simplified quantification of stormwater runoff using the law of Darcy, it can be shown that horizontal runoff can be ignored, despite the lack of knowledge on the dynamical behaviour of highway runoff. Van Der Steen (2005) empirically determined vertical and horizontal permeabilities of porous asphalt in the beginning of its lifetime and found values between 0.8 to 1.4 $\times 10^{-3}$ m/s. The law of Darcy is as follows;

$$Q = -iKA \tag{B.8}$$

in which Q represents the discharge ($L^3T^{-1}$), K refers to the hydraulic conductivity (L/T) and i is the hydraulic gradient (-). According to the law of Darcy (Equation B.8) a maximum discharge inside porous asphalt of Q = 1.32 $\times 10^{-4} m^3$/min per m road length can be generated in a porous asphalt layer with a thickness of 0.11m, a hydraulic conductivity of $1 \times 10^{-3}$ m/s and a hydraulic gradient i of 2% (representative values for the case area). An extreme precipitation event of P = 38 mm/hr on a five-lane road with a width w of 22m generates a surface discharge of $Q = P \times w = 22 \times (38/1000/60) = 1.39 \times 10^{-2} m^3$/min per m road length. The difference between the runoff fluxes inside the porous asphalt and on the surface is a factor 2 and therefore the runoff inside the porous asphalt can be regarded negligible. A higher precipitation intensity causes an increase in the factor. Thus, the more precipitation, the better the assumption of ignoring horizontal runoff holds.

2. Using the empirical formula of Kirpich to compute the time for runoff from the remotest point on the highway towards the stormwater sewer, it can be illustrated that routing can be ignored. The empirical formula of Kirpich is as follows (Van De Ven, 2009);

$$t = 0.01947 \frac{L^{0.77}}{S^{0.385}} \tag{B.9}$$

with t = time of runoff (min), L is the length of the flow path (m) and S is the slope (m/m). The Kirpich formula only demands two inputs, which can be derived from the Dutch Digital Elevation Model AHN3 and are therefore not constrained by the lack of information on porous asphalt roughness. The Kirpich method is applicable to small catchments with slopes between 0.002 and 0.1 m/m (Roussel et al., 2005; Fang et al., 2008). Along the A2 under study the longitudinal road slope is smaller than the cross-sectional road slope. Thereafter, it is assumed that precipitation will run off perpendicular to the road length, following the width of the road. As an example to substantiate the assumption, a travel distance of 22m under a slope of 2% are inserted in Equation B.9. The distance and slope correspond with a five-line asphalt road and therefore indicate the maximum distance for a drop of precipitation to travel from the porous asphalt towards the verge. Equation B.9 reveals a time of runoff of less than a minute, i.e. routing of runoff towards the verge can be ignored in the infiltration model.

- **Infiltration:** Two infiltration mechanisms can be distinguished; infiltration excess overland flow and saturation excess overland flow;
  - In case of infiltration excess overland flow, the rainfall rate is larger than the soil infiltration capacity and therefore ponded infiltration starts occurring (Brevnova, 2001; Hendriks, 2010). The process of infiltration excess overland flow can be physically approximated by the Green and Ampt 1D infiltration model (Figure B.5). The model simplifies infiltration through a step-like approximation (Figure B.5), assuming a sharp wetting front (Brevnova, 2001; Hendriks, 2010; Kale and Sahoo, 2011), a constant saturated hydraulic conductivity and a constant capillary suction. The latter two assumptions imply the absence of soil layering and a deep groundwater table.

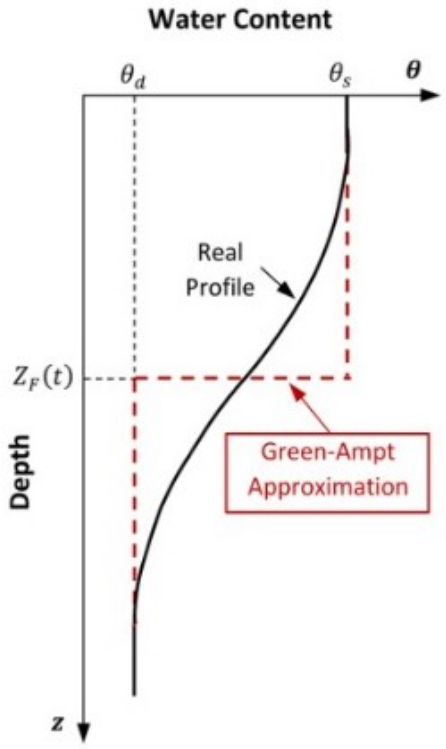


Figure B.5: Instantaneous water content profile in a dry soil (solid line) and its step-like Green-Ampt approximation (dashed red line). $Z_F$ represents the depth of the wetting front, $\theta_s$ is the soil moisture content at saturation and $\theta_d$ represents the initial soil moisture content (Alastal and Ababou, 2019).

Equivalent to the law of Darcy (Equation B.8), the Green and Ampt equation expresses the total gradient;

$$f = K\frac{L + S_f + h_0}{L} \tag{B.10}$$

with infiltration rate f $[L/T^{-1}]$, effective hydraulic conductivity K $[L/T^{-1}]$, capillary suction $S_f$ [L], ponded water height at the soil surface $h_0$ [L] and wetting front depth L (Hendriks, 2010). By definition, the effective hydraulic conductivity is smaller than the saturated conductivity. The change in ponded water height at the soil surface $h_0$ throughout the precipitation event can be neglected, because it can be regarded small in comparison to the increase in L (Brevnova, 2001). From equation B.10 it can be derived that as infiltration continues L increases, a decrease of the total gradient and consequently a gradual decline of the infiltration rate takes place. Moreover, the gradient will reduce to a value of 1 after some time has passed, since L in that case will largely exceed $S_f$ and $h_0$. Due to the decrease of the infiltration rate throughout the precipitation event, there is usually some time prior to ponding during which the infiltration capacity exceeds precipitation intensity $P$. Therefore, the infiltration process consists of two-stages; infiltration before ponding and after ponding (Brevnova, 2001). Using the time to ponding $t_p$ (Equation B.11) and neglecting $h_0$, the cumulative two-stage infiltration F can be iteratively computed according to Equation B.12.

$$t_p = \frac{KS_f\Delta\theta}{P(P-K)} \tag{B.11}$$

$$F - Pt_p - S_f\Delta\theta\ln\frac{S_f\Delta\theta + F}{S_f\Delta\theta + Pt_p} = K(t - t_p) \tag{B.12}$$

The Green-Ampt model is modified in several ways to account for local conditions at the case area;

1. To account for the runoff from porous asphalt into the verge, precipitation intensity $P$ includes both the runoff from the verge that forms a depression depth (Equation B.4) as well as precipitation that directly falls on the verge.

2. An effective hydraulic conductivity is used instead of a saturated conductivity for several reasons. Firstly, the effective hydraulic conductivity is believed to account for hysteresis [1] (Kale and Sahoo, 2011; Tügel et al., 2021). Secondly, the hydraulic conductivity was found to be smaller than the saturated hydraulic during short, extreme precipitation events (Tügel et al., 2021). Brevnova (2001) suggests to use half the saturated conductivity as the effective hydraulic conductivity. Thirdly, Jotisankasa and Sirirattanachat (2017) states that grass roots, which are present throughout the verge in the case area, can decrease the permeability of the soil.

– In case of saturation excess overland flow, on the other hand, the soil infiltration capacity is larger than the precipitation intensity throughout the precipitation event and the water table rises to the land surface due to a limited amount of available storage in the unsaturated zone (Hendriks, 2010). In this case the time of ponding depends on the initial storage in the unsaturated zone $\theta_i$, the porosity n and the depth of the groundwater table $l_{wt}$;

$$t_p = (n l_{wt} - \theta_i)/P \tag{B.13}$$

The infiltration rate simply equals the precipitation rate (which can also include runoff from the road) until the time of ponding is reached. Afterwards runoff takes place (Hendriks, 2010).

- **Stormwater sewer system** Quantification of the stormwater sewer overflow has been done for the trajectories separately through the rational method and hydraulic calculations.
To start with, the rational method is a robust, stationary modelling approach (Butler et al., 2018) and requires the input of a rainfall intensity that causes the sewer system to operate at steady state. Operation at steady state arises when the duration of rainfall is equal to the time of concentration in the area. The time of concentration ($t_c$) is the time required for surface runoff to flow from the remotest part of the catchment area to the point under consideration, including both overland flow time ($t_e$, coincides with $t$ in Equation B.9) as well as sewer flow time ($t_s$) (Van De Ven, 2009);

$$t_c = t_e + t_s \tag{B.14}$$

The rational method can be expressed by

$$Q = iCA \tag{B.15}$$

in which Q represents the discharge through a pipe [$L^3T^-1$], C is the runoff coefficient [-], A is the catchment area [$L^2$], and i is the critical rainfall intensity [$L^3T^{-1}L^{-2}$] associated with a time window equal to the concentration time. The size of the contributing catchment areas to each pipe-section (A) is based on the length of the pipe segments and the cross-slope of the road; areas sloping towards pipe sections contribute to the pipe section. The longer the pipe segment, the larger the discharge area that belongs to the pipe segments. As a discharge model with initial losses is assumed, the runoff coefficient C is 100%. For each sewer trajectory, the cumulative discharges have been determined.
Secondly, implementing the findings from the rational method into hydraulic calculations allows the determination of the occurrence of flooding. Flooding occurs when the hydraulic gradient line exceeds the ground level. The hydraulic gradient is made up of friction losses, which are due to friction between the water and the sewer pipe, and local losses, due to disruptions such as bends and changes in the cross-section (Butler et al., 2018). Friction losses can be represented by the Darcy Weisbach-equation:

$$h_{friction} = \lambda \frac{Lu^2}{D2g} \tag{B.16}$$

in which $h_{friction}$ represents the head loss per pipe segment due to friction [m], $\lambda$ is the friction factor [-], L represents the length of the pipe segment [m], u refers to the actual flow velocity [$ms^-1$], D is the internal pipe diameter [m] and g represents the gravitational acceleration constant [9.81 $ms^-2$]. Local losses can be expressed in terms of velocity head as follows;

$$h_{local} = k_L \frac{u^2}{2g} \tag{B.17}$$

[1] Hysteresis refers to the dependency of an equilibrium state in the soil moisture characteristic on history of the physical system and on the process which occurs, i.e. drying or wetting (Hendriks, 2010

where $h_{local}$ is the local head loss (m) and $k_L$ is a constant for the particular type of fitting [-], u refers to the actual flow velocity [$ms^{-1}$], and g represents the gravitational acceleration constant [9.81 $ms^{-2}$]. For straight manholes on a gravity sewer which is surcharged, $k_L$ equals 0.15. The total hydraulic gradient is as follows;

$$\Delta h = h_{local} + h_{friction} = k_L \frac{u^2}{2g} + \lambda \frac{Lu^2}{D2g} \tag{B.18}$$

Using the White-Colebrook equation

$$\lambda = \frac{1}{(2\log\frac{3.71D}{k})^2} \tag{B.19}$$

the frictional factor was quantified. For the PVC pipes present in the case area, an average roughness of $k$ = 0.045 mm was implemented (Butler et al., 2018). The actual velocity in each pipe segment is determined by

$$u = \frac{4Q_{tot}}{\pi D^2} \tag{B.20}$$

in which D represents the inner diameter [m].

Using the weirs as a starting point, hydraulic gradient calculations have been executed for the sewer trajectories. The water levels over the weirs have been modelled by assuming flow over a standard weir with free flow;

$$h_{weir} = \frac{Q}{1.7 c_v c_d b}^{2/3} \tag{B.21}$$

with weir discharge Q [$m^3 s^{-1}$] (obtained through rational method), velocity correction coefficient $c_v$ [-], crest coefficient $c_d$ [-] and the width of the weir b [m]. The standard weir formula was apprehended due to a lack of knowledge on the outflow location dimensions. $c_v$ and $c_d$ values of 1 have been apprehended and a value of b was assumed to equal 0.8m (based on Asbuilt drawings). It is important to note that for computation of the hydraulic heads at the outflow locations, the blue trajectories are characterized by set up walls of 1.85 NAP m (connected to the large culvert (As built drawings)), whereas 2.15 m NAP walls are assumed at the outflow locations near 119.1. This assumption is based on level of Dungense ditch, the absence of connecting culvert and the lost storage assumption. The crest height and $h_{weir}$ constitute the input for hydraulic calculations.

In case the hydraulic gradient rises above the ground level somewhere on the sewer trajectory flooding occurs and the tipping point is reached.

- **Drainage:** The drainage pipes can be regarded the interaction between the groundwater and the surface water, since the drainage pipes collect groundwater and transport the groundwater to the Dungense ditch through connection with the storm sewer system. Since limited information on the effect of drainage on the groundwater level is available, it is assumed that the drainage capacity is at maximum 7 mm/d (Van De Ven, 2009). It was decided not to model the drainage capacity using Hooghoudt due to the presence of many disturbances such as the water sheet piles, the impermeable road foundation and heterogeneous soil layers and uncertainties regarding location of the southern highway stormwater and drainage facilities, the drain entry resistance and clogging. However, regarding the design drainage capacity of 7 mm/d, it can be assumed that the inflow into drainage pipes during a rainstorm is negligible. Moreover, it can be speculated that the drainage pipes are functioning poorly at 119.1, since the groundwater level at that location is never restored to the invert level of the drains; the MLGL is higher than the invert level of the drains. Therefore, the capacity of the drainage pipes might be close to 0 mm/d.

- **Percolation, capillary rise, recharge, and seepage**: The fluxes associated with groundwater dynamics are encapsulated by the MHGL and MLGL groundwater statistics retrieved in Chapter 4.

- **Pumping:** The pumping capacity of the two pumps in the Segers pumping station equals 63 $m^3/min$. The Segers pumping stations drains a surface area of 1600 hectares, resulting in a capacity of 0.0039 mm/min of each pump. The Segers pumping station is not of direct influence to the catchment of the road.

# B.2. Implementation of measures in bucket models

## B.2.1. Adaptation measures related to increasing discharge

The adaptation measures related to increasing discharge are implemented in the bucket approach as follows;

- **Install manholes with holes:** Implementation of installing manholes with holes at 119.1 is established in a similar way to cross-section 119.95, i.e. by a discharge model with initial losses, according to the rational method in combination with hydraulic calculations (Appendix B.1).
- **Increase in sewer capacity:** Increasing the sewer capacity of the existing sewer lay-out is established in the model by an increase in pipe diameters. For cross-section 119.1, all pipe diameters undergo an increase to the successive commercially available diameter; from 250 mm to 315 mm. For cross-section 119.95, all critical pipes (i.e. the most upstream pipe diameters) undergo an increase to the successive commercially available diameter; from 160 mm to 250 mm, from 250 mm to 315 mm and from 315 mm to 400 mm.
- **New sewer layout:** A re-iteration process was executed according to the rational method and hydraulic calculations in order to choose the most cost-effective solution to meet the requirement of no flooding for the T=10 year design storm that occurs in 2050 according to the Dutch climate scenarios (Table 7.1). Flooding occurs when the hydraulic gradient line exceeds the ground level and it can be prevented by enlarging internal pipe diameters. The design of the weir contributes largely to the overflowing discharge and thereby the hydraulic gradients. A weir with a crest height of 2.85 m NAP was chosen to avoid groundwater from flowing into the sewer system. Using the outflow weir as a starting point, head calculations were executed for the sewer trajectories.

## B.2.2. Adaptation measures related to increasing storage

The adaptation measures related to increasing storage on the road are implemented in the bucket approach as follows;

- **Clean ZOABTW:** It is assumed that after cleaning ZOABTW, the entire storage capacity of the porous asphalt bucket (23.8 mm) is available for precipitation in any scenario.
- **Increase storage ZOABTW:** In all scenarios, the thickness of the porous asphalt is increased to 18 cm (an increase of 7 cm with respect to the current situation), based on the thickness values of porous asphalt in the Adaptation Pathways map of Leijstra et al. (2018). The increase in thickness results in an increase of interception capacity to 38.9 mm, assuming the porosity values of Bles et al. (2020). Moreover, as a result of the addition of 7 cm of porous asphalt, the depression storage bucket in the verge will be enlarged according to the area ratios of the buckets.
- **Plastic Road:** According to Koudstaal Jorritsma (2015), the PlasticRoad can store 0.3 $m^3/m^2$. Thereafter, it is assumed that the capacity of the porous asphalt bucket is enlarged to 300 mm.

The adaptation measures related to increasing storage in the verge are implemented in the bucket approach as follows;

- **Remove top layer verge and descending verge:** The removal of the top layer of the verge and the descending verge increase the depression storage in the verge by 10 cm and 5 cm respectively. Thereafter, the length to water table will be decreased by 10 cm and 5 cm respectively in every scenario and the depression storage bucket in the verge will be enlarged according to the area ratios of the buckets.
- **Infiltration verge:** The infiltration trench design with its corresponding parameters is based on Van De Ven (2009). It is assumed that installing an infiltration trench between ground level and the MHGL results in a change of the infiltration model parameters. As it is assumed that the infiltration trench will be filled with course stones, the following infiltration model values are apprehended; porosity n = 0.4, effective hydraulic conductivity K = 25 m/d, suction $S_f$ = 0.015 m.
- **Raise the road:** In this case it is assumed that no porous asphalt will be added, but that the entire road will simply be raised by 10 cm. This results in an extra depression storage of 10 cm in the verge, which is applied in the model according to the area ratios of the buckets.